Summer 9-1-2014

Host-Microbial Interactions that Modulate Luminal IgA

Clara Moon
Washington University in St. Louis

WASHINGTON UNIVERSITY IN ST. LOUIS

Division of Biology & Biomedical Sciences

Immunology

Dissertation Examination Committee:
Thaddeus S. Stappenbeck, Chair
Paul M. Allen
Deepta Bhattacharya
Marco Colonna
David A. Hunstad
Herbert W. Virgin

Host-Microbial Interactions that Modulate Luminal IgA

by

Clara Moon

A dissertation presented to the
Graduate School of Arts and Sciences
of Washington University in
partial fulfillment of the
requirements for the degree
of Doctor of Philosophy

August 2014

St. Louis, Missouri

TABLE OF CONTENTS

LIST OF FIGURES AND TABLES

CHAPTER 2

CHAPTER 3

CHAPTER 4

LIST OF ABBREVIATIONS

AID	Activation-induced (cytidine) deaminase
APRIL	A proliferation-inducing ligand; Tnfsf13
Atoh1	Atonal homolog 1
BAFF	B-cell activating factor; Tnfsf13B
Caco-2	human colorectal adenocarcinoma cell line, epithelial
CD	Crohn's Disease
CM	Conditioned media (from L-WRN cells)
DAPT	N-[(3,5-Difluorophenyl)acetyl]-L-alanyl-2-phenyl]glycine-1,1-dimethylethyl ester (γ-secretase inhibitor)
dIgA	Dimeric immunoglobulin A
dsRNA	double stranded RNA
DSS	Dextran sodium sulfate
EDTA	Ethylenediaminetetraacetic acid
ELISA	Enzyme-linked immunosorbent assay
EPEC	Enteropathogenic *E.coli*
hBD1	Human beta defensin 1
HT-29	Human colorectal adenocarcinoma cell line, epithelial
IBD	Inflammatory bowel disease
IEC-18	Rat ileal cell line
IFNγ	Interferon gamma
IgA	Immunoglobulin A
IgA1	Human IgA subclass 1
IgA2	Human IgA subclass 2
IGAD	IgA deficiency
IgG	Immunoglobulin G
IgJ	Immunoglobulin J; J chain
IgM	Immunoglobulin M
IL-1β	Interleukin-1β
IL-2	Interleukin-2
IL-4	Interleukin-4
IL-5	Interleukin-5
IL-10	Interleukin-10
IL-17	Interleukin-17
ILF	Isolated lymphoid follicle
IRF1	Interferon regulatory factor 1
LL-37	Cathelicidin antimicrobial peptide
LPS	Lipopolysaccharide
LTi	Lymphoid tissue inducer cells
L-WRN	L-cells expressing Wnt3a, R-spondin3, and Noggin
MDCK	Madin-Darby canine kidney epithelial cell line
MHC	Major histocompatibility complex
Muc2	Mucin 2
Myd88	Myeloid differentiation primary response gene 88
NFκB	Nuclear factor kappa B

OVA	ovalbumin
pIgR	Polymeric immunoglobulin receptor
RAG	Recombination activating gene
RegIIIγ	Regenerating islet-derived 3 gamma
ROCK	Rho kinase inhibitor, Y-27632
SC	Secretory component (cleaved form of pIgR that is bound to dIgA)
SCID	Severe combined immunodeficiency
SIgA	Secretory immunoglobulin A (composed of SC bound to dIgA)
STAT6	Signal transducer and activator of transcription 6
T84	Human colorectal carcinoma cell line, epithelial
TCR	T cell receptor
TER	Transepithelial electrical resistance
TGFβ	Transforming growth factor beta
TLR	Toll like receptor
TLR4	Toll-like receptor 4
TNFα	Tumor necrosis factor alpha
TRUC	*Tbet*$^{-/-}$ *Rag*$^{-/-}$ ulcerative colitis (mouse model)
UEA-1	Ulex europaeus agglutinin 1 (lectin)
Vil1	Villin 1
ZapA	Metalloprotease from *Proteus mirabilis*
ZO-1	Zonula occludens 1 / Tjp1 (Tight junction protein 1)

ACKNOWLEDGEMENTS

First and foremost, I would like to thank my parents for always supporting me and encouraging me in all of my endeavors. They have sacrificed so much to provide me with the best life possible, and I cannot express in words the gratitude and love that I have for them. They have taught me the importance of education and the value of hard work, but most importantly they have taught me about perseverance and determination. I may still be a pessimist at heart, but I will never truly give up on anything or anyone because of them. They have been tremendous role models, and I wouldn't be the same person I am today without their example.

I would also like to thank Thad for being a wonderful mentor and giving me the opportunity to train in his laboratory. Despite his busy schedule, he always made time to talk to his students and trainees; his door was always open to us and I truly appreciate that. Though my project had bumps, unexpected turns, and even some dead ends along the way, he was always able to find the good in the bad, and his enthusiasm for science is contagious. Because of this, I've learned much more than just how to think scientifically.

I would like to thank all the members of my thesis committee – Paul, Deepta, Marco, David, and Skip – for their time, encouragement, and guidance to help me become a better scientist. I couldn't have asked for better mentors.

I was very lucky to have the privilege of working with Megan Baldridge, who was a wonderful collaborator, mentor, and friend. All of the work performed in chapter 3 was with her help, and without her this story would not have been the same. She was the one that encouraged and helped me to push this project past the striking initial observations, and I am truly grateful to have worked with her on this story.

Thank you to all the members of the Stappenbeck lab, past and present. It was wonderful to be surrounded by people from such different scientific backgrounds, who approached each question from a different perspective. Our conversations have been invaluable in my growth as a scientist. In addition, I've made some truly great friends who have made the lab a lively and enjoyable place to work.

I'd also like to thank Darren Kreamalmeyer for his help with mice throughout the years. He always has kind words of encouragement for me every time we meet.

I am very grateful to Jerri Smith, Bonnie Meltzer, Janet Casmaer, Ann Winn, and Jennifer Schwierjohn, who have all been so generous with their help throughout the years. Melanie Relich has been there for me since the day I applied to the program, and I'm very appreciative for all her help and guidance.

I would like to thank my wonderful friends – I couldn't have gotten through this without their support. They've been there for me through all the ups and downs of grad school, and have reminded me to take time to breathe and enjoy life as well.

Funding for this work has been provided by NIH training grant T32-AI007172 (Infectious Diseases/Mechanisms of Microbial Pathogenesis, 2009-2010) and NIH training grant T32-AI007163 (Immunology and Immunogenetics, 2011-2014).

ABSTRACT OF THE DISSERTATION

Host-Microbial Interactions that Modulate Luminal IgA

by

Clara Moon

Doctor of Philosophy in Biology and Biomedical Sciences
Immunology

Washington University in St. Louis, 2014

Professor Thaddeus S. Stappenbeck, Chair

IgA is the most abundant immunoglobulin produced in the body, most of which can be found at mucosal sites such as the intestine where it plays an important role at a critical intersection between the host immune system and the microbiota. In the work detailed here, I sought to investigate IgA delivery and stability using *in vitro* and *in vivo* methods. First, I developed a primary intestinal epithelial monolayer system, and utilized this system to evaluate factors that modulate IgA transcytosis. *In vivo,* I interrogated baseline levels of fecal IgA in WT mice and surprisingly observed a binary phenotype in fecal IgA levels between cages. I found that the dichotomous IgA levels were heritable, transmissible, and microbially driven. In addition, the IgA-Low phenotype was dominant and functionally resulted in increased intestinal injury by DSS. Utilizing the primary epithelial monolayer system and IgA transcytosis assay, I found that anaerobically cultured microbes from IgA-Low mice had proteolytic activity capable of degrading secretory component (SC) *in vitro*. These findings support the idea that degradation of SC *in vivo* would make IgA more susceptible to degradation itself. These studies highlight the ability of the microbiota to produce phenotypic effects through IgA modulation.

CHAPTER ONE

Introduction: IgA in the Intestine

The intestine

The intestinal mucosa is comprised of three main layers: the single cell epithelial layer that lines the inner surface of the intestine, the underlying lamina propria that is populated by many cell types from different lineages, and the muscularis mucosae that separates the mucosal layer from the underlying submucosa and muscularis layers. In the colon, the epithelial layer forms structures called crypts, whereas the small intestinal epithelium covers fingerlike projections called villi as well as the crypts. There are several different cell types found in the intestinal epithelium. Stem cells and progenitors found near the base of the crypts are important for the high turnover of epithelial cells. Absorptive enterocytes function in nutrient and water absorption. Secretory cell types include the hormone-secreting enteroendocrine cells, mucus secreting goblet cells, and small intestinal Paneth cells that secrete antimicrobial peptides in addition to mucus.

The lamina propria contains many different cell types including immune cells such as dendritic cells, macrophages, and plasma cells. Mucosal sites are locations where the host is in direct contact with the environment, which includes approximately 10^{14} commensal bacteria present in the intestinal lumen[1]. The immune system must be able to respond to any breaches in the epithelial barrier but at the same time control its responses to prevent chronic inflammation. It is thought that diseases such as inflammatory bowel disease (IBD) may arise from the dysregulation of the immune response to the commensal bacteria[2].

Plasma cells and IgA production

Another highly secretory cell type found in the intestine is the immunoglobulin-secreting plasma cell. 75% of the total immunoglobulin produced in the body is made in the intestine,

where immunoglobulin A (IgA) is the predominant isotype produced[3]. Humans secrete ~3g of IgA in the intestine per day. While IgA can be found as a monomer in serum, the dimeric form (dIgA) covalently linked by the J chain (IgJ) is the predominant form at mucosal sites.

Plasma cells develop from B cells after stimulation in either a T cell-dependent or T cell-independent manner[4]. *Ex vivo* studies have found that transforming growth factor β (TGFβ) and interleukin (IL)-4 could promote naïve B cells to undergo IgA class switch when non-specifically stimulated[5]. Furthermore, once IgA class switch has occurred, IL-2, IL-5, and IL-10 had a synergistic effect in increasing IgA levels.

In co-culture studies, dendritic cells were shown to be able to induce IgA class switch with or without the presence of T cells. Further studies using T cell receptor (TCR) β and δ chain deficient mice as well as CD40 deficient mice showed a substantial decrease but not absence of IgA. These studies suggested a T cell-independent pathway of IgA production. It is thought that in this pathway, intestinal epithelial cells and dendritic cells can produce cytokines such as APRIL and BAFF that can directly activate B cells to class switch to IgA without the need for antigen presentation on class II MHC, TCR engagement, or co-stimulation by CD40-CD40L. This is thought to mainly occur in isolated lymphoid follicles (ILFs), which require lymphoid tissue inducer (LTi) cells for their formation[6].

It has been hypothesized that the T-independent pathway may be important for protection against commensals, whereas the T-dependent pathway (which leads to affinity maturation by somatic hypermutation, and therefore more specific antibodies) might play a large role in defense against pathogens and toxins such as cholera toxin[7]. Using an activation-induced deaminase (AID) mutant mouse that can undergo class switch recombination but not somatic hypermutation, Wei et al observed that in the absence of affinity-maturation, a protective IgA

response to cholera toxin could not be generated[8]. More recent studies have shown however that the majority of IgA gene sequences in the gut are heavily mutated, arguing for the T-dependent IgA pathway as the major and dominant pathway for IgA production[9].

In the intestine, B cells can be found in the secondary lymphoid tissues such as Peyer's Patches (T-dependent) and ILFs (T-independent). Upon stimulation, these cells develop into plasmablasts and eventually into mature plasma cells as they enter circulation through the lymphatics and home back to the lamina propria[5], where a large number of mature IgA-secreting plasma cells can be normally found along the entire length of the gastrointestinal tract.

IgA transcytosis and the polymeric immunoglobulin receptor

While plasma cells produce and secrete dIgA locally in the lamina propria, most of its hypothesized roles are thought to occur in the lumen. To get from the lamina propria into the lumen, dIgA must bind to the polymeric immunoglobulin receptor (pIgR), which is expressed basolaterally on epithelial cells. The J chain, a 15 kDa polypeptide, is crucial for the ability of dIgA to bind to pIgR. In addition to dIgA, other multimeric immunoglobulins that possess the J chain (such as pentameric IgM) can also bind to pIgR as well[10,11]. The dIgA-pIgR complex is then endocytosed in clathrin-coated vesicles and transcytosed through the cell to the apical surface. At the cell surface, the receptor is cleaved[12], releasing the dIgA still bound to the extracellular portion of pIgR (known as the secretory component; SC). This SC-bound dIgA (called secretory IgA; SIgA) is thought to be more resistant to cleavage by intestinal proteases due to the presence of the SC, J chain, and additional glycosylation residues[13,14].

The pIgR protein is a 120 kDa type I transmembrane protein expressed specifically in epithelial cells. Its expression can be found along the entire length of the gastrointestinal tract as

well as at other mucosal sites[15]. In rodents, there is also robust expression in the liver due to the hepatobilliary transport of IgA in these animals[16,17]. The extracellular portion of pIgR is composed of 5 immunoglobulin domains that are important for interacting with dIgA[11,18-20]. A small region, containing putative pIgR cleavage sites, separates these immunoglobulin domains from the transmembrane domain. The cytoplasmic C-terminal region contains a number of intracellular sorting signals. A great deal of work has been done *in vitro* using MDCK and human intestinal epithelial cell lines to dissect out the intracellular trafficking signals and pathways[21-25]. The binding of dIgA to pIgR has been shown to enhance pIgR transcytosis, however the unoccupied receptor can traffic to the surface to some extent as well[21,22,25]. Furthermore, this unoccupied pIgR can also be cleaved and released into the lumen, where it can play a role in host-defense independent of IgA. Free SC, which can be found in high concentrations in human colostrum and milk[19], has been shown to bind to certain bacteria (enteropathogenic *E.coli*; EPEC) and antigens (*C. difficile* toxin A) to prevent their interaction with intestinal epithelial cells[26-28].

The enzyme that cleaves pIgR at the apical surface *in vivo* is still unknown[20]. The *in vitro* systems used to study pIgR have been comprised of many different cell types (intestine, liver, kidney; from multiple species). Yet in all of these systems, cleavage of pIgR has been observed, leading to the hypothesis that the enzyme of interest is either a widely expressed host protease, or there are multiple different proteases able to carry out this function. Further attempts to characterize the enzyme(s) involved have shown the protease involved to be sensitive to protease inhibitors leupeptin, antipain, E-64, and Aprotinin[12]. In addition, characterization of domain 6 of SC from human secretions did not find a consensus cleavage site[29,30]. These data suggest that

there are potentially multiple different enzymes that cleave pIgR *in vivo*, or that there is additional processing by host/bacterial peptidases after the initial cleavage event.

Regulation of pIgR expression

The expression of pIgR in the intestinal epithelium is regulated by bacterial stimuli[19,31-35]. *In* vitro studies have shown that stimulation of HT-29 cells with microbial factors such as heat killed bacteria, lipopolysaccharide (LPS), butyrate, and dsRNA can upregulate pIgR expression[32,33]. In addition, pro-inflammatory cytokines produced in response to microbial stimuli, such as interferon-γ (IFNγ), tumor necrosis factor-α (TNFα), IL-1β, IL-4 and IL-17 have also been shown to increase pIgR expression *in vitro*[19,36]. *In vivo* studies also support this idea, as germ-free mice monocolonized with *Bacteroides thetaiotamicron* have a 3-fold increase in pIgR expression in the ileum[31].

Promoter analysis of mouse and human pIgR has revealed binding sites for multiple transcription factors including IRF1, STAT6, and NFkB[37,38]. This is in agreement with the *in vitro* studies showing the ability of IFNγ (signaling through IRF1), IL-4 (signaling through STAT6), and TNFα (signaling though NFkB) to induce pIgR expression. Furthermore, bacterial ligands can signal through different toll like receptors (TLR) via Myd88 and NFkB to directly induce pIgR expression[38,39]. Epithelial-specific deletion of Myd88 showed a ~50% decrease in pIgR expression, suggesting a contribution of both Myd88-dependent and -independent pathways normally occurring *in vivo*.

Regulation of intestinal IgA induction

Germ-free animals have markedly reduced intestinal plasma cell numbers and IgA, demonstrating the important role of microbes in the production of intestinal IgA[40]. To take a closer look at the timing and specificity of the IgA produced in the intestine, Hapfelmeier et al performed an elegant study using a novel reversible germ-free system[41]. In those experiments, an *E. coli* mutant requiring nutrients not produced by mammalian hosts was used. These mutants were able to survive in a nutrient-supplemented culture, but could not replicate and colonize the intestinal tract. Germ-free mice gavaged with this mutant strain became germ-free within 72 hours. Despite the lack of colonization, a specific IgA response was observed, although a high dose of live bacteria was required to induce this response. This suggested an intrinsic threshold (between 10^8-10^9 bacteria) for the intestinal IgA response to occur. After exposure to this single bacterial strain, the plasma cells persisted for >16 weeks, despite the fact that germinal center B cells returned to baseline by 2-6 weeks in the absence of bacteria. In the presence of additional bacterial species however, the *E.coli*-specific IgA is rapidly lost due to ongoing induction of IgA by the colonized microbes. This result showed that the IgA response changed to the changing microbial population, allowing the mucosal immune system to adapt to the bacteria that are currently present.

Older studies have shown that the average half-life of intestinal plasma cells was 5 days, with a maximum lifetime of 6-8 weeks in conventional mice[42]. These studies demonstrate the quicker turnover of plasma cells and most likely the changing IgA specificities in the presence of a diverse commensal microbiota.

What is the role of SIgA in the intestine?

Several knockout mice lacking luminal IgA have been created to look at the role of IgA in the intestine. Two different *pIgR*$^{-/-}$ mice have been created by different groups, targeting different exons of the *pIgR* gene[43,44]. Both mice show essentially no IgA in the feces or luminal content, indicating the essential role of pIgR in the transport of IgA into the lumen. In addition, there is a significant increase in serum IgA levels (especially dIgA), as well as an increase in lamina propria IgA staining in the *pIgR*$^{-/-}$ mice compared to heterozygous and wild type littermate controls. Further studies showed that there is an increase in IgA^{+} plasma cell numbers in the lamina propria of the *pIgR*$^{-/-}$ mice[45]. The *IgJ*$^{-/-}$ mouse also shows a similar phenotype as the *pIgR*$^{-/-}$, with decreased luminal IgA and increased serum IgA[46,47]. Additional mice lacking luminal IgA (among other things) include the immunodeficient SCID and *RAG*$^{-/-}$ mice, class-switch deficient *AID*$^{-/-}$ mouse as well as the *IgA*$^{-/-}$ mouse[48]. The *IgA*$^{-/-}$ mice show an increase in other immunoglobulin isotypes, and there is concern in the field of disregulated class switching due to the fact that the IgA switch region was targeted in addition to several of the Cα exons.

The functional significance of this lack in luminal IgA has been tested using several models, and there are several hypotheses in the field. Infection studies looking at intestinal and lung pathogens in *pIgR*$^{-/-}$ and *IgJ*$^{-/-}$ mice show that SIgA is important in **protecting against secreted toxins** at the mucosal sites[47,49] and **preventing colonization** of bacterial pathogens[49,50]. However, systemic immune responses seem to be intact, as *pIgR*$^{-/-}$ mice are able to survive and clear systemic infection with *Salmonella typhimurium* and *Streptococcus pneumoniae* after mucosal immunization just as well as wild type mice. In addition, uninfected *pIgR*$^{-/-}$ mice show increased translocation of gut commensal bacteria to the MLNs compared to wild type mice along with an increase in serum IgA and IgG reactivity to the commensal bacteria[51]. This

supports the idea that luminal IgA is important in **limiting bacterial translocation** across the epithelium. Furthermore, IgA may play a role in **regulating the composition** of the normal commensal bacterial population, as *AID*$^{-/-}$, *RAG*$^{-/-}$, and SCID mice all show alterations in their intestinal microbiota compared to wildtype or littermate controls[4,52]. Finally, using OVA-specific TCR transgenic mice, it has been shown that epithelial cells can transport antigen-bound dIgA from the lamina propria into the lumen via pIgR, thereby **eliminating antigens** that have crossed the intestinal epithelial barrier[53].

Despite these many hypothesized roles and experimental systems utilized to address these hypotheses, direct and definitive evidence for the exact function of IgA *in vivo* is still lacking and there is still debate in the field as to its functional significance[7].

Selective IgA deficiency in humans

In humans, IgA deficiency (IGAD) is the most common primary immunodeficiency, with frequencies ranging between 1:223 and 1:1000 in different US populations[54]. It is defined as decreased or absent serum IgA in the presence of normal IgM and IgG. Most people with IGAD are asymptomatic and many more are thought to go undiagnosed due to the general nature of the symptoms. Patients with this disorder develop allergies, autoimmune manifestations, and recurrent infections at mucosal sites. Additionally, selective IgA deficiency has been associated with several gastrointestinal disorders including celiac disease, colon cancer, and IBD. These manifestations suggest an important role for IgA at mucosal sites, however, IgA levels at mucosal sites have not been thoroughly investigated in humans, as diagnosis is usually limited to serum-based methods. As the mucosal immune compartment is thought to be distinct and separate from the systemic immune compartment, there could be IgA deficiencies specifically at

mucosal sites through several different mechanisms that have not been observed or investigated in the context of mucosal diseases such as IBD.

In 1976, a case study was published on a 15 year old patient with normal serum immunoglobulins, but specifically lacking mucosal IgA[55]. This patient was breast fed until 3.5 months of age, after which he developed persistent intermittent diarrhea. Antibiotic treatment and dietary changes did not resolve the symptoms, and multiple stool samples were negative for parasites. Small intestinal biopsy samples revealed increased lamina propria lymphoid cells, and *in vitro* stimulation of peripheral blood lymphocytes showed normal proliferation and immunoglobulin secretion. Unlike IGAD patients, free secretory component was not found in saliva or jejunal fluid. At this time the role of SC and the identity of pIgR were unknown, however the evidence presented here suggests that the patient may have a defect in IgA transcytosis by pIgR. This case study shows the significance of maternally transferred IgA, as well as the role of IgA in maintaining intestinal homeostasis.

A recent study looking at Crohn's Disease (CD) patients identified a subset of patients with reduced pIgR expression in the colon along with elevated serum IgA levels and increased IgA staining in the lamina propria[56]. This mirrors what is observed in the *pIgR*$^{-/-}$ mice. These two examples demonstrate potential consequences of the lack of luminal SIgA in the presence of normal or even elevated systemic IgA, and further supports the idea that serum IgA cannot necessarily be used as a read-out for mucosal IgA.

Commensal bacteria in the intestine

There is an estimated 10^{14} microbes present in the intestinal lumen representing at least 500-1000 individual species[1]. These commensal bacteria are acquired shortly after birth, and

many of these microbes are thought to be maternally transmitted[57-59]. Sequencing of the gut microbiome has revealed *Bacteroidetes* and *Firmicutes* as the two major phyla found in the intestine[60,61]. Despite the fact that these commensal bacteria greatly outnumber host cells, the idea that microbes can modulate host phenotypes is sometimes overlooked in studies using genetically modified mice. While there are many phenotypes that are a clear and direct consequence of host genetics, there have been many cases where the assumed genetically-induced phenotype may in fact be driven solely by differences in the commensal microbiota[62-67]. In some cases, opposing results using the same genetic knockout mouse in different facilities has led to controversy and argument in the field[62,68,69]. It has therefore become crucial to take into account both host genetic and microbial factors in studies, especially those involving mucosal sites.

Degradation of SIgA by pathogenic bacteria

Although there is still debate over the role and even significance of IgA, the fact that there are pathogenic bacteria that can degrade IgA strongly supports the idea that IgA plays an important role in host-microbial interactions and intestinal homeostasis. Beginning in the 1970s, several groups have identified pathogenic bacteria producing related proteases that specifically cleave human IgA1 at Pro-Ser and Pro-Thr residues in the IgA hinge region[70-72]. The bacterial strains, isolated from human patients, include *Neisseria gonorrheae*, *Neisseria meningitides*, *Haemophilus influenza*, and *Streptococcus pneumonia*. Importantly, the related non-pathogenic members/commensal species of these bacteria did not even possess the IgA1 protease genes, suggesting that these genes could be virulence factors[73,74].

A recent study showed one mechanism of how this ability to degrade IgA can benefit the bacterial pathogen[75]. Janoff et al showed *in vitro* that exogenously and endogenously produced IgA1 protease cleaved capsule-specific monoclonal human IgA1 antibodies that recognized the bacterial surface of *S. pneumonia*. This in turn inhibited the Fc-mediated phagocytic killing of the microbe, and furthermore left the Fab fragments still bound to the antigenic residues on the bacterial surface, making these bacteria in effect immunologically hidden.

While human IgA1 is more abundant at non-mucosal sites, the identification of bacterial IgA1 proteases led to the idea that there could be pathogens that cleave the mucosally-dominant human IgA2. In fact, several examples of bacteria able to cleave human IgA2 have been identified[73,76,77]. Like the classical IgA1 proteases, these proteases have been isolated from bacterial pathogens (*Clostridial species* from IBD and *Proteus species* from urinary tract infections). While the some of the identified proteases may be more specific for IgA, *Proteus mirabilis* has been shown to produce a metalloprotease called ZapA that is able to cleave a wide variety of proteins, including immunoglobulins (IgA1, IgA2, IgG), SC, complement (C1q, C3), antimicrobial peptides (hBD1, LL-37), and structural proteins (collagen, fibronectin, laminin, actin, tubulin)[78,79].

The bacterial IgA proteases identified to date have great specificity for their host species. For example, the bacterial IgA1 proteases from human isolates have limited reactivity and are only specific for human IgA1, and in some cases chimpanzee and gorilla IgA1[80,81]. Furthermore, multiple strains of canine *Ureaplasma* isolates were shown to cleave canine IgA, but did not have proteolytic activity against human or murine IgA[81]. The identification of these broad and specific IgA proteases produced by pathogenic bacteria with host specificity highlights the

significant impact that IgA has played in the evolutionary conversation between the host and microbes.

Modeling the intestine in vitro

Many advances in the last few decades have made the study of gastrointestinal tract possible, including the development of genetically and microbially defined animal models, animal models of injury and repair, and immortalized cell lines. Most recently, the ability to grow and propagate primary intestinal epithelial cells *in vitro* has greatly advanced the field.

Sato et al developed an intestinal crypt culture system from single $Lgr5^+$ cells isolated from the mouse intestine that required exogenous growth factors in the media (EGF, R-spondin1, and Noggin)[82]. The single $Lgr5^+$ cells, suspended in Matrigel, were shown to form crypt-villus structures termed organoids, and contained multiple cell types including enterocytes, Paneth cells, goblet cells, and enteroendocrine cells. These organoids could be dissociated and re-plated to form new organoids every 14 days. While this was a major breakthrough in the field, the exogenous factors required to maintain these cells are expensive and can be cost-prohibitive to maintain for the large-scale cultures that are required for standard *in vitro* assays.

Miyoshi et al developed a system to culture enriched gastrointestinal stem cells using conditioned medium from a supportive cell line (L-WRN) containing Wnt3a, R-spondin3, and noggin[83,84]. This system not only provided a cost-effective method to grow primary intestinal stem cells, it also allowed for the use of whole tissue as starting material, eliminating the need to sort and purify stem cells prior to the start of culture. Despite the heterogeneous cell population in the starting material, the culture conditions here specifically allowed for the growth and propagation of the stem cell population. Unlike the organoid system, these enriched stem cells

did not form budding structures and instead formed spheroids. However, these cells were able to differentiate into multiple cell types by decreasing the amount of conditioned media and adding the γ secretase inhibitor DAPT. Furthermore, these cells could be passaged every 3 days, as opposed to the 14 days required by the organoid system. In addition, the L-WRN conditioned media has allowed for establishment of epithelial spheroid cultures from human gastrointestinal tissue and biopsy samples (VanDussen et al in press).

Prior to the ability to grow primary intestinal epithelial cells, colon cancer cell lines have been widely used to model physiologic and cell biologic intestinal processes *in vitro*, and these studies have provided great insight into epithelial cell biology. However, there are many well-recognized limitations to these lines including prolonged time to attain mature and differentiated monolayers (~20 days in culture for some lines), aneuploidy, and the presence of numerous undefined DNA mutations. Additional alternatives to human cancer cell lines have been developed and include the use of virally-transformed intestinal epithelial cells such as rat IEC-18 cells, or non-intestinal epithelial cells such as MDCK cells, but these systems have their own limitations[85,86]. One major advantage these various cell lines have over the current primary intestinal epithelial culture method is their ability to form polarized monolayers in Transwells. This has provided the means to study many epithelial cell processes including interactions with other host cell types, interactions with microbes, drug absorption, and intracellular trafficking[85,87,88]. The development of a primary intestinal epithelial monolayer system would allow for a more physiologic model to investigate these different intestinal epithelial processes *in vitro.*

CHAPTER TWO

Development of a Primary Intestinal Epithelial Monolayer Culture System to Evaluate Factors that Modulate IgA Transcytosis

ABSTRACT

There is significant interest in the use of primary intestinal epithelial cells in monolayer culture to model intestinal biology. However, it has proven to be challenging to create functional, differentiated monolayers using current culture methods, likely due to the difficulty in expanding these cells. Here, we adapted our recently developed method for the culture of intestinal epithelial spheroids to establish primary epithelial cell monolayers from the colon of multiple genetic mouse strains. These monolayers contained differentiated epithelial cells that displayed robust transepithelial electrical resistance. We then functionally tested them by examining IgA transcytosis across Transwells. IgA transcytosis required induction of pIgR expression, which could be stimulated by a combination of lipopolysaccharide and inhibition of γ-secretase. In agreement with previous studies using immortalized cell lines, we found that TNFα, IL-1β, IL-17, and heat-killed microbes also stimulated pIgR expression and IgA transcytosis. We used wild-type and knockout cells to establish that among these cytokines, IL-17 was the most potent inducer of pIgR expression/IgA transcytosis. IFNγ, however, did not induce pIgR expression, and instead led to cell death. This new method will allow the use of primary cells for studies of intestinal physiology.

INTRODUCTION

The study of intestinal epithelial biology has been made feasible through advances in the field of gastroenterology during the last few decades. Some of these technical advances have included the development of genetically and microbiologically defined animal models, animal models of injury and repair, and immortalized epithelial cell lines for *in vitro* studies. Most recently, the ability to propagate primary intestinal epithelial cells *in vitro* has greatly advanced the field[82-84].

Prior to the ability to grow primary intestinal epithelial cells, colon cancer cell lines have been widely used to model physiologic and cell biologic intestinal processes *in vitro*. Studies using these lines have provided initial insights into epithelial biology in many areas. For example, Caco-2, HT-29, and T84 cells can form monolayers of differentiated cells[89-91]. However, colon cancer cell lines have many well-recognized limitations including prolonged time to attain mature monolayers (~20 days in culture for some lines), aneuploidy, and the presence of numerous undefined DNA mutations. Additional alternatives to human cancer cell lines have been developed and include the use of virally-transformed intestinal epithelial cells such as rat IEC-18 cells, or non-intestinal epithelial cells such as MDCK cells, but these systems also have limitations[85,86].

One advantage these various cell lines have over the current primary intestinal epithelial cell culture method is their ability to form polarized monolayers in Transwells. This has provided the means to study many epithelial cell processes including interactions with other cell types, interactions with microbes, drug absorption, and intracellular trafficking[85,87,88]. One such intestinal epithelial cell process that has been well-dissected and characterized using these cell lines is IgA transcytosis via pIgR[11,19,38].

The majority (75%) of the total immunoglobulin produced in the body is made in the intestine, where IgA is the predominant isotype produced[3]. Humans secrete ~3 g of IgA in the intestine per day. While IgA can be found as a monomer in serum, the dimeric form (dIgA) connected by the J chain (IgJ) is the predominant form at mucosal sites[20].

Plasma cells produce and secrete dIgA locally in the lamina propria. For the IgA to enter the intestinal lumen, dIgA must bind to its receptor pIgR[92,93], which is expressed basolaterally on epithelial cells. The dIgA-bound pIgR is then endocytosed in clathrin-coated vesicles and transcytosed across the cell through several distinct compartments to the apical surface[11,19,94]. At the cell surface, as of yet unidentified enzymes cleave the receptor, releasing the dIgA still bound to the extracellular portion of pIgR (known as the secretory component, or SC). This secretory IgA (SIgA), protected by the J chain as well as the SC, is more resistant to cleavage by intestinal proteases[13,14].

Several studies have shown that the expression of pIgR in the intestinal epithelium is regulated by bacterial stimuli. Germ free mice have a 3-fold increase in pIgR expression in the ileum upon monocolonization with *Bacteroides thetaiotamicron*[31]. *In vitro* studies have shown that stimulation of HT-29 cells with microbial factors (such as LPS, butyrate, and dsRNA) or heat-killed bacteria can upregulate pIgR expression[32,33]. Pro-inflammatory cytokines produced in response to microbial stimuli, such as IFNγ, TNFα, IL-1, and most recently IL-17 have also been shown to increase pIgR expression *in vitro*[19,36,38,95-98].

Here for the first time, we establish a system to grow primary intestinal epithelial cell monolayers. This will assist in the study of intestinal epithelial cell processes *in vitro* using primary cells. We chose to focus on the process of IgA transcytosis using this system. We were able to adapt the previously established three dimensional (3D) primary intestinal epithelial stem

cell culture system into a 2D monolayer in a Transwell. These cells are able to express pIgR after stimulation with LPS, and transcytose IgA across the monolayer. TNFα, IL-1β, and IL-17 were able to induce pIgR expression and IgA transcytosis in a dose-dependent manner. Importantly, perhaps demonstrating a distinction with previous methodologies using immortalized cell lines, IFNγ did not enhance pIgR expression. Heat-killed bacteria were also able to stimulate these processes to differing extents. Finally, this system will be readily adaptable for the use with available genetically modified mice to study different genes of interest: primary intestinal epithelial cells from *pIgR*$^{-/-}$ mice do not show IgA transcytosis into the supernatants, while cells from *Tlr4*$^{-/-}$ mice have reduced pIgR expression and IgA transcytosis after LPS stimulation compared to wild-type cells.

MATERIAL AND METHODS

Mice. Animal protocols were approved by the Washington University Animal Studies Committee. All mice were maintained in a specific pathogen-free barrier facility. *pIgR*$^{-/-}$ mice (B6.129P2-Pigr^{tm1Fejo}/Mmmh[43]) were initially obtained from Mutant Mouse Regional Resource Center (Columbia, MO). *Tlr4*$^{-/-}$ mice were provided by the laboratory of Dr. William F. Stenson (B6.B10ScN-TLR4$^{lps-del}$/JthJ from Jackson Laboratory[99]). All mice used were 8-10 weeks of age.

3D spheroid cell culture. Primary colonic epithelial stem cells were isolated, grown, and maintained as 3D spheroid cultures in Matrigel (BD Biosciences; San Jose, CA) as described in Miyoshi et al[83,84]. Cells were kept in 50% L-WRN conditioned media (CM). Media was changed every two days, and cells were passaged every three days (1:3 split).

Formation of Transwell monolayers. To form monolayers of intestinal epithelial cells, spheroids were taken from three-day-old 3D cultures for plating in Transwells (Corning Costar 3413; Tewksbury, MA). The Transwells were coated in 0.1% gelatin for ≥1 hour at 37°C. Spheroids were recovered from Matrigel by first washing in a solution of 0.5 mM ethylenediaminetetraacetic acid (EDTA), and then dissociated for 4 minutes at 37°C using a solution of 0.05% Trypsin/0.5 mM EDTA. The trypsin was then inactivated using DMEM/F12media containing 10% FBS. The spheroids were then dissociated by vigorous pipetting (using a 1000 µl pipet). The cells were then passed through a 40 µm cell strainer (BD Biosciences) and re-suspended in 50% L-WRN CM containing 10 µM Y-27632 (ROCK inhibitor; Tocris Bioscience and R&D Systems; Minneapolis, MN). On average, spheroids from three wells of a 24-well plate were plated into the upper compartment of a single Transwell in

100µl of media. An additional 600 µl of media was added to the lower compartment of the Transwells.

Cell treatments. On day one (24 hours after seeding the Transwells) the 50% L-WRN CM supplemented with Y-27632 was removed and replaced with 0% CM (Advanced DMEM/F12 containing 20% FBS, 100 units of Penicillin, 0.1 mg/ml Streptomycin and 2mM L-glutamine). At this time, any additional treatments were also administered to the cells: LPS (Sigma L4391; Saint Louis, MO), DAPT γ-secretase inhibitor (Millipore 565784; Billerica, MA), recombinant mouse IL-1β (R&D Systems 401-ML), recombinant mouse IFNγ (R&D Systems 485-ML), recombinant mouse TNFα (R&D Systems 410-MT), recombinant mouse IL-17 (R&D Systems 421-ML), and heat-killed *E. coli* (lab stocks, mouse adapted strain)[100]. Cells were given fresh media with the respective treatments on day two, and were treated for a total of 48 hours before being used for IgA transcytosis, histology, or RNA extraction on day three.

Transepithelial electrical resistance (TER) measurements. TER was measured for cells in Transwells using an epithelial volt-ohm meter (World Precision Instruments, Inc.; Sarasota, FL). Resistance of the intestinal epithelial cell monolayer was calculated by subtracting the resistance of the (membrane + media) from the resistance of the (membrane + media + cells). Each Transwell was measured in triplicate and the average value was taken. This value was then multiplied by the area of the Transwell membrane (0.33 cm^2) to obtain a final value in Ωcm^2.

IgA transcytosis assay. On day three, the Transwells were removed from the various treatment conditions and washed with 0% CM. 600 µl of 0% CM containing mouse IgA (for early studies:

Santa Cruz Biotechnology sc-3900; Dallas, TX; later studies: BD Pharmingen 553476) was added to the lower compartment. Both sources of IgA contained a mixture of monomeric and polymeric IgA, according to each company. For the lot of BD Pharmingen IgA used in these studies, the amount of dimeric IgA was ~85% according to the manufacturer. 100 µl of 0% CM alone was added to the upper compartment and collected at different time points to evaluate the amount of IgA transcytosed by ELISA (Immunology Consultants Labs E-90A; Portland, OR).

Immunostaining and histologic analysis. Cells in the Transwells were washed with PBS and fixed in either 10% formalin or Bouins fixative for 10 minutes. The cells were then washed three times in 70% ethanol and the Transwell membranes were cut out from the Transwell inserts using a surgical blade. The membranes were processed for paraffin embedding. 5 µm thick transverse sections were cut for hematoxylin and eosin staining and immunostaining. For this procedure, the sections were de-paraffinized, hydrated, boiled in Trilogy solution (Cell Marque; Rocklin, CA) for 20 minutes, rinsed in PBS, blocked with 1% bovine serum albumin/0.1% Tritin-X100 for 30 minutes, and incubated with primary antibody at 4°C overnight. Primary antibodies include: rabbit anti-ZO-1 (1:100, Invitrogen/Life Technologies; Grand Island, NY), mouse anti-chicken Villin1 (1:100, AbDSerotec; Raleigh, NC), and goat anti-pIgR (1:500, R&D Systems). The slides were rinsed three times in PBS and then incubated with AlexaFluor594- or AlexaFluor488-conjugaed species-specific secondary antibodies for one hour at room temperature (1:500, Invitrogen/Life Technologies). Slides were washed three times in PBS and stained with bis-benzimide (Hoescht 33258, Invitrogen/Life Technologies) to visualize nuclei and mounted with a 1:1 PBS:glycerol solution. Staining was visualized with a Zeiss (Oberkochen, Germany) Axiovert 200 microscope with an Axiocam MRM digital camera.

For whole mount immunostaining, cells were fixed and washed in the Transwells as described above, then washed three times with PBS before they were cut out from the Transwell inserts and placed in the wells of a 24-well plate. The membranes were then blocked and stained as described above. Nuclei counts were made using ImageJ[101]. For whole tissue immunostaining, mouse colons were harvested and prepared as previously described[102].

Gene expression analysis. RNA was isolated from cells in the Transwells on day three after seeding using the NucleoSpin RNA II isolation kit (Macherey-Nagel; Bethlehem, PA). Complementary DNA (cDNA) synthesis was performed using 0.2 μg of RNA and the SuperScript III reverse transcriptase (Life Technologies). Quantitative PCR reactions (qPCR) were performed with SYBR Advantage qPCR Premix (Clontech; Mountain View, CA). Expression levels were determined in triplicate per sample and normalized to the expression of glyceraldehyde 3-phosphate dehydrogenase (Gapdh). Primers used include: Gapdh for 5'-AGG TCG GTG TGA ACG GAT TTG-3', Gapdh rev 5'- TGT AGA CCA TGT AGT TGA GGT CA-3', pIgR for 5'-ATG AGG CTC TAC TTG TTC ACG C-3', pIgR rev 5'-CGC CTT CTA TAC TAC TCA CCT CC-3', Villin1 for 5'-ATG ACT CCA GCT GCC TTC TCT-3', Villin1 rev 5'-GCT CTG GGT TAG AGC TGT AAG-3', Reg3g for 5'-CATCAACTGGGAGACGAATCC-3', Reg3g rev 5'-CAGAAATCCTGAGGCTCTTGACA-3', Muc2 for 5'-ATG CCC ACC TCC TCA AAG AC-3', Muc2 rev 5'-GTA GTT TCC GTT GGA ACA GTG AA-3', Atoh1 for 5'-GAG TGG GCT GAG GTA AAA GAG T-3', and Atoh1 rev 5'-GGT CGG TGC TAT CCA GGA G-3'.

RESULTS

Developing a Transwell system for mouse primary intestinal epithelial cells

A critical roadblock to understanding intestinal physiology has been the lack of an experimental system to model primary intestinal epithelial cells as a polarized, confluent monolayer. The use of primary cells is of interest due to the differentiation potential of these cells *in vitro*[82] as well as the need to evaluate cells from genetically modified mice. It has been challenging to adapt primary intestinal epithelial cells to Transwell culture as monolayers because this technique requires substantial numbers of viable cells.

We have solved this problem using an *in vitro* experimental system that allowed for significant expansion of intestinal epithelial stem/progenitor cells[83,84]. To obtain cells for a single Transwell, we harvested colonic spheroids from three wells (400-500 spheroids/well) of a 24-well plate that were cultured as spheroids for three days in Matrigel using 50% L-WRN (L-cells expressing Wnt3a, R-spondin3, and Noggin) conditioned media (CM). This produced ~$5x10^5$ cells that were seeded onto a single 0.33 cm^2 Transwell insert of a 24-well plate. Typically this cell input created a monolayer of ~$2.5x10^5$ cells. At the time of seeding cells in Transwells, we used 50% L-WRN CM that also contained 10 μM of the ROCK inhibitor Y-27632 (**Figure 2.1**). The media was maintained for one day post-seeding.

On day one after seeding, the 50% CM was replaced with 0% CM supplemented with or without specific treatments that were designed to facilitate the study of IgA transcytosis. The treatment included a combination of the γ-secretase inhibitor DAPT to differentiate the cells[103,104], and LPS to induce the expression of pIgR (which is known to be regulated by microbial and/or cytokine signaling)[31]. The cells were treated for two days in this media prior to

evaluation for differentiation by histology and gene expression analysis, as well as functional assays such as IgA transcytosis.

We next evaluated the effects of DAPT+LPS on differentiation and lineage allocation of primary epithelial monolayers. Cells were fixed on the Transwell membrane, which was then cut out of the insert and processed for paraffin embedding. Histologic sections were cut and stained with hematoxylin and eosin. We observed that both untreated and DAPT+LPS-treated cells showed a single layer of cells overlying the Transwell membrane (**Figure 2.2a**). To confirm that differentiation of enterocytes occurred both with and without DAPT+LPS treatments, we performed immunostaining using antisera against ZO-1 and Villin (**Figure 2.2b,c**). ZO-1 is a tight junction marker[105] and Villin1 marks microvilli[106]. In addition, both of these proteins showed appropriate apical localization throughout the monolayer and this pattern was present regardless of treatment. We also found that a basolateral marker, CD138, showed appropriate localization in Transwell cultures (**Figure 2.2d**). Taken together, the localization of these markers is consistent with polarized epithelial cells. We stained for markers of additional colonic epithelial lineages including enteroendocrine cells (chromogranin A[107]) and goblet cells (lectin UEA-1[108]). Whole mount images of immunostained Transwells showed that both of these cell types were present in DAPT+LPS-treated monolayers with lower fractional representation than absorptive enterocytes (**Figure 2.3**). This lineage allocation is similar to what is observed *in vivo* for the surface epithelium of the mouse colon (**Figure 2.4**).

To adapt this experimental system for the study of IgA transcytosis, we evaluated the expression of pIgR both *in vivo* and *in vitro*. The colonic epithelium, including surface epithelial cells, expressed pIgR *in vivo* (**Figure 2.5**). *In vitro*, pIgR could be induced in epithelial monolayers that were treated with DAPT+LPS, as shown by immunostaining (**Figure 2.2e**). To

quantify the relative effects of DAPT and LPS on pIgR expression, we performed qRT-PCR of mRNAs isolated from epithelial cells grown on Transwells for three days. The addition of DAPT+LPS stimulated a robust increase in pIgR mRNA expression compared to untreated cells (~100-fold increase) (**Figure 2.6**). This finding corroborated the effects of DAPT+LPS on protein expression as determined by immunostaining (**Figure 2.2e**). Single treatment with either LPS or DAPT did not stimulate pIgR mRNA expression to the extent that was achieved by the combination of these factors. As a positive control for LPS treatment, expression of RegIIIγ[109] was increased after DAPT+LPS treatment (**Figure 2.7a**). As a negative control, Villin1 expression (which is not microbially regulated *in vivo*[110]) was similar in all groups of treated and untreated cells (**Figure 2.7b**). Thus, we were able to show that wild-type primary colonic epithelial cells on Transwells were responsive to DAPT+LPS.

To perform IgA transcytosis experiments, a complete monolayer of cells is required. To demonstrate that the seeded cells formed a functional monolayer, we measured transepithelial electrical resistance (TER) in the Transwells on day three (**Figure 2.8**). For this experiment, we used cells at a density of ~$2.5x10^5$ cells/0.33 cm^2. The average TER of untreated cells was 3333 Ωcm^2. The TER of DAPT+LPS-treated cells was similar to the TER of untreated cells (2877 Ωcm^2).

Developing an IgA transcytosis assay using primary mouse Transwell cultures

One of the critical functions of the intestinal epithelium is the transcytosis of IgA from the lamina propria to the lumen of the intestine. This process involves pIgR trafficking across the intestinal epithelium which can occur at a slower rate in the absence of IgA[25]. To determine if the primary intestinal epithelial monolayers were capable of IgA transcytosis, we developed an assay

utilizing these cells. At day three post-plating on Transwell inserts, the cells were washed and placed in wells containing normal mouse IgA in the lower compartment (**Figure 2.9a**). This media is in contact with the basolateral surface of the epithelial monolayer. Media alone was added to the upper compartment (apical surface). The cells were incubated at 37°C for different periods of time to allow for receptor binding and transcytosis to occur before the media in the upper compartment was sampled for analysis by enzyme-linked immunosorbent assay (ELISA) (**Figure 2.9b**). Colonic cells isolated from *pIgR*$^{-/-}$ mice were used as a negative control for all transcytosis experiments.

Consistent with the pIgR mRNA expression data, cells treated with DAPT+LPS showed measurable IgA in the apical media whereas the other three groups (untreated, DAPT alone, and LPS alone) had levels at or below the limit of detection (**Figure 2.10**). Apical media from *pIgR*$^{-/-}$ cells did not contain IgA regardless of treatment. This genetic control indicated that IgA is actively transported through epithelial cells and does not use paracellular transport.

To determine the optimal conditions for transcytosis experiments, we performed IgA dose curve and time course experiments using DAPT+LPS-treated cells. One hour after the addition of IgA to the basal compartment, no IgA was detected in the apical media (**Figure 2.11**). Therefore, one hour was not sufficient for IgA in the basal compartment to bind pIgR and transcytose across cells to the apical compartment. This result also showed that the monolayer was intact and thus did not allow the IgA to freely diffuse into the apical media. Because of this result, we utilized the one hour time point as an additional internal control in all subsequent experiments. Additional time points were taken three hours (four hours after the addition of IgA) and six hours later (ten hours after the addition of IgA). Both of these time points showed

progressively higher levels of IgA in the apical media (**Figure 2.11**). In subsequent experiments, all three of these time points were evaluated.

In choosing the optimal dose of IgA, the amount of IgA in the apical compartment at three and six hour time points needed to be in linear range of the ELISA. We initially used normal mouse IgA from Santa Cruz Biotechnology at a dose of 40 µl/well (**Figure 2.12a**). In later experiments, we used normal mouse IgA from BD Pharmingen at a comparable dose, which allowed for a more precise measurement of IgA concentration and decreased variability between experiments (**Figure 2.12b**). For this source of IgA, we were able to calculate the IgA concentration used to 5 µg/ml, or a total of 3 µg/well.

As it was unclear how sensitive primary wild-type colonic epithelial cells were to LPS, we performed a dose-response curve for LPS using both IgA transcytosis and pIgR expression as readouts (**Figure 2.13**). Both transcytosis and pIgR mRNA expression responded in a dose-dependent manner. In all subsequent experiments, we used 1 µg/ml LPS as this was in linear range of the response of wild-type cells.

Although LPS has been used as a standard in the field to efficiently induce pIgR expression in different cell types, there is growing interest in the study of the effects of specific microbes in the intestine and how they stimulate IgA[32-34,39,111]. To model an example of such host-microbial interactions *in vitro*, cells were treated with heat-killed *E. coli* to analyze its ability to induce IgA transcytosis and pIgR expression (**Figure 2.14**). A dose equivalent to 10^7 CFU/ml *E. coli* was found to induce similar levels of IgA transcytosis and pIgR expression as that demonstrated for to 1 µg/ml LPS.

Cell density affects IgA transcytosis and pIgR expression in Transwell cultures

We noticed that there was occasional experiment-to-experiment variability of the amount of IgA transcytosed. Further scrutiny of the Transwells utilized in these experiments led us to hypothesize that the cellular density plays a role in the level of IgA transcytosis *in vitro*. To test this idea, we performed two-fold serial dilutions of the cells seeded in the Transwells (**Figure 2.15a**). Both the undiluted (using ~$5x10^5$ cells as above) and a 1:2 dilution showed similar amounts of transcytosed IgA. However, a 1:4 dilution reproducibly showed significantly less transcytosed IgA. Furthermore, apical media collected from a 1:8 dilution showed IgA at levels below the limit of detection. This result suggested that there was an intact monolayer at this cell density but no detectable IgA was transcytosed. At a 1:16 dilution, we could not reproducibly achieve a monolayer, as in some experiments, IgA was readily detected in the apical compartment at levels similar to the basolateral chamber. TER measurements corroborated these findings. Higher cell densities all showed resistance values of >2500 Ωcm2 (**Figure 2.15b**). The TER for the 1:8 cell dilution was more variable, with average values of ~1240 Ωcm2. The TER for the 1:16 dilution was near baseline values.

The cell density was quantified for each dilution by nuclei counts of whole mount images of bis-benzimide-stained Transwell membranes (**Figure 2.16**). A 1:2 dilution of input cells resulted in only a small change in the number of seeded cells on the Transwell, indicating that maximum cell numbers were seeded at these two input densities. Each successive two-fold dilution showed a ~two-fold decrease in cell density. We next tested whether the correlation of cell density to IgA transcytosis was due to cell number and/or pIgR expression. Co-staining of cells with anti-pIgR antisera showed detectable staining in the majority of cells in Transwells with higher cell densities (no dilution, 1:2 and 1:4). We observed a substantial decrease in the

number of cells that were positive for pIgR in 1:8 dilution samples. There was no detectable staining for pIgR in the 1:16 dilution samples. To confirm this observation, we performed gene expression analysis for pIgR at each dilution (**Figure 2.17**). The highest relative expression of pIgR was observed at the 1:2 and 1:4 dilution samples. We observed a threshold effect whereby pIgR expression was substantially lower in the 1:8 and 1:16 dilution samples. Our interpretation is that the decrease in IgA transcytosis that occurred between the 1:2 and the 1:4 dilutions is likely due to changes in cell density while the decrease in IgA trancytosis in the 1:8 dilution is likely further driven by diminished pIgR expression. One other possibility is that global differentiation is altered by decreased density. We found that markers of secretory lineages (Muc2 and Atoh1) were diminished in a density-dependent manner while a general marker of epithelial cells (Vil1) was not altered (**Figure 2.18**).

Cytokines induce pIgR expression and IgA transcytosis in the primary Transwell cultures

Several different cytokines were previously shown to induce pIgR expression in tumor cell lines including IL-1β, TNFα, IFNγ, and most recently, IL-17[19,36,38,95-98]. We wanted to test if primary intestinal epithelial cells responded similarly to these cytokines, and if so, what was the relative potency. To do this, we performed a dose titration using these four cytokines with IgA transcytosis and pIgR expression as readouts (**Figure 2.19-2.21**). IL-17 was the most potent cytokine tested. A dose of 0.5 ng/ml resulted in higher levels of IgA transcytosis than LPS treatment (**Figure 2.19a**). IL-1β and TNFα were both significantly less potent than IL-17, as a 100 ng/ml dose of these cytokines only induced half the levels of IgA transcytosis as LPS (**Figure 2.20a, 2.21a**). Apical media from *pIgR*$^{-/-}$ cells at all doses of IL-1β, TNFα, and IL-17

contained no IgA (**Figure 2.19-2.21**). For all three of these cytokines the dose response curves for pIgR expression mirrored the IgA transcytosis (**Figure 2.19-2.21**).

Of note, the results for IFNγ treatment were distinct from that of the other cytokines as well as previously published literature using immortalized cell lines (**Figure 2.22**). At 0.1-1 ng/ml, the epithelial monolayer did not remain intact, as apical media from wild-type and *pIgR*$^{-/-}$ cells both contained IgA levels similar to the media in the lower compartment (**Figure 2.22a**). Furthermore, TER measurements of cytokine-treated cells showed no measureable resistance after IFNγ treatment while treatment with IL-1β, TNFα, and IL-17 showed comparable TER values with LPS-treated cells (**Figure 2.23**). At lower doses (0.001-0.01 ng/ml), less IgA was present in the apical media, however none of these conditions led to an increase of pIgR mRNA expression (**Figure 2.22b**). Our conclusion is that IgA uses a paracellular route in IFNγ-treated cells that could either be due to cell death or leaky junctions.

Colonic epithelial cells generated from *Tlr4*$^{-/-}$ mice show reduced IgA transcytosis and pIgR expression after LPS but not IL-17 treatment

One advantage of this system is the ability to isolate cells directly from different genetically modified mice for experiments. As a proof of principle, cells were harvested from *Tlr4*$^{-/-}$ mice to generate colonic spheroids. These cells lack the LPS receptor, Tlr4, and therefore should have a reduced response to LPS stimulation. As expected, IgA transcytosis and pIgR expression was reduced to ~50% of that of wild-type cells (**Figure 2.24**). The ability of these cells to respond to other stimuli for IgA transcytosis was not affected, as IL-17 treatment of the *Tlr4*$^{-/-}$ cells showed no difference from wild-type cells (**Figure 2.25**).

DISCUSSION

We have established a new method to grow primary intestinal epithelial cells in a functional monolayer. To do this, we adapted the previously established 3D primary intestinal epithelial stem cell culture system[83,84] to a 2D monolayer in a Transwell. The system we have developed has three important components. Firstly, the use of the L-WRN CM system allowed us to attain large cell numbers that are required to form monolayers in Transwells. Secondly, cells only needed to be grown in Matrigel culture for three days prior to recovery and seeding into Transwells. Lastly, seeded cells quickly formed polarized monolayers and demonstrated high TER values within three days. In contrast, previously established intestinal epithelial monolayer systems that utilize immortalized cell lines require as many as twenty days in culture to form differentiated, polarized monolayers[89-91].

This system will be useful for the study of many different physiologic processes. Here, we chose to focus on IgA transcytosis. For this process to occur, epithelial cells must express the IgA receptor pIgR, which has been shown to be regulated by microbial products[31]. LPS has been used as a standard in the field to induce pIgR expression *in vitro*. Typically immortalized cell lines have been used. Here we showed that LPS-treated primary intestinal epithelial cells were also able to induce pIgR expression. In addition, we found that maximal pIgR expression required DAPT treatment in addition to LPS, suggesting that the intestinal epithelial cells require differentiation for efficient pIgR expression. To demonstrate the robustness of primary intestinal epithelial cells for IgA transcytosis, we carefully analyzed several key factors including time, IgA dose, and LPS dose. We titrated the assay and chose to use 10 μM DAPT, 1 μg/ml LPS, and 5 μg/ml IgA as our optimal conditions. The time course of a typical experiment is 10 hours with multiple samples taken from each Transwell.

Interestingly, we found that cell density also affected IgA transcytosis. After recovery from the Matrigel, two-fold serial dilutions were made before seeding the cells in the Transwells. As it might be expected, we observed a cell density-dependent decrease in the amount of IgA transcytosed. However, this decrease in IgA was not just due to the decrease in cell number. Gene expression analysis of *pIgR* showed a substantial decrease at the lowest cell densities. Immunofluorescence staining for pIgR correlated with the mRNA expression data, showing fewer pIgR-positive cells at the lowest cell densities. We hypothesized the lower density cells may be in a less differentiated state, which has been shown in other *in vitro* cell systems[112-114]. We therefore tested the expression of other cell differentiation markers, including goblet cell marker *Muc2* and a secretory cell lineage marker *Atoh1*, and found both to show a correlation of expression with cell density. This suggests that cell-to-cell endogenous signaling, and not solely exogenous chemical stimuli, regulate colonic cell differentiation in this culture system.

While LPS robustly induces pIgR expression, it is difficult to translate *in vitro* quantities to the biomass of intestinal microbes that generate this molecule. To make this system more applicable to specific bacteria, we utilized heat-killed bacteria. We therefore treated the cells with heat-killed *E. coli* and found that a dose of 10^7 CFU/ml stimulated IgA transcytosis and pIgR expression to a similar extent as 1μg/ml LPS. We feel that this system will be useful for future studies looking at host-microbial interactions *in vitro*.

Previous studies found that several host cytokines including IL-1β, TNFα, IFNγ, and IL-17 play a role in pIgR expression[36,38,95-98]. Similar to what has been shown in immortalized cell lines, IL-1β, TNFα, and IL-17 showed a dose-dependent induction of pIgR expression, with IL-17 being the most potent inducer of IgA transcytosis and pIgR expression of these cytokines. However, an important difference we found between our primary mouse intestinal epithelial cells

and human cancer cell lines is the ability of IFNγ to induce pIgR expression. IFNγ treatment did not lead to pIgR expression or IgA transcytosis at any dose tested, and actually resulted in cell death at higher doses. This may be a result that would otherwise be obscured by using immortalized cell lines, which can be resistant to cytokine-induced cell death. Furthermore, this does not appear to be species-specific phenomenon, as the mouse promoter for pIgR is highly conserved to the human promoter and also contains the IRF1 binding site[115].

One final important advantage of this system is the ability to readily use primary intestinal epithelial cells taken from different genetically modified mice. In this study, we utilized cells obtained from available lines of knockout mice for the *pIgR* and *Tlr4* genes. Monolayers of epithelial cells derived from these mice allowed us to directly address questions using cells with complete loss-of-function, as compared to the usual incomplete loss of function with shRNA knockdowns.

Prospectus- In summary, we developed a new system to culture primary intestinal epithelial cells in monolayer culture. While we have highlighted the capability of this system to be utilized for studies of IgA transcytosis, there are many other experimental avenues where this system should prove to be useful. These areas include barrier function, host-microbial interactions and epithelial-immune/stromal cell interactions. We propose that not only will this system be useful for mechanistic studies, but also for large-scale chemical biology screens in these arenas.

Figure 2.1. Timeline for primary intestinal epithelial monolayer formation.

Schematic of timeline for Transwell experiments. Primary intestinal epithelial stem cells originally isolated from the colons of wild type mice were passaged and maintained in 3D spheroid cultures in Matrigel. To seed into Transwells (day zero), three-day old spheroids were recovered from Matrigel, trypsinized, and dissociated by vigorous pipetting. Cells were passed through a 40 μm cell strainer and re-suspended in 50% L-WRN CM containing 10 μM Y-27632. On day one post-seeding, cells were treated with +/- 10 μM DAPT +/- 1 μg/ml LPS and utilized on day three post-seeding for various assays.

Figure 2.1. Timeline for primary intestinal epithelial monolayer formation.

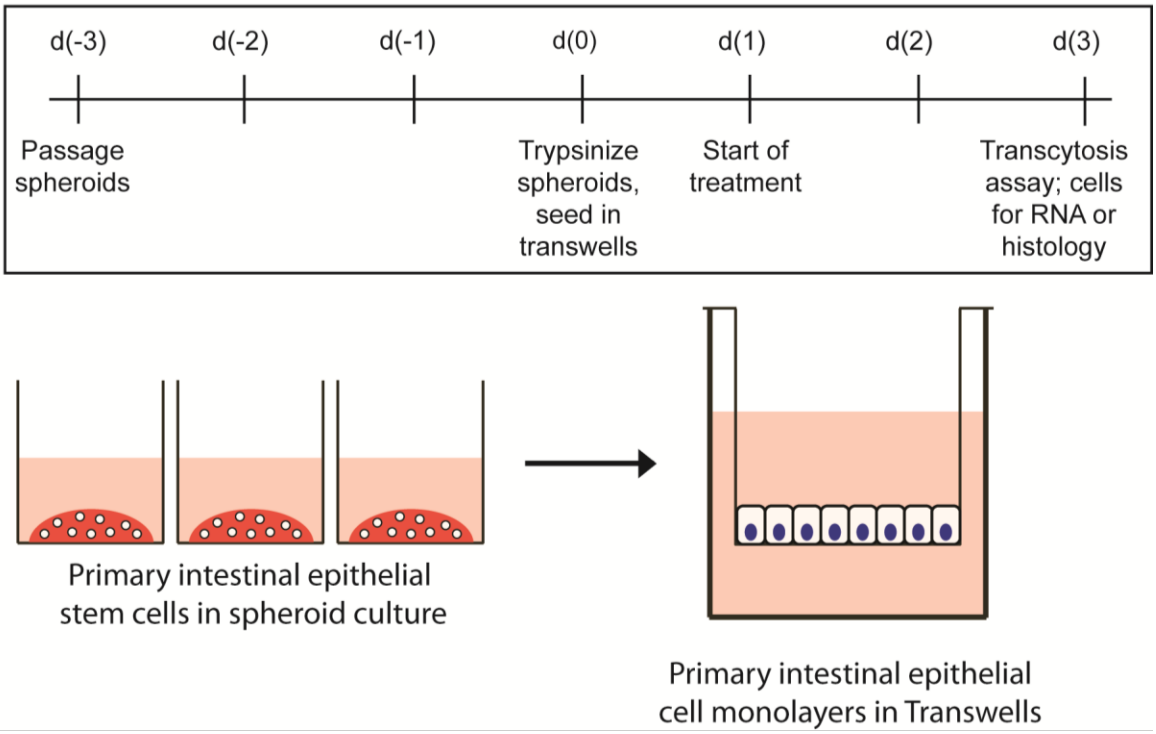

Figure 2.2. Primary IECs form a polarized monolayer that can be induced to express pIgR. Wild type cells were treated with +/- 10 μM DAPT +/- 1 μg/ml LPS and analyzed on day three post-seeding. Cells were fixed and paraffin-embedded on the transwell membranes. Sections were cut and stained with the following: **(a)** hematoxylin and eosin, **(b)** anti-ZO-1, **(c)** anti-villin, **(d)** anti-CD138, and **(e)** anti-pIgR. Bars = 50 μm. Representative images are shown.

Figure 2.2. Primary IECs form a polarized monolayer that can be induced to express pIgR.

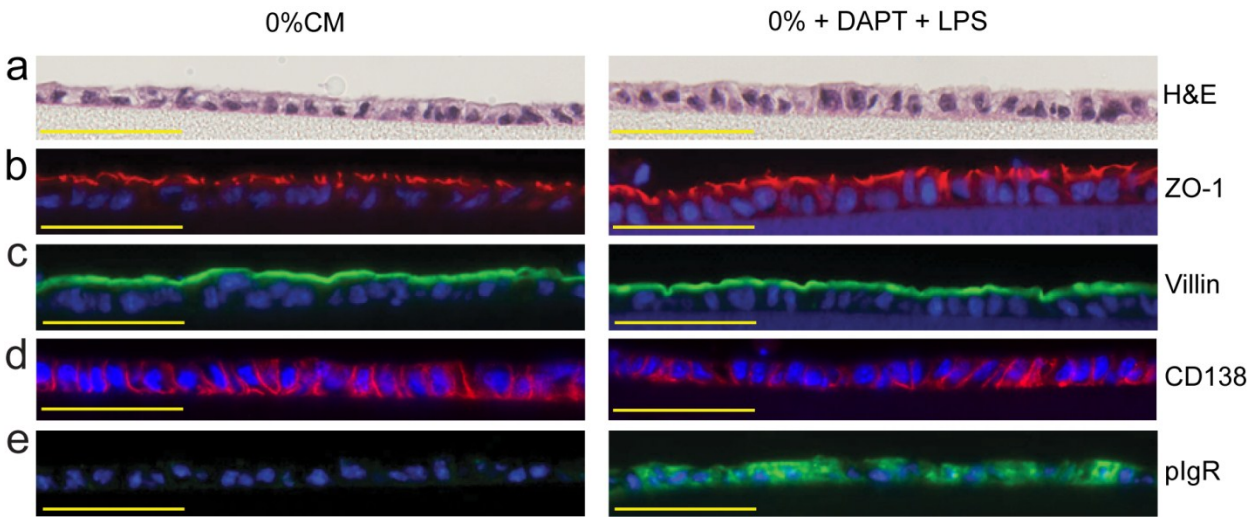

Figure 2.3. Primary IEC monolayers can differentiate into various cell types.

Wild type cells were treated with 10 μM DAPT and 1 μg/ml LPS and analyzed on day three post-seeding. Cells were fixed on the transwell membranes and stained for **(a)** Chromogranin A and **(b)** UEA-1 lectin (arrowheads). Representative whole mount images are shown.

Figure 2.3. Primary IEC monolayers can differentiate into various cell types.

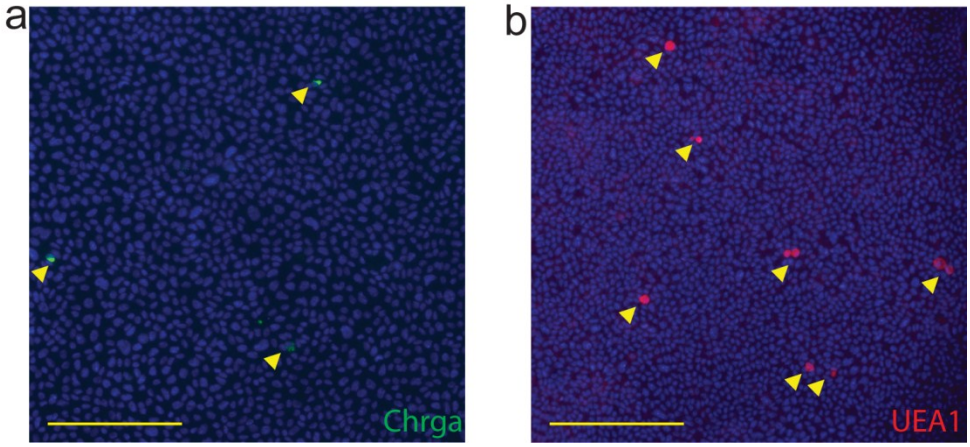

Figure 2.4. Primary IEC monolayers mirror *in vivo* staining patterns of the colonic surface epithelium.

Colons from wild type mice were harvested, bouins-fixed, and paraffin embedded. 5 μm histologic sections were cut and stained for **(a)** CD138, **(b)** chromogranin A, **(c)** UEA-1, **(d)** villin1, and **(e)** ZO-1. Bars = 200 μm. Yellow boxes denote area depicted in insets.

Figure 2.4. Primary IEC monolayers mirror *in vivo* staining patterns of the colonic surface epithelium.

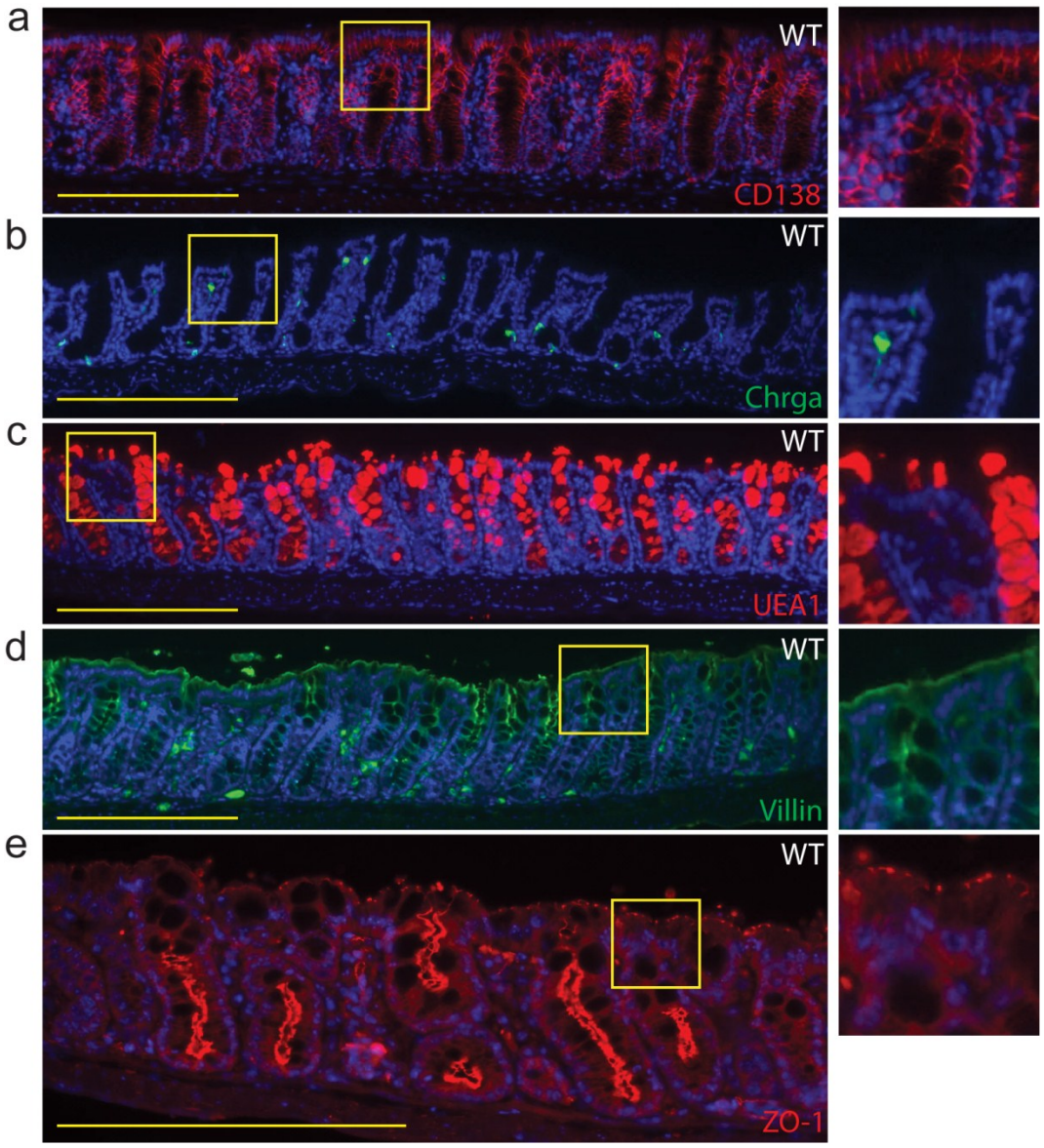

Figure 2.5. Colonic epithelial cells express pIgR *in vivo*.

Colons from **(a)** wild type mice or **(b)** *pIgR*$^{-/-}$ mice were harvested, bouins-fixed, and paraffin embedded. 5 μm histologic sections were cut and stained for pIgR. Bars = 200 μm. Yellow boxes denote area depicted in insets.

Figure 2.5. Colonic epithelial cells express pIgR *in vivo*.

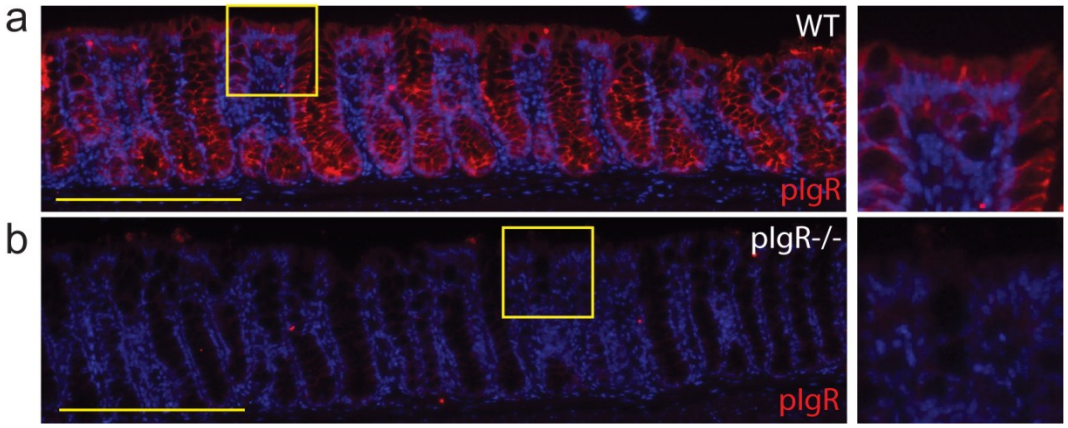

Figure 2.6. Primary IEC monolayers express pIgR mRNA *in vitro*.

Wild type cells were treated with +/- 10 μM DAPT +/- 1 μg/ml LPS and analyzed on day three post-seeding. Gene expression analysis was performed by qRT-PCR for pIgR. All samples were normalized to Gapdh mRNA, and data were presented as fold change relative to untreated (0% CM) cells (mean ± s.e.m.; $n \geq 3$ per condition). One-way ANOVA: $F = 96.02$, $P < 0.0001$. Means with different letters are significantly different by Bonferroni's multiple comparison test

Figure 2.6. Primary IEC monolayers express pIgR mRNA *in vitro*.

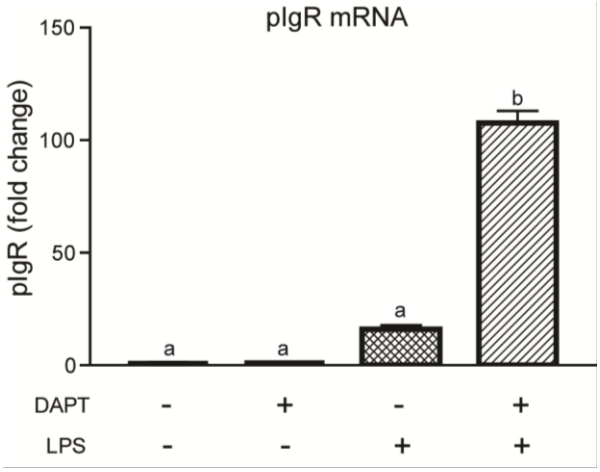

Figure 2.7. Primary IEC monolayers express Reg3g and Vil1 mRNA *in vitro*.

Wild type cells were treated with +/- 10 μM DAPT +/- 1 μg/ml LPS and analyzed on day three post-seeding. Gene expression analysis was performed by qRT-PCR for **(a)** Reg3g, and **(b)** Vil1. All samples were normalized to Gapdh mRNA, and data were presented as fold change relative to untreated (0% CM) cells (mean ± s.e.m.; $n \geq 3$ per condition). One-way ANOVA: **(a)** $F = 3.441$, $P < 0.0376$; **(b)** $F = 1.085$, $P < 0.3762$.

Figure 2.7. Primary IEC monolayers express Reg3g and Vil1 mRNA *in vitro*.

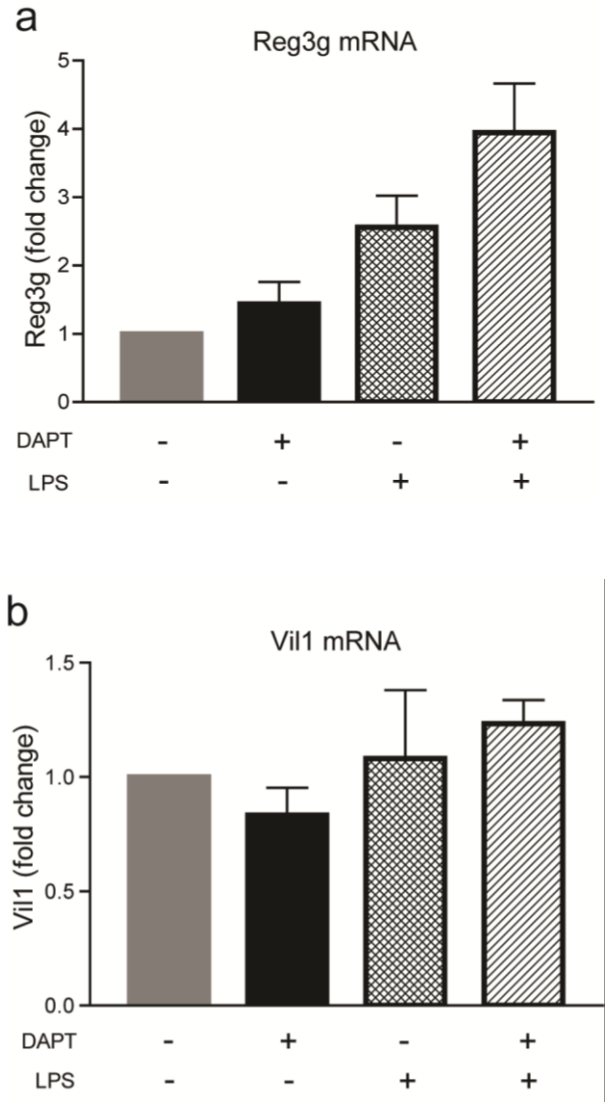

Figure 2.8. Primary IEC monolayers show robust transepithelial electrical resistance.

Wild type cells were treated with +/- 10 μM DAPT +/- 1 μg/ml LPS. Transepithelial electrical resistance was measured on day three post seeding. The (resistance x area) is shown for each condition (mean ± s.e.m., n = 6 per group). Statistical analysis by Student's t-test showed no significant difference between the two groups ($P < 0.4362$).

Figure 2.8. Primary IEC monolayers show robust transepithelial electrical resistance.

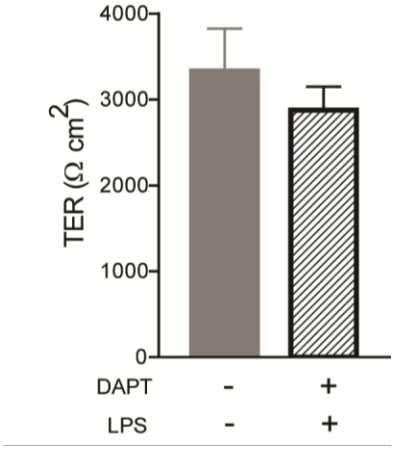

Figure 2.9. Schematic for IgA transcytosis assay.

Wild type and *pIgR*$^{-/-}$ cells were seeded in Transwells and treated with +/- 10 μM DAPT +/-1 μg/ml LPS as indicated. On day three post-seeding, 40 μl of normal mouse IgA (Santa Cruz) was added to the lower compartment of the Transwells **(a)**, and supernatants from the upper compartment were taken at six hours for the detection of IgA by ELISA **(b)**.

Figure 2.9. Schematic for IgA transcytosis assay.

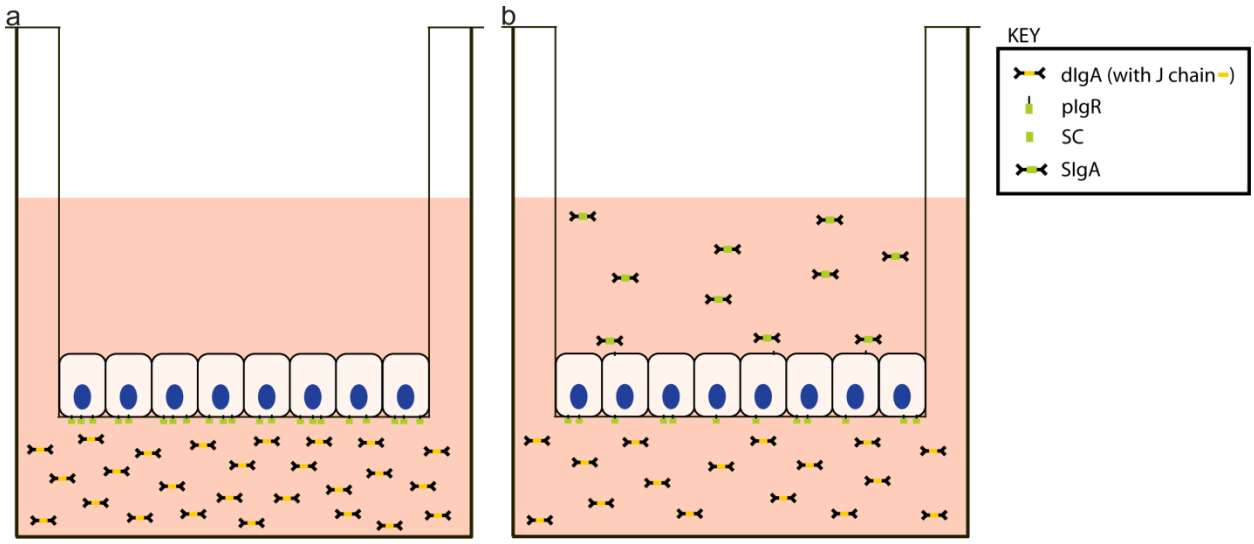

Figure 2.10. IgA transcytosis by primary IEC monolayers mirrors pIgR expression.

Wild type and *pIgR*$^{-/-}$ cells were seeded in Transwells and treated with +/- 10 μM DAPT +/-1 μg/ml LPS as indicated. On day three post-seeding, 40 μl of normal mouse IgA (Santa Cruz) was added to the lower compartment of the Transwells, and supernatants from the upper compartment were taken at six hours for the detection of IgA by ELISA. The dotted lines represent the limit of detection by the ELISA. All values are indicated as mean ± s.e.m. One-way ANOVA: $F = 573.3$, $P < 0.0001$, $n \geq 3$ per group. Means with different letters are significantly different by Bonferroni's multiple comparison test. N.D. = not detected.

Figure 2.10. IgA transcytosis by primary IEC monolayers mirrors pIgR expression.

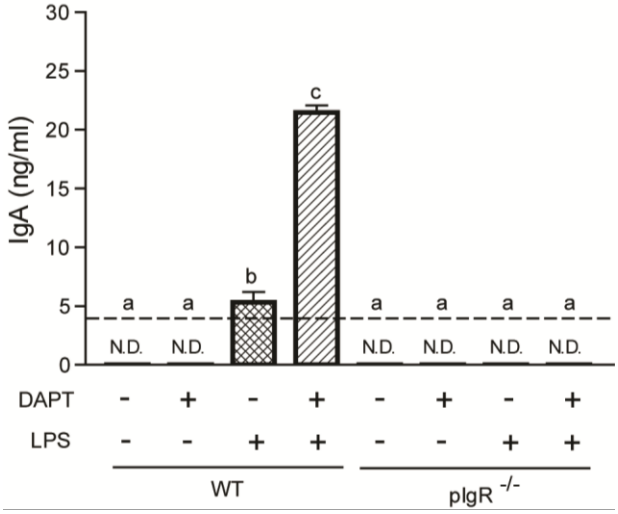

Figure 2.11. IgA transcytosis time course by primary IEC monolayers.

Wild type and *pIgR*$^{-/-}$ cells were seeded in Transwells and treated with +/- 10 μM DAPT +/-1 μg/ml LPS as indicated. On day three post-seeding, 40 μl of normal mouse IgA (Santa Cruz) was added to the lower compartment of the Transwells, and supernatants from the upper compartment were taken at various time points for the detection of IgA by ELISA. The dotted lines represent the limit of detection by the ELISA. All values are indicated as mean ± s.e.m. One-way ANOVA: $F = 539.2$, $P < 0.0001$, $n \geq 12$ per group. Means with different letters are significantly different by Bonferroni's multiple comparison test. N.D. = not detected.

Figure 2.11. IgA transcytosis time course by primary IEC monolayers.

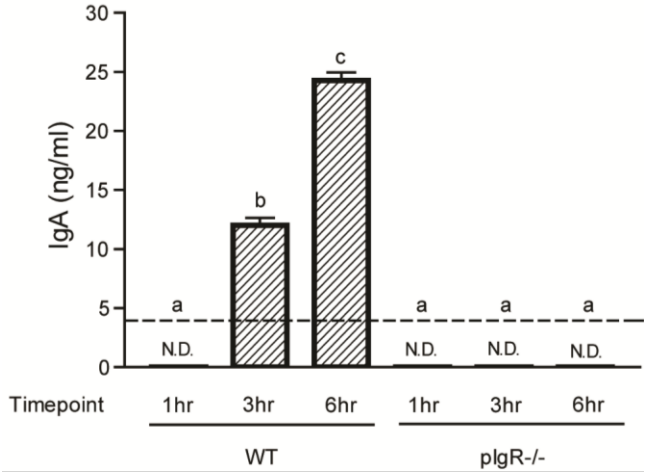

Figure 2.12. Determining the optimal IgA concentration for IgA transcytosis.

Wild type and *pIgR*$^{-/-}$ cells were seeded in Transwells and treated with +/- 10 μM DAPT +/-1 μg/ml LPS as indicated. On day three post-seeding, various concentrations of normal mouse IgA was added to the lower compartment of the Transwells, and supernatants from the upper compartment were taken at three and/or six hours for the detection of IgA by ELISA. The dotted lines represent the limit of detection by the ELISA. **(a)** Normal mouse IgA from Santa Cruz Biotechnology was evaluated, and 40 μl/well was chosen for experiments. **(b)** Determining a comparable IgA dose from BD Pharmingen.

Figure 2.12. Determining the optimal IgA concentration for IgA transcytosis.

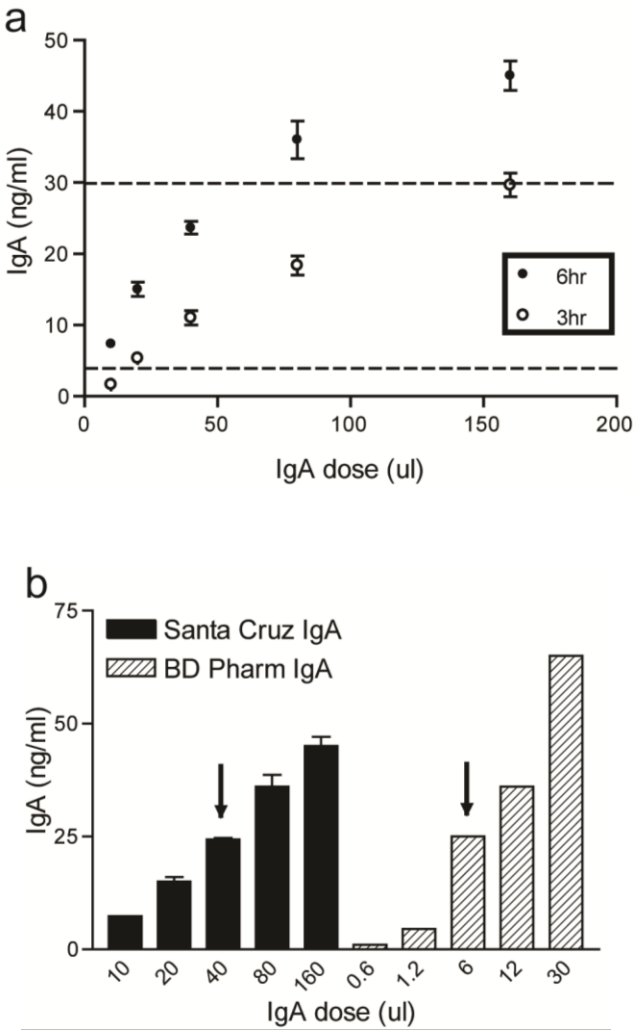

Figure 2.13. Determining the optimal LPS concentration for IgA transcytosis.

An LPS dose curve was performed on WT and *pIgR*$^{-/-}$ cells to determine whether IgA transcytosis **(a)** and pIgR expression **(b)** were dose dependent. All LPS-treated cells were also treated with 10 μM DAPT. For IgA transcytosis, results from the ELISA were normalized to the 1 μg/ml LPS treatment group (= 100%). Gene expression analysis by qRT-PCR for pIgR was performed by normalizing to Gapdh, and data are presented as fold change relative to untreated cells. The dotted lines represent the limit of detection by the ELISA. All values are indicated as mean ± s.e.m. One-way ANOVA: **(a)** $F = 675.7$, $P < 0.0001$, $n \geq 3$ per group; **(b)** $F = 46.22$, $P < 0.0001$, $n \geq 6$ per group. Means with different letters are significantly different by Bonferroni's multiple comparison test. N.D. = not detected.

Figure 2.13. Determining the optimal LPS concentration for IgA transcytosis.

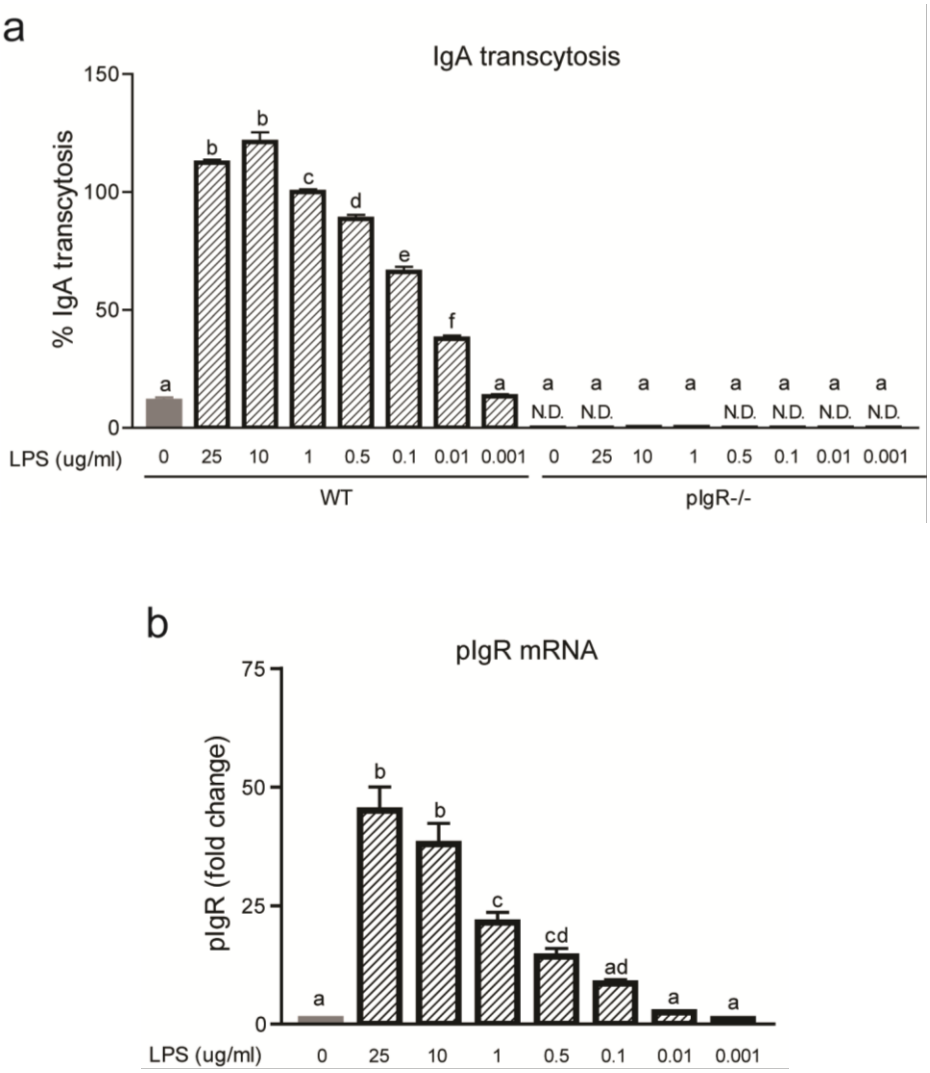

Figure 2.14. Heat-Killed *E.coli* can induce IgA transcytosis and pIgR expression.

Wild type and *pIgR*$^{-/-}$ cells were seeded in Transwells and treated with 10 μM DAPT and 1 μg/ml LPS or 10^7 CFU/ml heat-killed *E.coli* as indicated. **(a)** IgA transcytosis was analyzed by ELISA, and results were normalized to the WT+DAPT+LPS group (= 100%). **(b)** Gene expression analysis by qRT-PCR of pIgR was performed and all samples were normalized to Gapdh. Data are presented as fold change relative to untreated (0% CM) cells. All values are indicated as mean ± s.e.m. One-way ANOVA: **(a)** $F = 426.2$, $P < 0.0001$, $n \geq 6$ per group, means with different letters are significantly different by Bonferroni's multiple comparison test; **(b)** $F = 11.47$, $P < 0.0008$, $n \geq 5$ per group. Means with different letters are significantly different by Bonferroni's multiple comparison test. N.D. = not detected.

Figure 2.14. Heat-Killed *E.coli* can induce IgA transcytosis and pIgR expression.

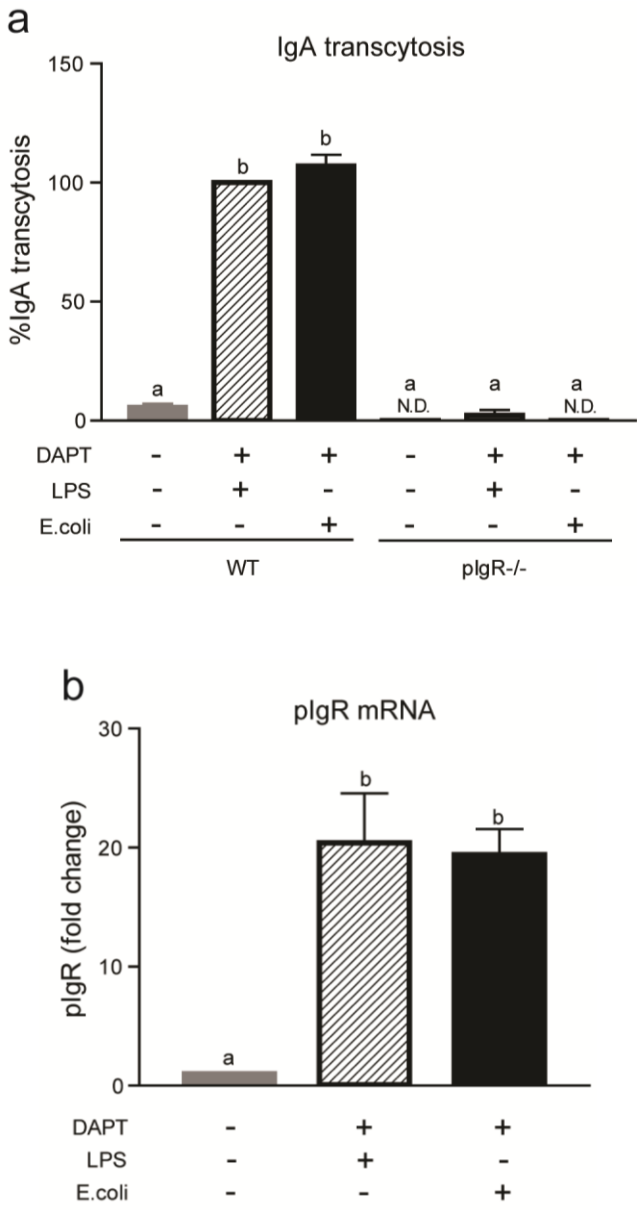

Figure 2.15. Cell density affects IgA transcytosis and monolayer formation.

Two-fold serial dilutions of wild type cells were seeded into Transwells and treated with 10 μM DAPT and 1 μg/ml LPS. **(a)** IgA transcytosis was performed on day three post-seeding, and measurement of IgA in the supernatants at the six hour time point is shown. The dotted lines represent the limit of detection by the ELISA. All values are indicated as mean ± s.e.m. One-way ANOVA: **(a)** $F = 53.11$, $P < 0.0001$, $n \geq 6$ per group. Means with different letters are significantly different by Bonferroni's multiple comparison test. **(b)** Transepithelial electrical resistance was measured on day three. The (resistance x area) is shown for each condition (mean ± s.e.m., n > 4 per group). N.D. = not detected.

Figure 2.15. Cell density affects IgA transcytosis and monolayer formation.

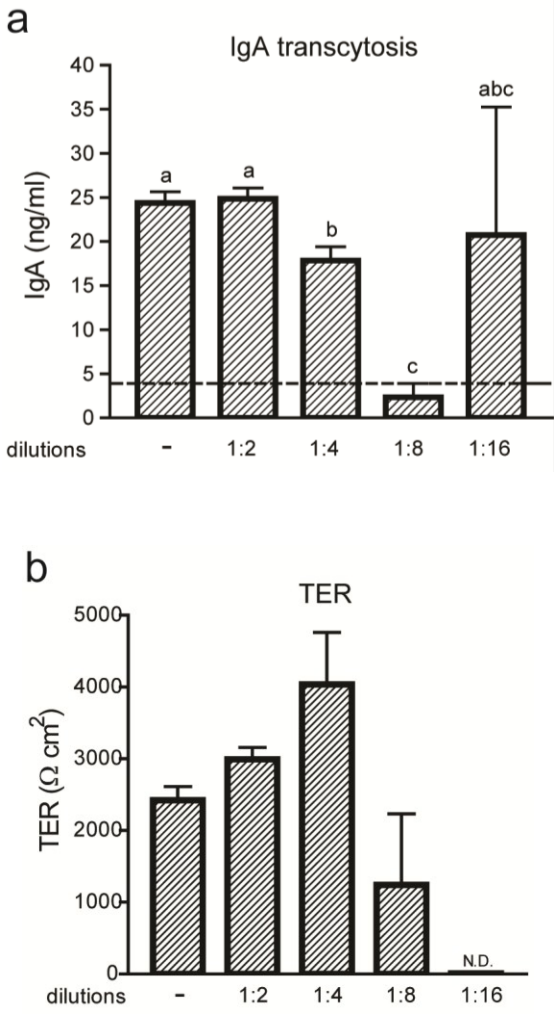

Figure 2.16. Cell density affects pIgR protein expression.

Two-fold serial dilutions of wild type cells were seeded into Transwells and treated with 10 μM DAPT and 1 μg/ml LPS. Cells were fixed and stained on the Transwell membranes **(a)** with anti-pIgR (green) and bis-benzamide dye (blue). Bars = 200 μm. **(b)** Quantification of cell density of cells on Transwells was performed using ImageJ software. All values are indicated as mean ± s.e.m. One-way ANOVA: **(b)** $F = 183.2$, $P < 0.0001$, $n \geq 15$ per group. Means with different letters are significantly different by Bonferroni's multiple comparison test.

Figure 2.16. Cell density affects pIgR protein expression.

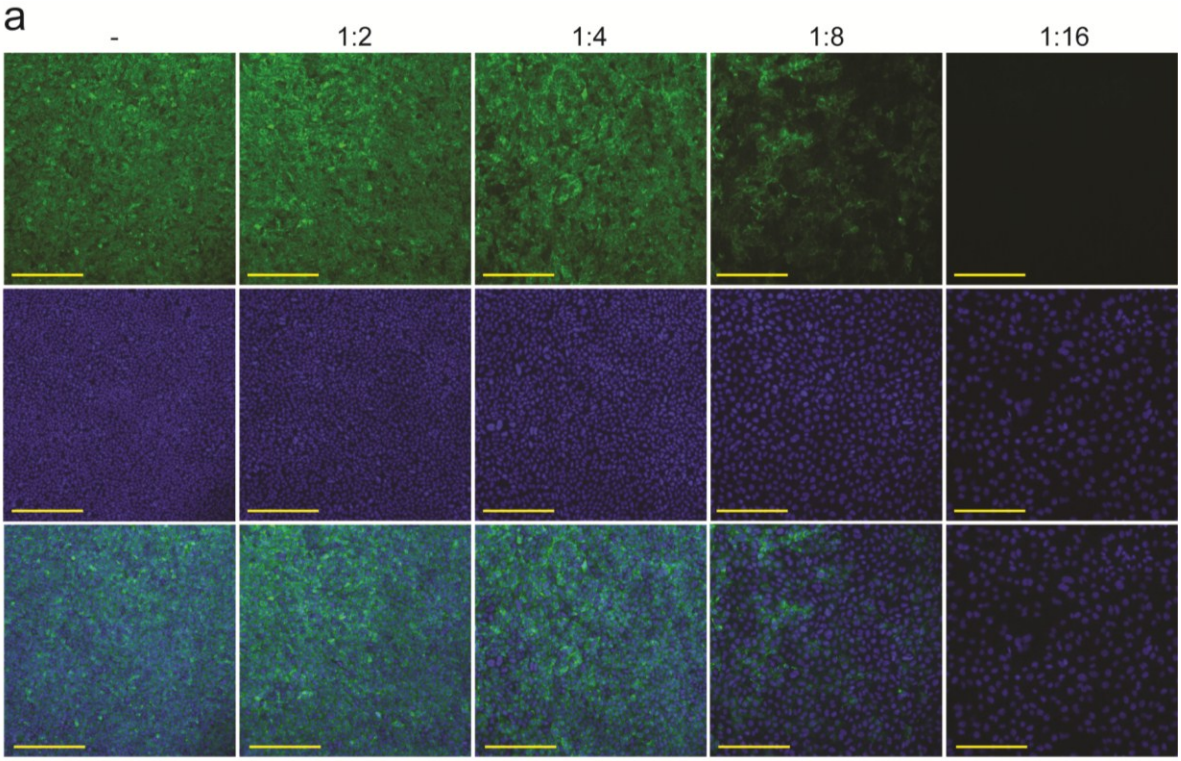

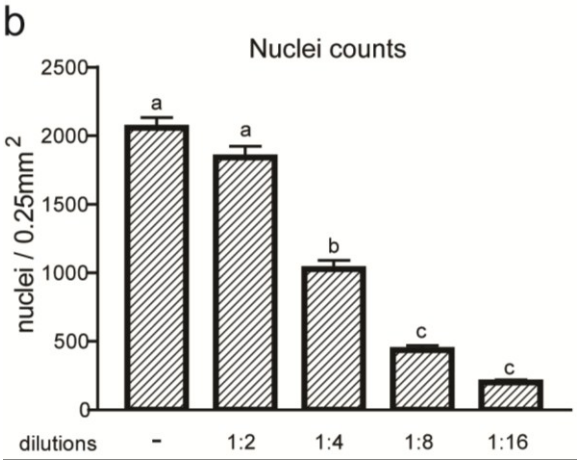

Figure 2.17. Cell density affects pIgR mRNA expression.

Two-fold serial dilutions of wild type cells were seeded into Transwells and treated with 10 μM DAPT and 1 μg/ml LPS. Gene expression analysis was performed by qRT-PCR for pIgR. All samples were normalized to Gapdh, and data are presented as fold change relative to untreated (0% CM) cells. All values are indicated as mean ± s.e.m. One-way ANOVA: $F = 39.02$, $P < 0.0001$, $n \geq 3$ per group. Means with different letters are significantly different by Bonferroni's multiple comparison test.

Figure 2.17. Cell density affects pIgR mRNA expression.

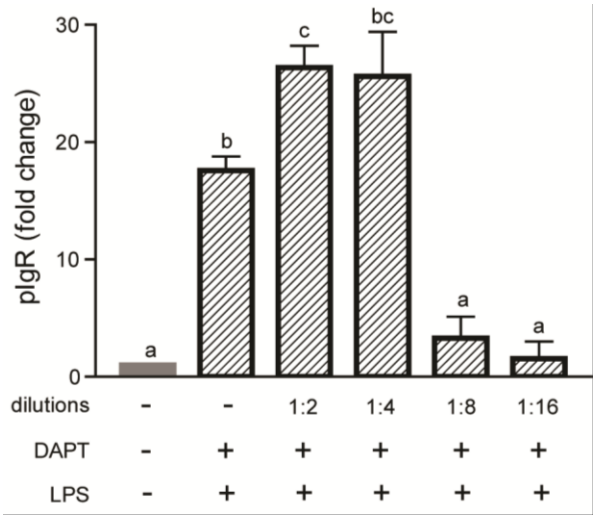

Figure 2.18. Cell density affects intestinal epithelial monolayer differentiation.

Two-fold serial dilutions of wild type cells were seeded into Transwells and treated with 10 μM DAPT and 1 μg/ml LPS. Gene expression analysis was performed by qRT-PCR for **(a)** Muc2, **(b)** Atoh1, and **(c)** Vil1. All samples were normalized to Gapdh, and data are presented as fold change relative to untreated (0% CM) cells. All values are indicated as mean ± s.e.m. One-way ANOVA: **(a)** $F = 11.07$, $P < 0.0001$, $n \geq 3$ per group; **(b)** $F = 3.436$, $P < 0.0183$, $n \geq 3$ per group; **(c)** $F = 2.186$, $P < 0.0894$, $n \geq 3$ per group. Means with different letters are significantly different by Bonferroni's multiple comparison test.

Figure 2.18. Cell density affects intestinal epithelial monolayer differentiation.

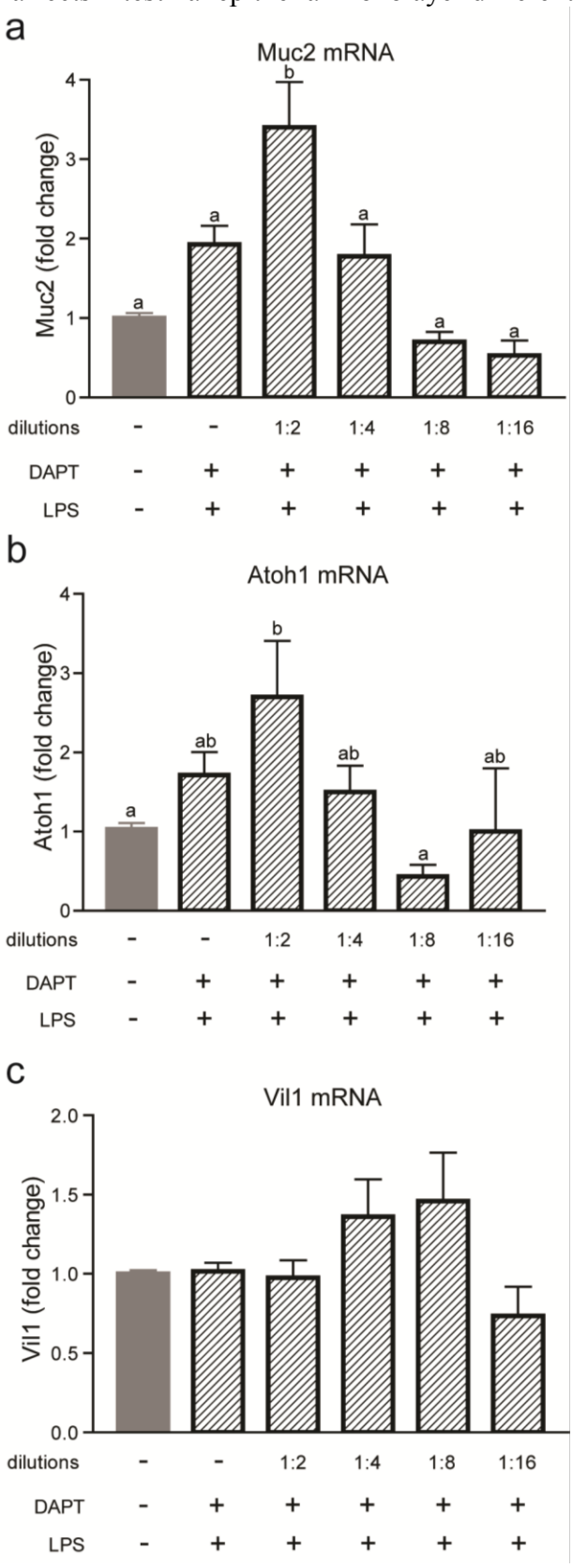

Figure 2.19. IL-17 robustly induces IgA transcytosis and pIgR expression.

Wild type and *pIgR*$^{-/-}$ cells were treated with 10 μM DAPT and varying doses of IL-17. **(a)** IgA transcytosis was analyzed by ELISA, and results were normalized to the WT+DAPT+LPS group (= 100%). **(b)** Gene expression analysis of pIgR was performed and all samples were normalized to Gapdh. Data are presented as fold change relative to untreated (0% CM) cells. All values are indicated as mean ± s.e.m. One-way ANOVA: **(a)** $F = 152.3$, $P < 0.0001$, $n \geq 3$ per group; **(b)** $F = 119.5$, $P < 0.0001$, $n \geq 4$ per group. Means with different letters are significantly different by Bonferroni's multiple comparison test. N.D. = not detected.

Figure 2.19. IL-17 robustly induces IgA transcytosis and pIgR expression.

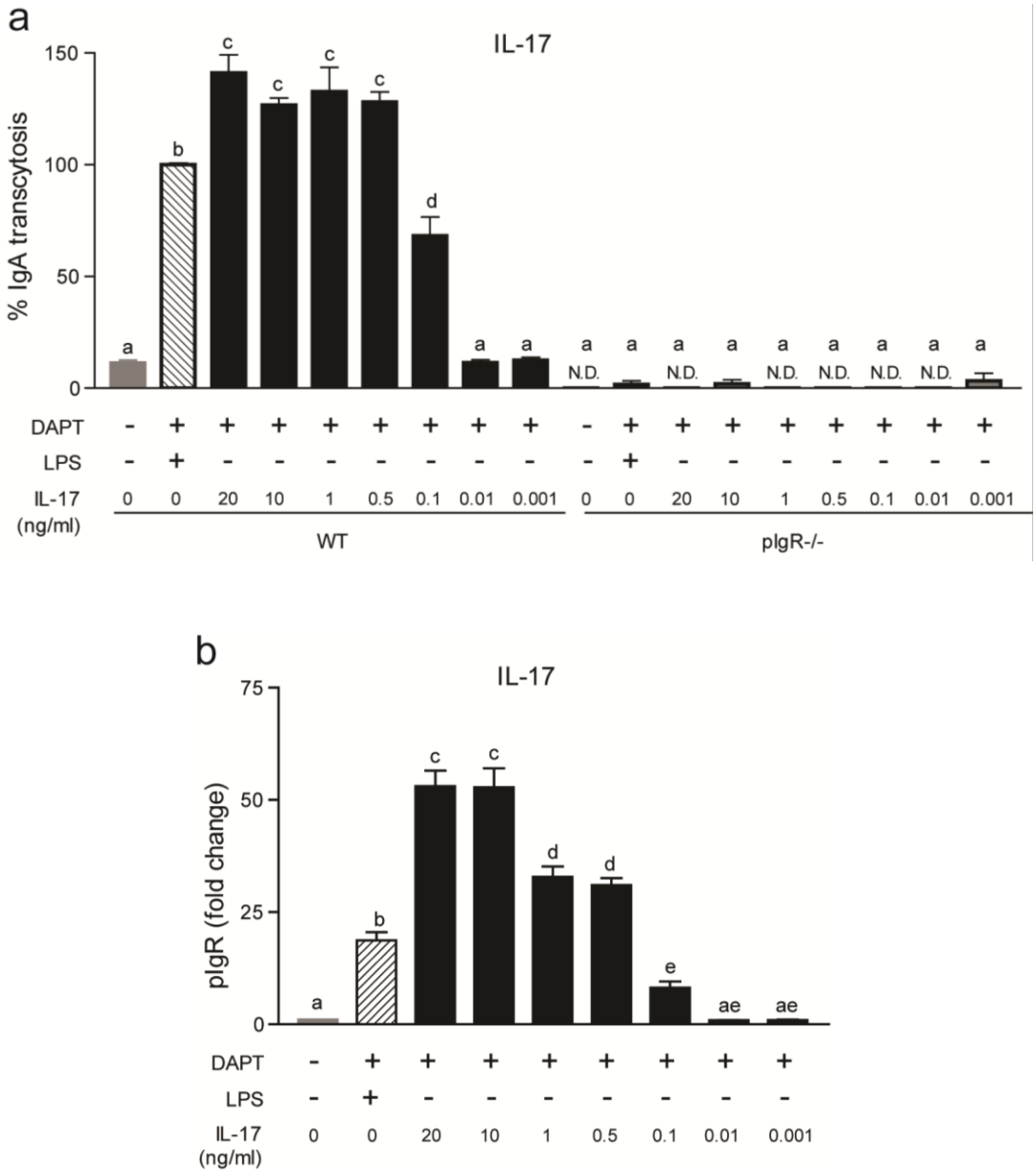

Figure 2.20. IL-1β can induce IgA transcytosis and pIgR expression.

Wild type and *pIgR*$^{-/-}$ cells were treated with 10 μM DAPT and varying doses of IL-1β. **(a)** IgA transcytosis was analyzed by ELISA, and results were normalized to the WT+DAPT+LPS group (= 100%). **(b)** Gene expression analysis of pIgR was performed and all samples were normalized to Gapdh. Data are presented as fold change relative to untreated (0% CM) cells. All values are indicated as mean ± s.e.m. One-way ANOVA: **(a)** $F = 187.9$, $P < 0.0001$, $n \geq 3$ per group; **(b)** $F = 49.92$, $P < 0.0001$, $n \geq 5$ per group. Means with different letters are significantly different by Bonferroni's multiple comparison test. N.D. = not detected.

Figure 2.20. IL-1β can induce IgA transcytosis and pIgR expression.

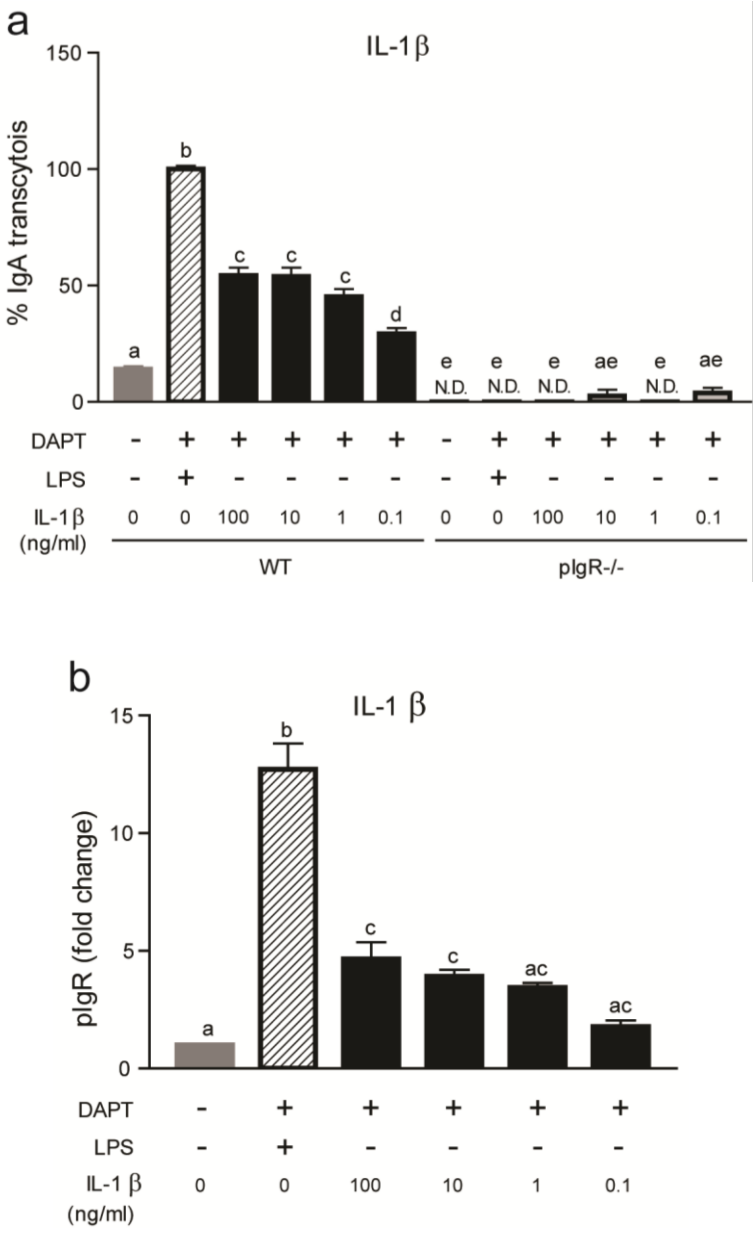

Figure 2.21. TNFα can induce IgA transcytosis and pIgR expression.

Wild type and *pIgR*$^{-/-}$ cells were treated with 10 μM DAPT and varying doses of TNFα. **(a)** IgA transcytosis was analyzed by ELISA, and results were normalized to the WT+DAPT+LPS group (= 100%). **(b)** Gene expression analysis of pIgR was performed and all samples were normalized to Gapdh. Data are presented as fold change relative to untreated (0% CM) cells. All values are indicated as mean ± s.e.m. One-way ANOVA: **(a)** $F = 376.7$, $P < 0.0001$, $n \geq 3$ per group; **(b)** $F = 28.29$, $P < 0.0001$, $n \geq 4$ per group. Means with different letters are significantly different by Bonferroni's multiple comparison test. N.D. = not detected.

Figure 2.21. TNFα can induce IgA transcytosis and pIgR expression.

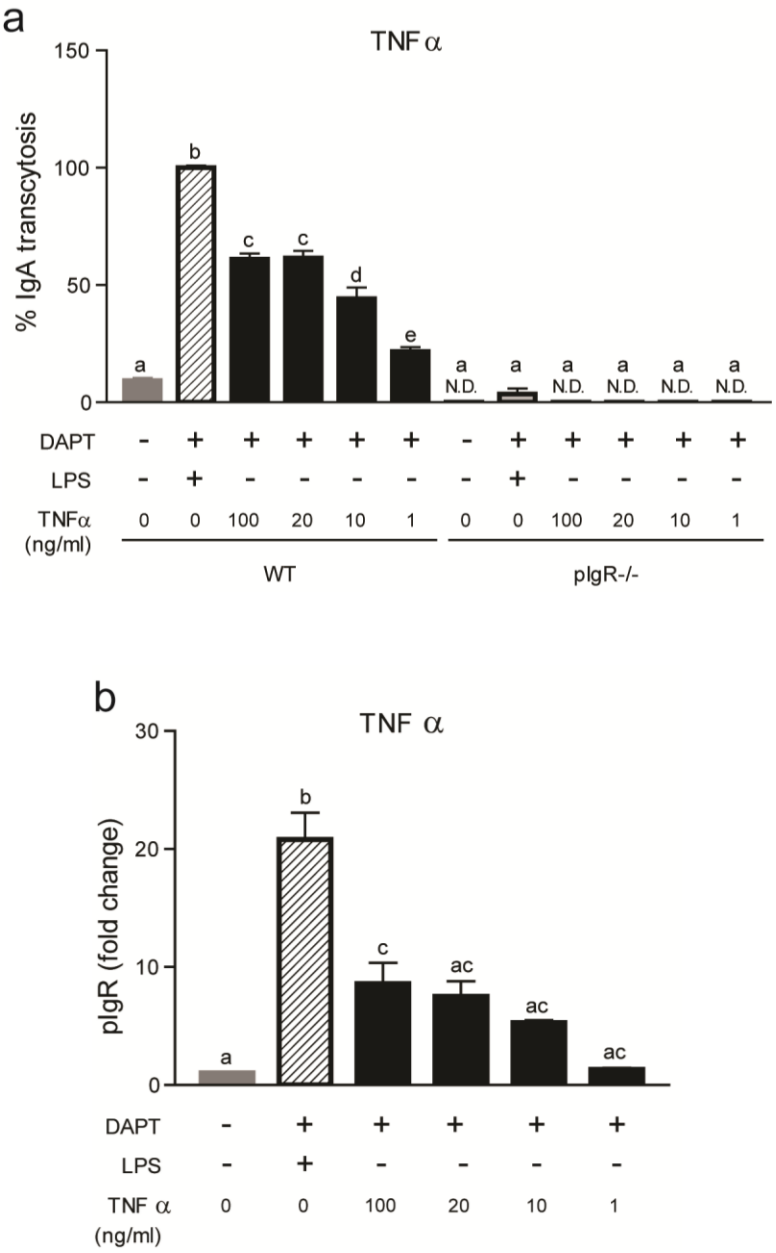

Figure 2.22. IFNγ does not induce pIgR expression.

Wild type and pIgR$^{-/-}$ cells were treated with 10 μM DAPT and varying doses of IFNγ. **(a)** IgA transcytosis was analyzed by ELISA, and results were normalized to the WT+DAPT+LPS group (= 100%). The no cell group indicates the amount of IgA that freely diffuses into the apical supernatant in the absence of cells in the Transwell. **(b)** Gene expression analysis of pIgR was performed and all samples were normalized to Gapdh. Data are presented as fold change relative to untreated (0% CM) cells. All values are indicated as mean ± s.e.m. One-way ANOVA: **(b)** $F = 35.17$, $P < 0.0001$, $n \geq 5$ per group. Means with different letters are significantly different by Bonferroni's multiple comparison test. N.D. = not detected.

Figure 2.22. IFNγ does not induce pIgR expression.

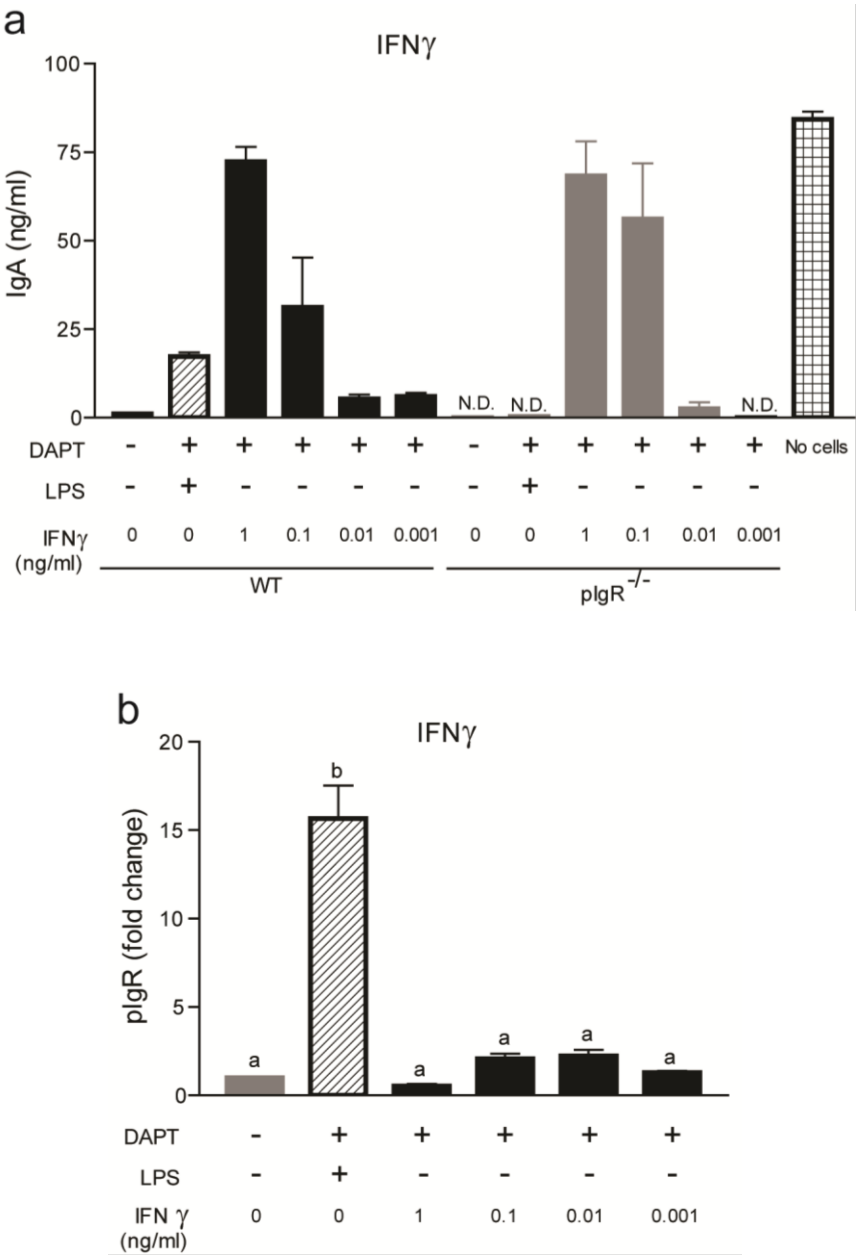

Figure 2.23. IFNγ-treated cells do not maintain an intact monolayer.

Transepithelial electrical resistance measurements were taken on day three after treatment with 10 μM DAPT and the highest previously used dose of various cytokines (100 ng/ml IL-1β, 100 ng/ml TNFα, 20 ng/ml IL-17, 1 ng/ml IFNγ). All values are indicated as mean ± s.e.m. One-way ANOVA: $F = 19.23$, $P < 0.0001$, $n \geq 4$ per group. Means with different letters are significantly different by Bonferroni's multiple comparison test. N.D. = not detected.

Figure 2.23. IFNγ-treated cells do not maintain an intact monolayer.

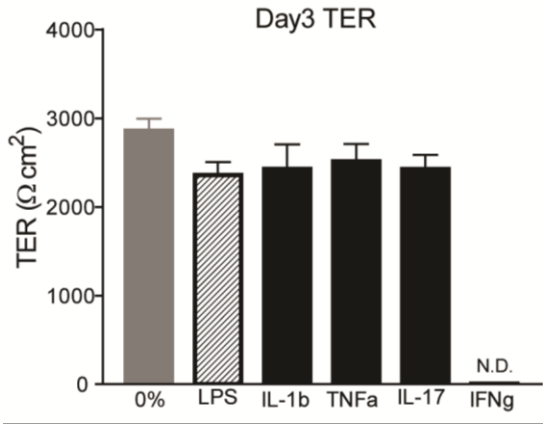

Figure 2.24. Cells from *Tlr4*$^{-/-}$ mice have an impaired IgA transcytosis response to LPS.

Wild type Tlr4 and *Tlr4*$^{-/-}$ were treated with 10 μM DAPT and 1 μg/ml LPS. **(a)** IgA transcytosis was measured by ELISA and results were normalized to the WT group (= 100%). Values are indicated as mean ± s.e.m.; $n = 8$ per group. Wilcoxon signed rank test: $P = 0.0039$. **(b)** Gene expression analysis of pIgR was performed and all samples were normalized to Gapdh. Data are presented as fold change relative to untreated (0% CM) cells. All values are indicated as mean ± s.e.m. One-way ANOVA: $F = 40.92$, $P < 0.0001$, $n \geq 7$ per group. Means with different letters are significantly different by Bonferroni's multiple comparison test.

Figure 2.24. Cells from *Tlr4*$^{-/-}$ mice have an impaired IgA transcytosis response to LPS.

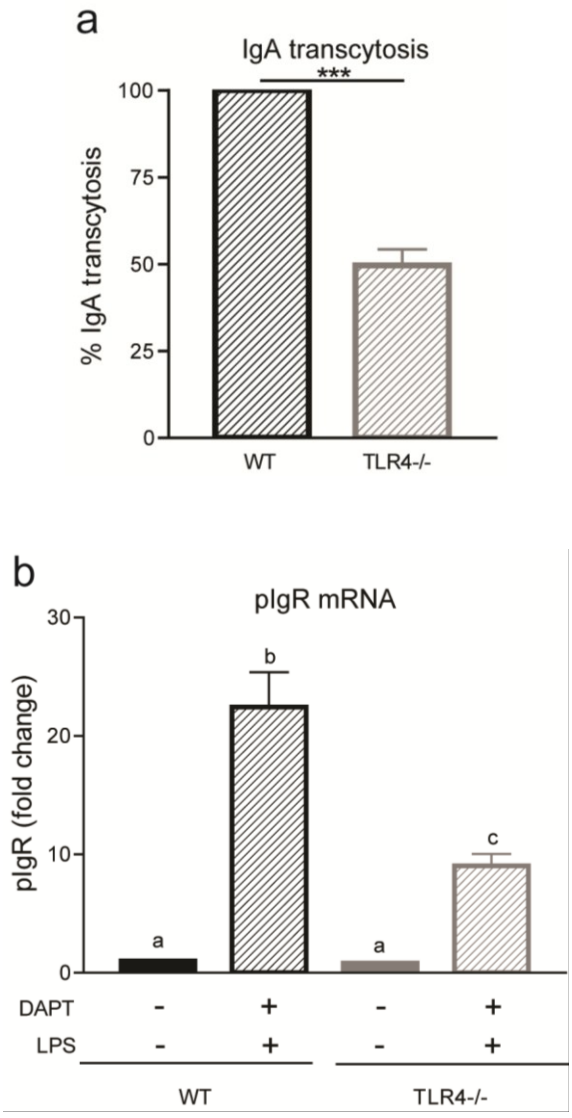

Figure 2.25. *Tlr4*$^{-/-}$ cells induce IgA transcytosis and pIgR expression in response to IL-17. Wild type Tlr4 and *Tlr4*$^{-/-}$ cells were treated with 10 μM DAPT and varying doses of IL-17. **(a)** IgA transcytosis was analyzed by ELISA and results were normalized to the WT+D+L group (= 100%). Gene expression analysis of pIgR was performed **(b)** and all samples were normalized to Gapdh. Data are presented as fold change relative to untreated (0% CM) cells. All values are indicated as mean ± s.e.m. One-way ANOVA: **(a)** $F = 116.9$, $P < 0.0001$, $n \geq 3$ per group; **(b)** $F = 6.364$, $P < 0.0004$, $n \geq 3$ per group. Means with different letters are significantly different by Bonferroni's multiple comparison test. N.D. = not detected.

Figure 2.25. *Tlr4*$^{-/-}$ cells induce IgA transcytosis and pIgR expression in response to IL-17.

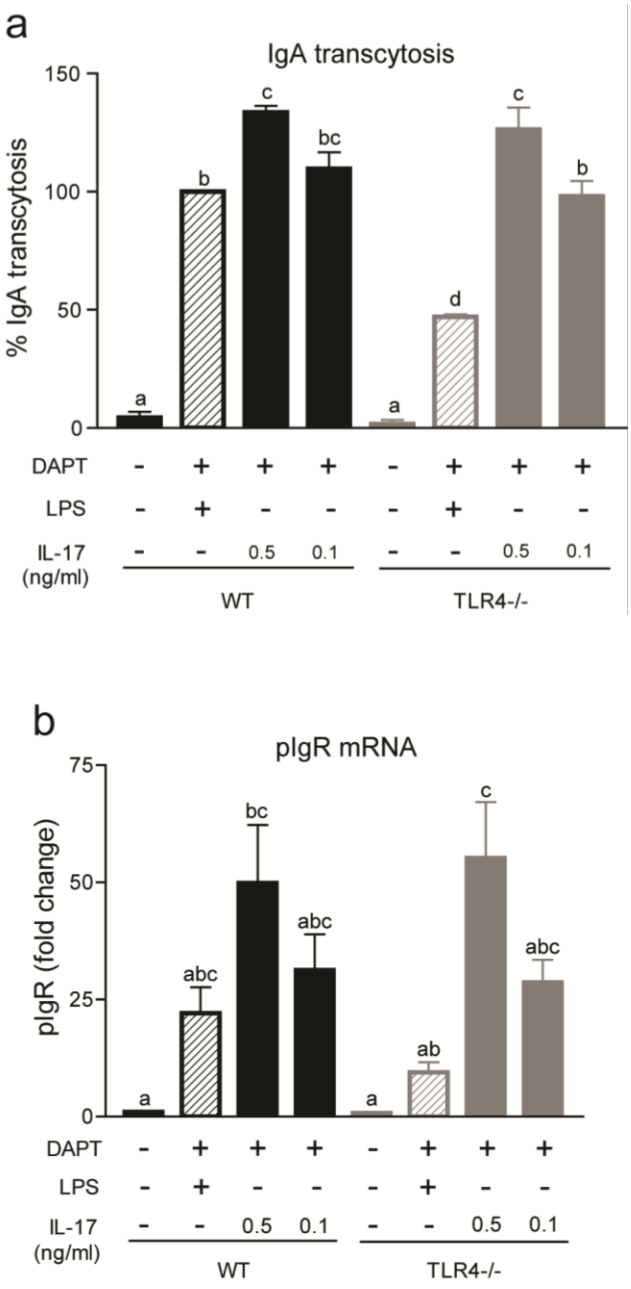

CHAPTER THREE

Heritable Luminal IgA Levels Distinguish Extra-Chromosomal Phenotypic Variation

ABSTRACT

IgA is the most abundant immunoglobulin produced in the body. The majority of the IgA can be found at mucosal sites such as the intestine where it plays an important role at a critical intersection between the host immune system and the microbiota. Mice of the same genetic background bred in the same facility were surprisingly found to have dichotomous fecal IgA levels. This phenotype was heritable and transmissible but was not due to a genetic effect. Furthermore, the IgA-Low phenotype was dominant and microbially driven. One functional consequence of the IgA-Low phenotype was increased damage in response to chemically-induced intestinal injury, which was observed to be directly dependent on the IgA status. In addition, these results indicate that the IgA-Low mice have biologically active microbes with proteolytic capability, leading to the degradation of SC and IgA *in vitro* and *in vivo*. Therefore, these data show that the microbiota can modulate fecal IgA levels, leading to phenotypic variation in mice.

INTRODUCTION

It is often assumed in mouse models that genotypic differences determine phenotypic differences as long as all experimental animals are bred in the same facility or are ordered from the same supplier. However, phenotypic variation of mice that are apparently genetically identical in different facilities is a well-recognized problem often leading to opposing conclusions[62,68,69]. There have been many examples showing that the bacterial microbiome (inherited from the dam in mice[57-59]) has major influences on intestinal phenotypes. Garrett et al have found that *K. pneumonia* and *P. mirabilis* correlates with the development of spontaneous disease in the TRUC (*Tbet*$^{-/-}$ *Rag*$^{-/-}$ ulcerative colitis) mouse model[63]. Through cross-fostering experiments, maternal transmission of bacteria was shown to be able to induce disease in the TRUC mice as well as the littermate controls that do not normally develop spontaneous disease (*Rag2*$^{-/-}$ and WT). Similarly, Elinav et al have shown that mice deficient in inflammasome components (*ASC*$^{-/-}$, *NLRP6*$^{-/-}$, *IL-18*$^{-/-}$) exhibit exacerbated intestinal injury to dextran sodium sulfate (DSS), which correlated with the presence of *Prevotella* species[64]. Cross-fostering experiments with these mice also revealed that the colitogenic activity of the microbiota was transferable to WT mice. Though one conclusion was that NLRP6 directly regulated the composition of the gut microbiota, since littermates were not used in the initial studies (or in the 16S sequencing studies), it is possible that the differences in the microbiota resulted from differences in ancestry. Several more examples of this can be seen in the literature[65,67].

A nice study performed by Ubeda et al showed that in contrast to what had been previously thought, deficiency in Myd88, TLR2, TLR4, TLR5, and TLR9 had minimal impact on the microbial composition relative to WT littermates under homeostatic conditions[66]. Therefore, their conclusions were that the differences previously found between these TLR-

deficient strains and their non-littermate WT controls reflected long-term divergence and drift of the microbiota that was maternally transmitted in these separate breeding schemes (despite being in the same mouse facility).

Though it is clear that the microbiota can change intestinal phenotypes such as the susceptibility of mice to intestinal injury, specific host-microbial mechanisms responsible have not been defined. Here, we investigated the surprising observation that wild-type mice bred within the same facility had dichotomous fecal IgA levels (IgA-High or IgA-Low). This phenotype was heritable, but not due to mouse genetics. Instead bacteria in IgA-Low mice dominantly lowered IgA levels in IgA-High mice after either co-housing or fecal transplantation. This property of inherited bacteria was not unique to a single facility. The dominant effect of bacteria from IgA-Low mice was stably passaged through mice lacking luminal IgA indicating that the heritable property of the IgA phenotype was not selected by the IgA itself. In response to DSS, IgA-Low mice showed increased colonic ulceration that was driven by fecal IgA differences. Serum IgA levels and intestinal plasma cell numbers were not altered, indicating that the B cell compartment did not drive the IgA-Low phenotype. Instead, bacteria from IgA-Low mice degraded the secretory component of SIgA. These studies highlight the ability of the microbiota to produce phenotypic effects through the modulation of IgA, and underscore the importance of taking into account the non-chromosomal hereditary variation between different breeders when making phenotypic comparisons between mice.

MATERIALS AND METHODS

Mice. Animal protocols were approved by the Washington University Animal Studies Committee. All mice were maintained in one of two a specific pathogen-free barrier facilities, with different procedures for maintaining food, water, and caging. In the SRF facility, complete cages (including food, bedding, isolator top, wires, and cage) are autoclaved after assembly, water is autoclaved and kept sterile, and a higher concentration of disinfectant is used (1:5:1 Clidox, Pharmacal Research Laboratories, Inc.). The CSRB facility also uses autoclaved cage components however the cages are assembled after autoclaving. The food is irradiated but not autoclaved, and a lower concentration of disinfectant is used (1:18:1 Clidox). *pIgR*$^{-/-}$ mice (B6.129P2-Pigr^{tm1Fejo}/Mmmh[43]) were initially obtained from Mutant Mouse Regional Resource Center and were backcrossed to 98% B6. All mice used were 3-6 months of age.

Mouse treatments. For fecal transplantation experiments, fecal samples were collected from mice and resuspended in sterile PBS to a final concentration of 200 mg/ml by weight. Mice were administered 25 μl of the fecal mixture on two consecutive days.

Antibiotics were administered in drinking water for 14 days. Treatments included 1 mg/ml vancomycin, 1mg/ml neomycin, 1mg/ml ampicillin, and 1mg/ml metronidazole.

For dextran sodium sulfate experiments, 2.5% DSS (TdB Consultancy) was administered in drinking water for 11 days. Mice were weighed daily and sacrificed at 70% of initial body weight if needed. Intestines were taken for histology.

Preparation of fecal samples for ELISA and immunoblotting. Fecal samples were collected from mice and resuspended in sterile PBS to a final concentration of 100 mg/ml by weight. Supernatants were collected and stored in -20°C until needed.

Preparation of fecal samples for bacterial culture. Fecal samples were collected from mice and resuspended in sterile PBS to a final concentration of 200 mg/ml by weight. 250 µl of this mixture was used to inoculate anaerobic chopped meat broth in Hungate tubes (Fisher Scientific) for overnight cultures in a 37°C shaking incubator. The fecal suspensions as well as the overnight cultures were used in epithelial co-culture experiments described below.

Primary intestinal epithelial cell culture. Primary colonic epithelial stem cells were isolated, grown, and maintained as 3D spheroid cultures in Matrigel (BD Biosciences) as described in Miyoshi et al[83,84]. Cells were kept in 50% L-WRN conditioned media (CM). Media was changed every two days, and cells were passaged every three days (1:3 split).

Primary intestinal epithelial cell monolayers were formed as described in Moon et al[116]. Briefly, spheroids were recovered from three-day-old 3D Matrigel cultures, trypsinized, dissociated to single cells by vigorous pipetting, and re-suspended in 50% L-WRN CM containing 10 µM Y-27632 (R&D Systems). These cells were plated in Transwell inserts (Corning Costar) coated with 0.1% gelatin.

Cell treatments. On day one (24 hours after seeding the Transwells) the 50% L-WRN CM supplemented with Y-27632 was removed and replaced with 0% CM (Advanced DMEM/F12 containing 20% FBS, 100 units of Penicillin, 0.1 mg/ml Streptomycin and 2 mM L-glutamine).

At this time, any additional treatments were also administered to the cells: 1 μg/ml LPS (Sigma), and 10 μM DAPT γ-secretase inhibitor (Millipore). Cells were given fresh media with the respective treatments on day two, and were treated for a total of 48 hours before being used for IgA transcytosis on day three.

IgA transcytosis assay. On day three, the Transwells were removed from the various treatment conditions, and switched to base media (Advanced DMEM/F12 supplemented with 2mM L-glutamine only; no FBS, no antibiotics). 600 μl of base media containing 3 μg of mouse IgA (BD Pharmingen) was added to the lower compartment (final concentration of IgA = 5 μg/ml). 100 μl of base media (with or without various treatments) was added to the upper compartment. Treatments included 1:10 fecal bacterial suspensions and 1:10 overnight anaerobic chopped meat bacterial cultures. The apical supernatant was collected at different time points to evaluate the amount of pIgR and IgA transcytosed by immunoblotting and ELISA (Immunology Consultants Labs).

Immunostaining and histologic analysis. For whole tissue immunostaining, mouse colons were harvested and prepared as previously described[102]. 5 μm thick transverse sections were cut for hematoxylin and eosin staining and immunostaining. For this procedure, the sections were de-paraffinized, hydrated, boiled in Trilogy solution (Cell Marque) for 20 minutes, rinsed in PBS, blocked with 1% bovine serum albumin/0.1% Tritin-X100 for 30 minutes, and incubated with primary antibody at 4°C overnight. Primary antibodies include: goat anti-mouse pIgR (1:500, R&D Systems) and goat anti-mouse IgA-AlexaFluor 488 (1:200, Serotec). The slides were rinsed three times in PBS and incubated with AlexaFluor594-conjugaed species-specific

secondary antibodies for one hour at room temperature (1:500, Invitrogen) if needed. Slides were washed three times in PBS and stained with bis-benzimide/Hoechst (Invitrogen) to visualize nuclei and mounted with a 1:1 PBS:glycerol solution. Staining was visualized with a Zeiss Axiovert 200 microscope with an Axiocam MRM digital camera.

Immunoblotting. Protein was isolated from intestinal tissue segments of ~1cm in 500 µl RIPA buffer with protease inhibitors using the Fastprep bead-beater system (MP Bio, BioSpec). Samples were subjected to 4 rounds of lysis at a speed 6 for 20 seconds, at 4°C. Primary intestinal epithelial cells were lysed in Transwells with 50 µl RIPA buffer with protease inhibitors (Sigma). Total protein was quantified using Pierce BCA Protein Assay Kit (Thermo Scientific). Supernatants from fecal samples and Transwells were taken as described above. Samples were run on either Any kD or 7.5% Mini-Protean TGX gels (Bio-Rad) and transferred onto nitrocellulose membrane (Bio-Rad). Membranes were blocked with 3% milk in 0.1% Tween-20 Tris-buffered saline for 1 h at room temperature and probed with goat IgG anti-pIgR (R&D) and rabbit IgG anti-Actin (Sigma) overnight at 4°C. Blots were incubated for 1 h with horseradish peroxidase-conjugated secondary antibodies (Invitrogen, BioRad) before development using the SuperSignal West Dura chemiluminescent kit (Thermo Scientific). Immunoblots were quantified using ImageJ software[101].

Statistical Analysis. Statistical significance between groups was determined using unpaired t-test, One-way analysis of variance, Two-way analysis of variance, and repeated measures Two-way analysis of variance in Prism GraphPad Software.

RESULTS

Low fecal IgA levels in WT C57BL/6 mice is heritable, transferable, and dominant

While interrogating baseline levels of fecal IgA in WT C57BL/6J mice (B6) bred in our mouse colony, we observed a binary phenotype in fecal IgA levels between cages (**Fig 3.1**): those with high fecal IgA (defined as greater than 0.05 μg IgA/mg feces), and those with nearly undetectable levels of fecal IgA (hereafter designated as IgA-High and IgA-Low mice). This differential IgA phenotype was observed in two separate facilities at our institution in WT B6 colonies that were independently derived (**Fig 3.2**). While both facilities are specific pathogen-free, the procedures, protocols, access, and personnel are unique. All experiments were performed in both facilities unless otherwise noted. Despite the profound difference in fecal IgA levels, serum IgA levels were similar between these two groups, suggesting an effect localized to the gut (**Fig 3.3**). The binary phenotype was vertically transmissible, indicating a heritable phenotype (**Fig 3.4**). Furthermore, this heritable phenotype was laterally transferable by co-housing IgA-High and IgA-Low WT B6 mice. Remarkably, both IgA-High and IgA-Low mice were found to be IgA-Low post-co-housing (**Fig 3.5**). This result also occurred by cross-transfer experiments which involved fecal transplantation between mice in our two facilities (**Fig 3.6**). Hence, the IgA-Low phenotype was dominant, indicating that IgA levels can be regulated by suppression and not only induction.

The IgA-Low phenotype is bacterially driven

We next tested if the fecal microbiome in the absence of IgA could create this binary phenotype. To address this experimentally, we used *pIgR*$^{-/-}$ mice that cannot transcytose IgA (and therefore lack luminal IgA)[43] as vessels to passage microbes independently of IgA (**Fig 3.7**).

Fecal samples from *pIgR*$^{-/-}$ mice transplanted with IgA-Low material were able to subsequently confer the IgA-Low phenotype to IgA-High WT recipient mice (**Fig 3.8**). As a control, WT IgA-High recipients maintained their phenotype when transplanted with samples from IgA-High-transplanted *pIgR*$^{-/-}$ mice. Thus, exposure to a novel environment lacking IgA (the *pIgR*$^{-/-}$ intestine) does not affect the ability of the fecal microbiota to regulate the IgA-High vs -Low phenotype.

Both commensal bacteria and viruses in the gut modulate mucosal IgA levels[117,118]. To assess whether dominant lowering of IgA levels was due to bacteria or alternatively viral or soluble factors, we transplanted IgA-High mice with fecal material from IgA-Low mice that had been either homogenized or filtered to remove large microbes (e.g. bacteria, fungi). IgA-High mice transplanted with filtered fecal material remained IgA-High, while mice transplanted with unfiltered fecal homogenate became IgA-Low (**Fig 3.9**). This result suggests the IgA-Low phenotype is induced by intestinal microbes, and excludes filterable viruses.

To determine if specific microbial pools could induce the IgA-Low phenotype, we pre-treated IgA-Low mice with a broad-spectrum antibiotic cocktail (vancomycin, neomycin, ampicillin, and metronidazole; VNAM) chosen to target a wide range of microbes[119,120] (**Fig 3.10a,b**), then transplanted them fecal samples from either IgA-High or IgA-Low mice. Transplantation with IgA-High microbes led to an increase of intestinal IgA levels, indicating that the IgA-Low-inducing microbes were eliminated by VNAM (**Fig 3.10b**). We then tested the role of specific antibiotics and found that ampicillin but not metronidazole was sufficient to reverse the IgA-Low phenotype (**Fig 3.10c,d**). These results show ampicillin-sensitive microbe(s) were responsible for the IgA-Low phenotype. Unlike VNAM, ampicillin treatment reversed the IgA-low phenotype even without transplantation with IgA-High samples. This

indicated that VNAM eliminated both the IgA suppressive and IgA-inductive microbes while ampicillin alone eliminated only the IgA-suppressive microbes. We assessed whether the IgA status of antibiotic-treated mice could be vertically transmitted, and found that VNAM-treated IgA-Low mice transplanted with IgA-High fecal samples gave rise to IgA-High progeny (**Fig 3.11**). Taken together, these results support a model where the IgA-low phenotype is bacterially-driven, dominantly transmissible, and heritable (**Figure 3.12**).

Functional consequences of low fecal IgA levels: increased susceptibility to colonic injury

We next determined if the IgA-Low phenotype affected intestinal injury responses as previous studies that showed *pIgR*$^{-/-}$ mice are more susceptible to DSS injury[121]. With DSS treatment, IgA-Low mice lost significantly more weight than their IgA-High counterparts (**Fig 3.13**), and exhibited increased distal colon ulceration (**Fig 3.14**). This DSS sensitivity could be secondary to either diminished IgA or the altered microbial composition.

To address this we re-colonized WT and *pIgR*$^{-/-}$ mice with IgA-High or IgA-Low fecal material for two weeks after VNAM treatment, as shown in Figure 3.7, prior to DSS treatment (**Fig 3.15**). As expected, WT IgA-Low mice showed enhanced DSS sensitivity compared to WT IgA High mice (**Fig 3.16, 3.17**). Consistent with previous reports[121], we observed that *pIgR*$^{-/-}$ mice exhibited increased weight loss and colonic ulceration compared to WT mice. Interestingly, this sensitivity was independent of the microbial composition. This finding implied that altered IgA levels, and not the microbes themselves, were responsible for the increased DSS damage in WT IgA-Low mice.

Identifying the mechanism: IgA-Low-associated microbes degrade SIgA

To study the mechanism by which IgA-Low microbes suppress fecal IgA levels, we assessed IgA production and IgA transport capacity by pIgR in IgA-High vs IgA-Low mice. Intestinal IgA is made in the lamina propria by plasma cells, but we found no difference in plasma cell numbers in small intestines or colons of these mice (**Fig 3.18**). Immunofluorescence staining for pIgR in the IgA-High and IgA-Low mice also failed to show obvious differences (**Fig 3.19**).

On the apical surface of intestinal epithelial cells, pIgR is cleaved and released into the intestine bound to dimeric IgA. This cleaved form of pIgR, called the secretory component (SC), is thought to help protect dimeric IgA from degradation by bacterial proteases[13,14]. We hypothesized that in IgA-Low mice, the absence of IgA may be secondary to degradation of SC. We therefore assessed levels of cleaved (SC) vs. full-length (membrane-bound) pIgR by immunoblots fecal samples and whole tissue (**Fig 3.20a**). While both IgA-High and -Low mice had comparable levels of pIgR in whole tissue (**Fig 3.20b,c**), IgA-Low mice had significantly reduced levels of SC in fecal samples (**Fig 3.20d**).

To define the mechanism for this observation, we developed an *in vitro* system. We first anaerobically cultured bacteria from IgA-High and IgA-Low fecal samples (**Fig 3.21a**), and administered these cultures to IgA-High recipients. While the IgA-High cultures maintained the IgA-High phenotype, mice administered IgA-Low cultures converted to the IgA-Low phenotype, indicating the causative IgA-Low microbes are culturable in these conditions (**Fig 3.21b**). We next generated polarized, differentiated monolayers of primary epithelial cells in Transwells[116] and assessed IgA transport from the basolateral to the apical compartment in the presence of the cultured bacteria (**Fig. 3.22**). Treatment with the γ-secretase inhibitor DAPT and LPS robustly

induces pIgR in these cells (**Fig. 3.23**), which is necessary for IgA transport (**Fig 3.24**). We then co-cultured epithelial monolayers with IgA-High or IgA-Low cultures by adding pelleted bacteria or culture supernatants to the apical compartment of the Transwells for three or six hours (**Fig 3.24**). In co-cultures with IgA-High pelleted bacteria, we detect SC in the apical supernatants at both time points, while co-cultures with IgA-Low pelleted bacteria exhibited substantially greater SC degradation over time. The bacterial culture supernatants did not lead to degradation, suggesting that the presence of the bacterial cells is required in this case. Epithelial cell lysates from all treatment conditions showed similar pIgR levels, indicating that differences in SC levels in the supernatant are not due to differences in epithelial pIgR expression (**Fig. 3.23**).

Taken together, these data suggest there are bacteria present in the IgA-Low microbiota capable of degrading SC *in vitro,* consistent with our observation of absent fecal SC *in vivo*. These findings are consistent with a model in which SC degradation by IgA-Low microbes makes IgA more susceptible to degradation itself (**Fig 3.25**). Bacteria have been shown to make proteases that can cleave human IgA1/IgA2 as well as SC[70-73,76-78], though this has not been addressed in murine models, and could be a potential means by which the causative IgA-Low microbes alter the host response.

DISCUSSION

Here, we show one driver of phenotypic variation between genetically identical mice bred in the same colonies. We found that fecal IgA levels show a binary phenotype in WT mice that was heritable and transferable. In addition, the IgA-Low phenotype was found to be dominant and microbially driven. One functional consequence of having low levels of luminal IgA was increased intestinal injury after DSS treatment in mice. Furthermore, *in vitro* co-culture experiments using primary epithelial monolayers and anaerobically cultured intestinal bacteria showed that cultured microbes from IgA-Low mice had proteolytic activity capable of degrading SC. Previous studies from multiple groups have shown that SC stabilizes and protects dIgA from degradation by proteases[13,14], thus these findings support the idea that degradation of SC *in vivo* would make IgA more susceptible to degradation itself, and thereby explain the IgA-Low phenotype.

This data reveals that the microbiome can potentially mimic the effects of chromosomal genes, such that phenotypes of mouse strains bred separately may reflect significant biological effects of the microbiome[122]. Therefore, in order to evaluate the effects of a chromosomal gene (especially in the intestine), the effects of the microbiome must be taken into consideration as well. In these studies, fecal IgA served as a readily measurable marker for relevant effects of the bacterial microbiome, and it is possible that its use might clarify variation that can occur within some mouse experiments. Furthermore, fecal transplantation and co-housing experiments could also serve as a methodological control for the phenotypic variation dependent on heritable factors that may be easily transmissible between hosts. Our findings may have broader implications for many animal experiments since the microbiome has also been shown to have systemic effects[123].

Figure 3.1. Wild type C57BL/6 mice have a binary fecal IgA phenotype.

Fecal IgA normalized by weight was measured by anti-mouse IgA enzyme linked immunosorbent assay (ELISA). The IgA-High phenotype was defined as having fecal IgA values >0.05 μg IgA/mg feces. The dotted lines represent the limit of detection by ELISA. All values are indicated as mean±s.e.m. Statistical analysis by unpaired *t*-test: $P<0.0001$, $n\geq34$ mice per group.

Figure 3.1. Wild type C57BL/6 mice have a binary fecal IgA phenotype.

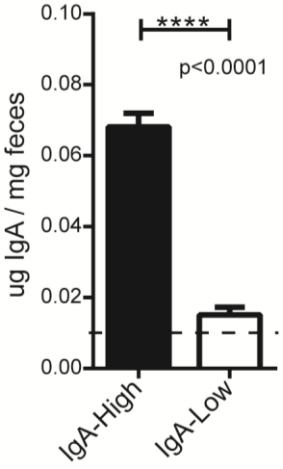

Figure 3.2. The binary fecal IgA phenotype is observed in two independent facilities.

Fecal IgA (normalized to fecal weight) from mice housed in either Facility 1 or Facility 2 was detected by anti-mouse IgA ELISA. The dotted lines represent the limit of detection by ELISA. All values are indicated as mean±s.e.m. One-way analysis of variance: $F=44.59$, $P<0.0001$, $n\geq12$ mice per group. Means with different letters are significantly different by Tukey's multiple comparison test.

Figure 3.2. The binary fecal IgA phenotype is observed in two independent facilities.

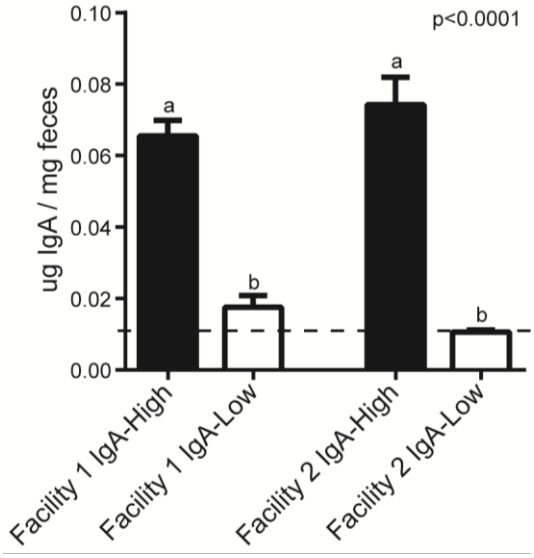

Figure 3.3. Serum IgA is comparable between IgA-High and IgA-Low mice.

Serum IgA was measured by anti-mouse IgA ELISA. All values are indicated as mean±s.e.m. Statistical analysis by unpaired *t*-test: $P<0.3991$, n=12 mice per group.

Figure 3.3. Serum IgA is comparable between IgA-High and IgA-Low mice.

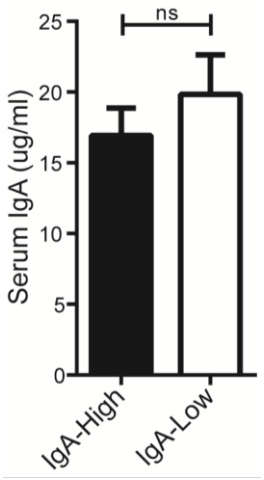

Figure 3.4. The binary fecal IgA phenotype is heritable.

Fecal IgA was analyzed from IgA-High/IgA-Low breeders and their progeny once they reached at least 8 weeks of age. The dotted lines represent the limit of detection by ELISA. All values are indicated as mean±s.e.m. One-way analysis of variance: $F= 45.95$, $P<0.0001$, $n\geq9$ mice per group. Means with different letters are significantly different by Tukey's multiple comparison test.

Figure 3.4. The binary fecal IgA phenotype is heritable.

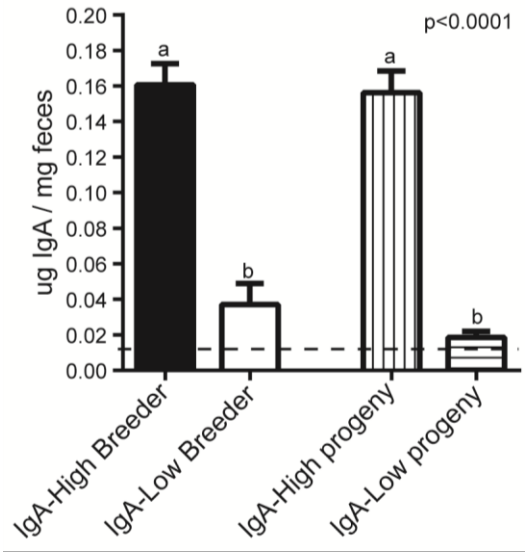

Figure 3.5. The IgA-Low phenotype is dominantly transferable by co-housing.

Fecal IgA was measured in IgA-High and IgA-Low mice before and after 14 days of 1:1 co-housing. The dotted lines represent the limit of detection by ELISA. All values are indicated as mean±s.e.m. One-way analysis of variance: $F= 15.56$, $P<0.0001$, $n\geq8$ mice per group. Means with different letters are significantly different by Tukey's multiple comparison test.

Figure 3.5. The IgA-Low phenotype is dominantly transferable by co-housing.

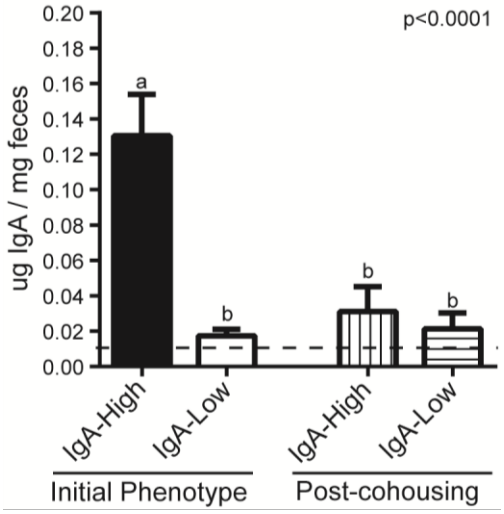

Figure 3.6. The IgA-Low phenotype is transferable between two independent mouse facilities.

WT IgA-High mice from one mouse facility were administered homogenized fecal material from WT IgA-High or IgA-Low mice from the other mouse facility, and fecal IgA was measured 14 days later by anti-mouse IgA ELISA. The dotted lines represent the limit of detection by ELISA. **(a)** Facility 1 mice pre- and post-fecal transplantation with Facility 2 fecal samples. **(b)** Facility 2 mice pre- and post-fecal transplantation with Facility 1 fecal samples. All values are indicated as mean±s.e.m. One-way analysis of variance: **(a)** $F=20.93$, $P<0.0001$, $n\geq8$ mice per group; **(b)** $F=12.92$, $P<0.0004$, $n\geq4$ mice per group. Means with different letters are significantly different by Tukey's multiple comparison test.

Figure 3.6. The IgA-Low phenotype is transferable between two independent mouse facilities.

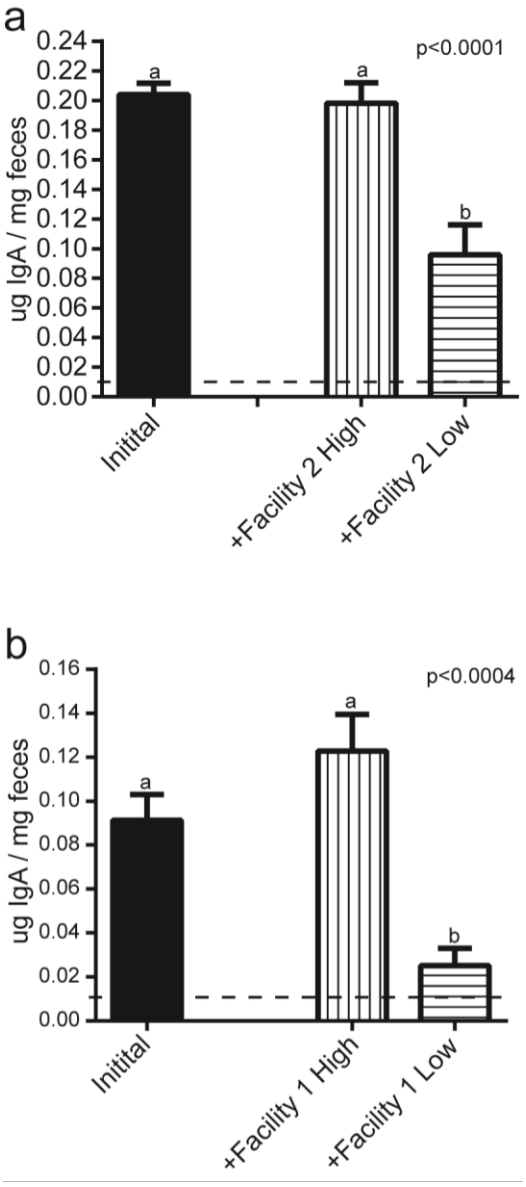

Figure 3.7. Schematic for passage experiment though *pIgR*$^{-/-}$ mice.

Schematic for re-population of antibiotic-treated *pIgR*$^{-/-}$ mice with microbes from WT IgA-High or IgA-Low mice by fecal transplantation (FT), followed by fecal transplantation of WT IgA-High recipients with samples from the re-populated *pIgR*$^{-/-}$ mice. VNAM = antibiotic cocktail containing vancomycin, neomycin, ampicillin, metronidazole.

Figure 3.7. Schematic for passage experiment though *pIgR*$^{-/-}$ mice.

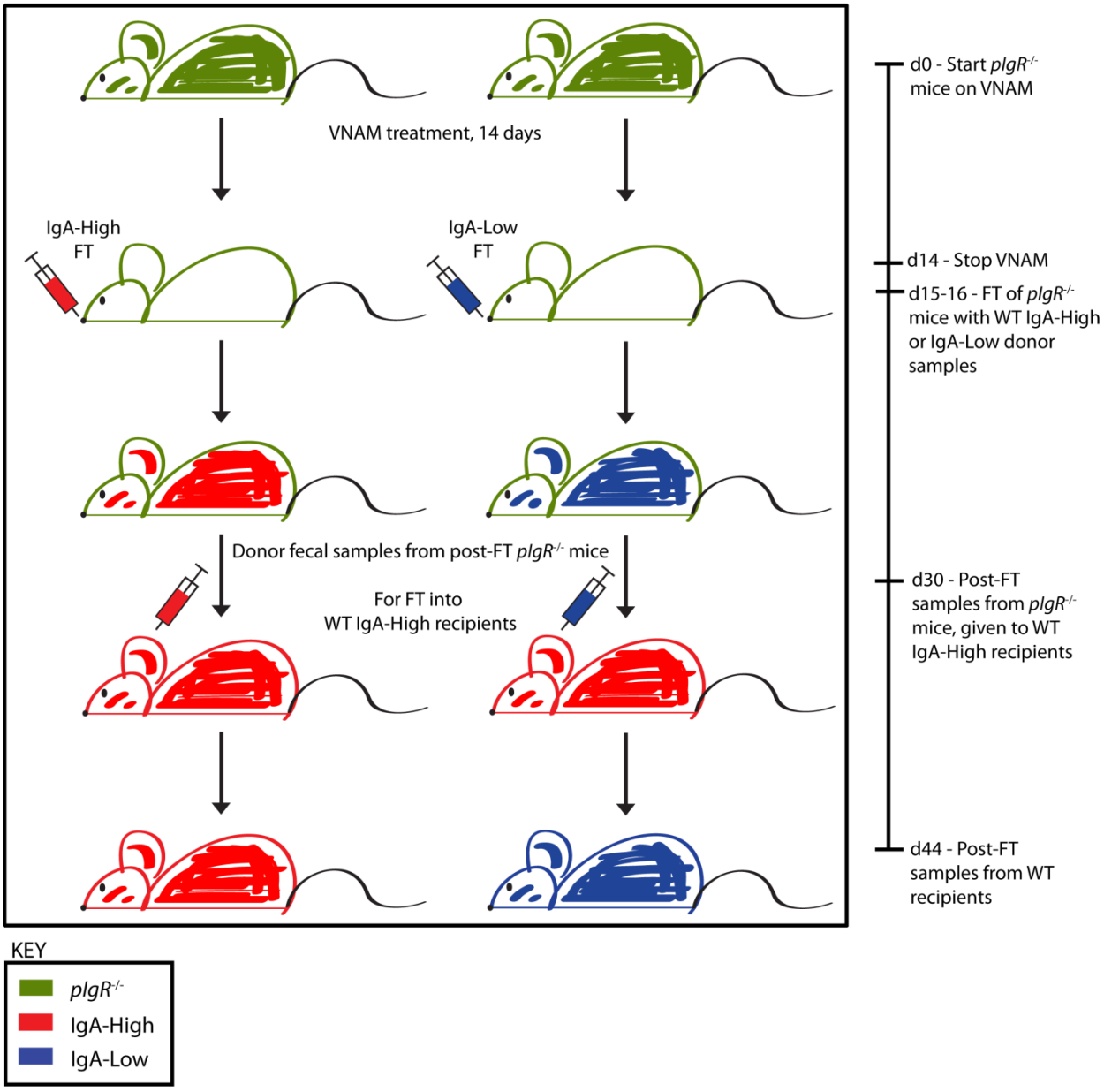

Figure 3.8. The binary IgA phenotype can be passaged though *pIgR*$^{-/-}$ mice.

Fecal IgA levels from mice on day 44 as depicted in Figure 3.7. The dotted lines represent the limit of detection by ELISA. All values are indicated as mean±s.e.m. Statistical analysis by unpaired *t*-test: $P<0.0003$, n=8 mice per group.

Figure 3.8. The binary IgA phenotype can be passaged though *pIgR*$^{-/-}$ mice.

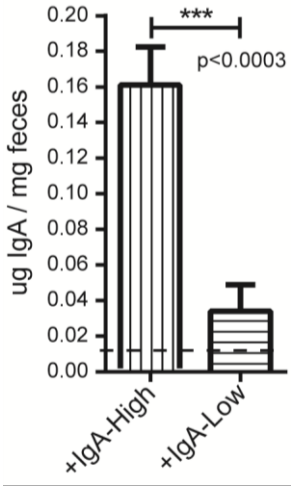

Figure 3.9. The IgA-Low phenotype can be transferred by fecal transplantation.

Fecal IgA levels from IgA-High mice pre- and post-fecal transplantation with unfiltered (Post-FT) or 0.45μm-filtered fecal material (Post-filter FT) from IgA-Low mice. The dotted lines represent the limit of detection by ELISA. All values are indicated as mean±s.e.m. One-way analysis of variance: $F=5.685$, $P<0.0076$, $n\geq5$ mice per group. Means with different letters are significantly different by Tukey's multiple comparison test.

Figure 3.9. The IgA-Low phenotype can be transferred by fecal transplantation.

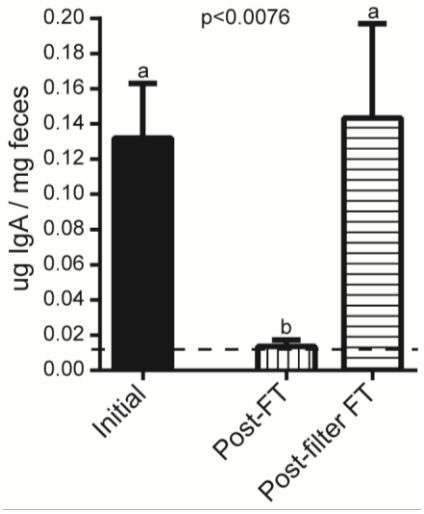

Figure 3.10. The IgA-Low phenotype is driven by ampicillin-susceptible bacteria.

(a) Schematic of antibiotic treatment + fecal transplantation experiments performed in **(b-d)**. Mice were treated with **(b)** a cocktail of antibiotics including vancomycin, neomycin, ampicillin, and metronidazole (VNAM), **(c)** ampicillin, or **(d)** metronidazole for 14 days prior to fecal transplantation with IgA-High or IgA-Low fecal samples. Fecal IgA levels were measured 14 days after transplantation. The dotted lines represent the limit of detection by ELISA. All values are indicated as mean±s.e.m. One-way analysis of variance: **(b)** $F=16.15$, $P<0.0001$, $n\geq9$ mice per group; **(c)** $F=22.96$, $P<0.0001$, $n\geq12$ mice per group; **(d)** $F=6.525$, $P<0.0012$, $n\geq5$ mice per group. Means with different letters are significantly different by Tukey's multiple comparison test.

Figure 3.10. The IgA-Low phenotype is driven by ampicillin-susceptible bacteria.

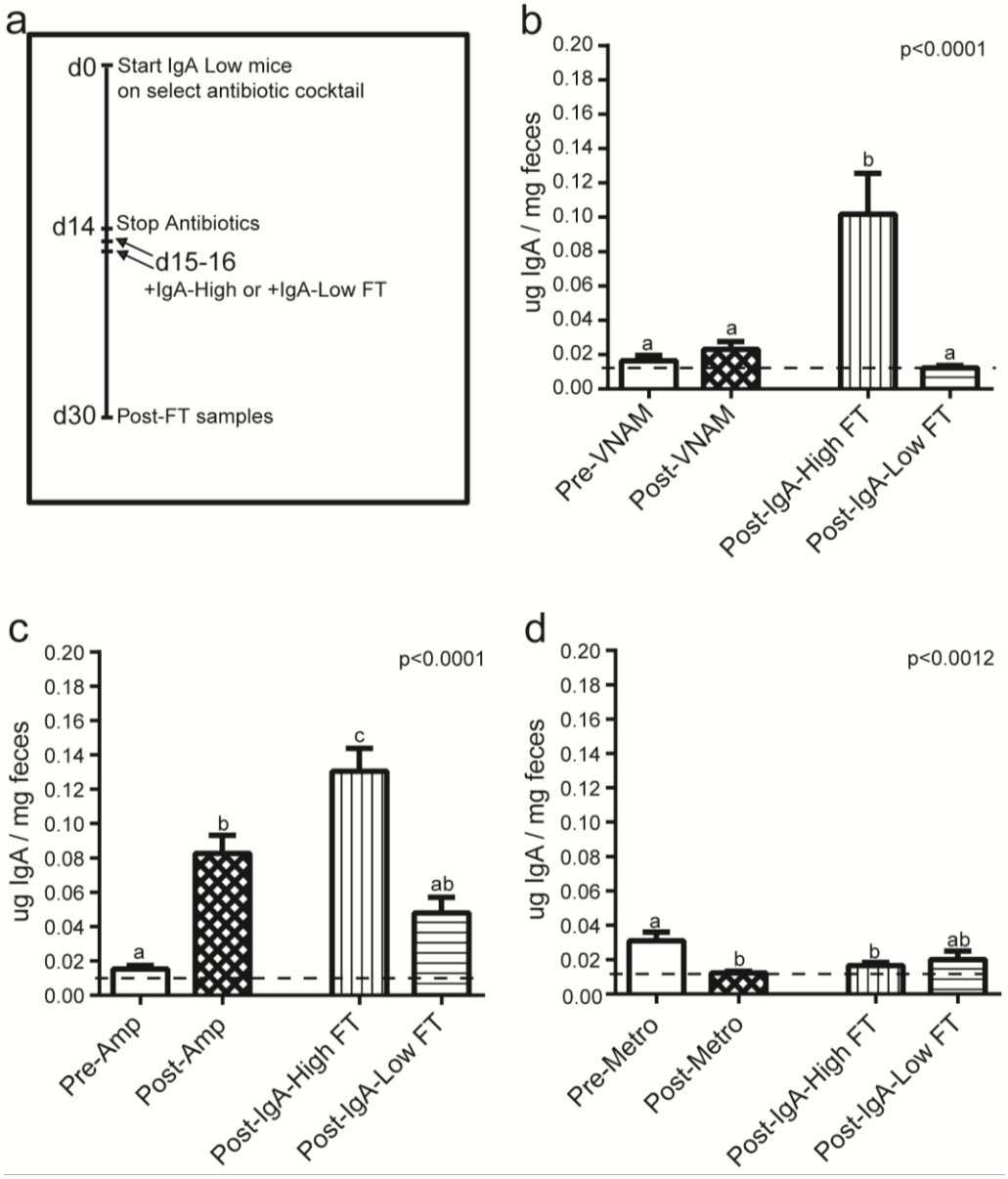

Figure 3.11. The converted IgA-High phenotype is stable and heritable.

IgA-Low mice converted to IgA-High from (**e**) were used to set up a breeding pair, and fecal IgA levels of their progeny were measured once they reached at least 8 weeks of age. The dotted lines represent the limit of detection by ELISA. All values are indicated as mean±s.e.m. One-way analysis of variance: $F=18.29$, $P<0.0002$, $n=2$ breeders and $n=10$ progeny from 4 litters. Means with different letters are significantly different by Tukey's multiple comparison test.

Figure 3.11. The converted IgA-High phenotype is stable and heritable.

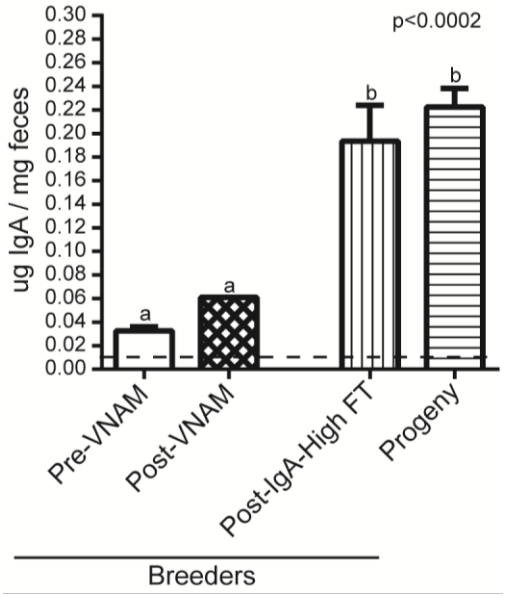

Figure 3.12. Summary model of the IgA phenotype.

Cartoon summarizing the IgA phenotype observed in WT mice in our mouse colonies. **(a)** The binary IgA phenotype is vertically transmitted and therefore heritable. **(b)** The IgA-Low phenotype is horizontally transmitted by co-housing in a dominant manner. **(c)** The IgA-Low phenotype is horizontally transmitted by fecal transplantation. Additional experiments suggest that the IgA-Low phenotype is driven by ampicillin-susceptible bacteria.

Figure 3.12. Summary model of the IgA phenotype.

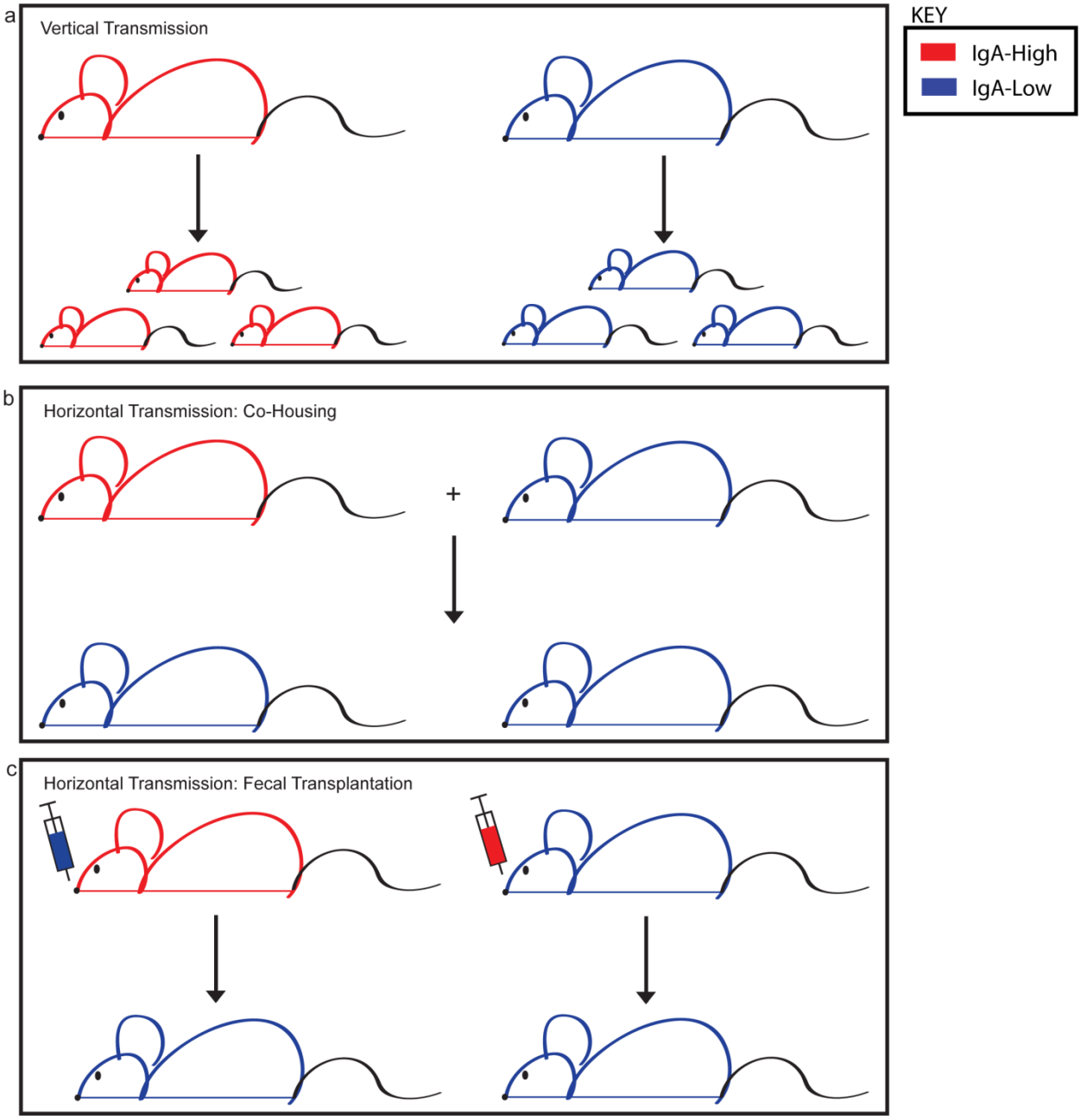

Figure 3.13. The IgA-Low mice have greater weight loss in DSS injury.

IgA-High and IgA-Low mice from both facilities were treated with 2.5% DSS in drinking water for 11 days. Mice were weighed daily and weight loss depicted as percent initial weight. All values are indicated as mean±s.e.m. Statistical analysis by Two-way repeated measures analysis of variance: column factor $P<0.0089$, $n\geq8$ mice per group. ***$P<0.001$ by Sidak's multiple comparison test for the final time point.

Figure 3.13. The IgA-Low mice have greater weight loss in DSS injury.

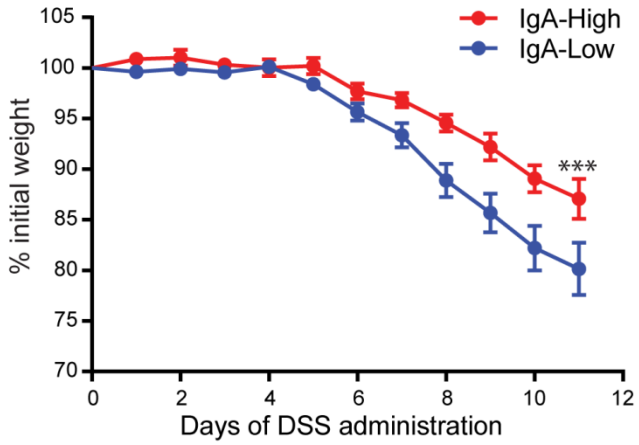

Figure 3.14. The IgA-Low mice have increased ulceration in DSS injury.

IgA-High and IgA-Low mice from both facilities were treated with 2.5% DSS in drinking water for 11 days, when colons were harvested for histology. **(a)** Representative hematoxylin and eosin stained histologic sections. Bars = 1 mm; boxes indicate areas of ulceration. **(b)** percentage of ulcerated distal colon. All values are indicated as mean±s.e.m. Statistical analysis by unpaired *t*-test: $P<0.0385$, $n\geq10$ mice per group.

Figure 3.14. The IgA-Low mice have increased ulceration in DSS injury.

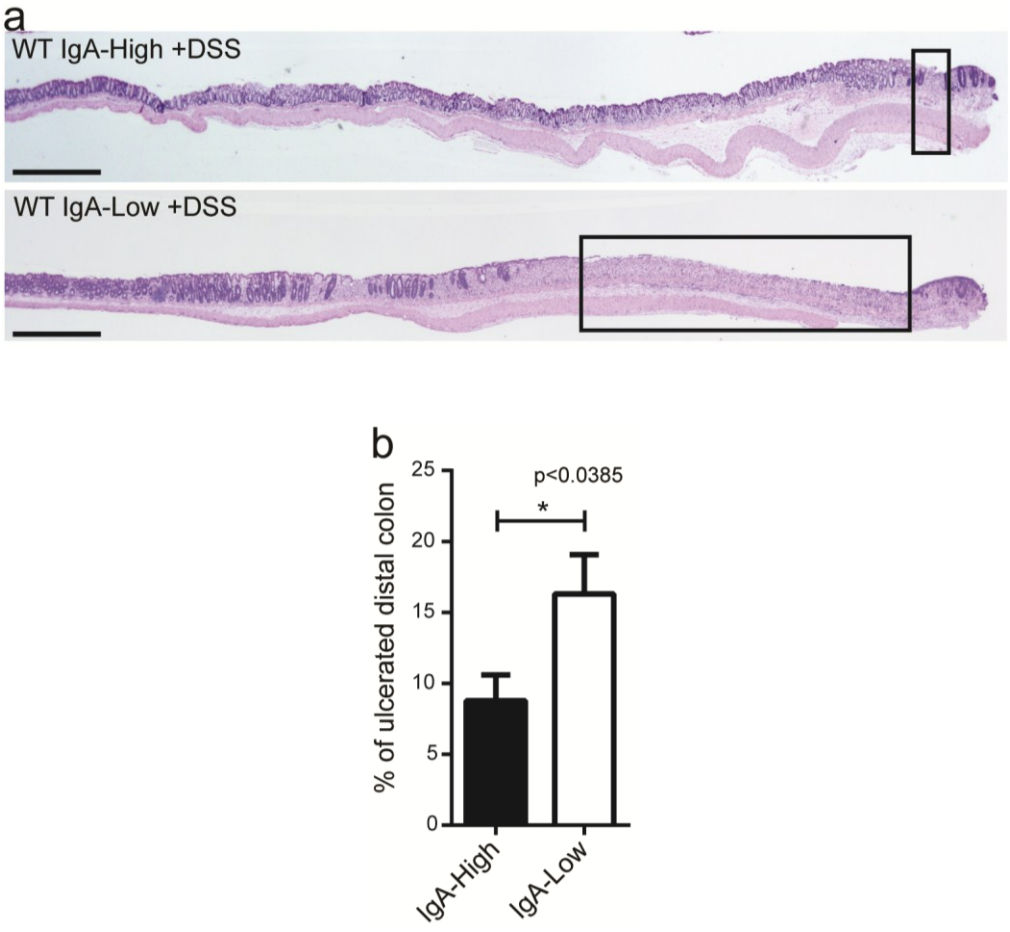

Figure 3.15. IgA status of mice after VNAM and FT, before the start of DSS treatment.

Fecal IgA levels were measured in mice from Figures 3.16 and 3.17 after VNAM treatment and IgA-High/IgA-Low fecal transplantation, prior to the start of DSS treatment. The dotted lines represent the limit of detection by ELISA. All values are indicated as mean±s.e.m. Statistical analysis by unpaired *t*-test: $P<0.0001$, n=7 mice per group.

Figure 3.15. IgA status of mice after VNAM and FT, before the start of DSS treatment.

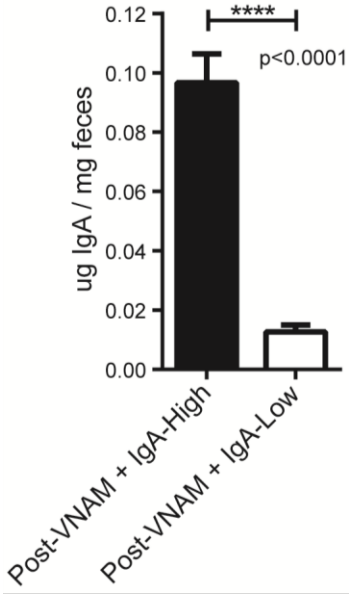

Figure 3.16. The increased DSS-induced weight loss of IgA-Low mice is due to altered IgA levels.

DSS treatment of WT and *pIgR*$^{-/-}$ mice from Facility 2 after 14 days of VNAM treatment and IgA-High/IgA-Low fecal transplantation. Mice were treated with 2.5% DSS in drinking water for 11 days, and weighed daily. Weight loss is depicted as percent initial weight. All values are indicated as mean±s.e.m. Statistical analysis by Two-way repeated measures analysis of variance: column factor $P<0.0001$, $n\geq15$ mice per group. Means with different letters are significantly different by Tukey's multiple comparison test for the final time point.

Figure 3.16. The increased DSS-induced weight loss of IgA-Low mice is due to altered IgA levels.

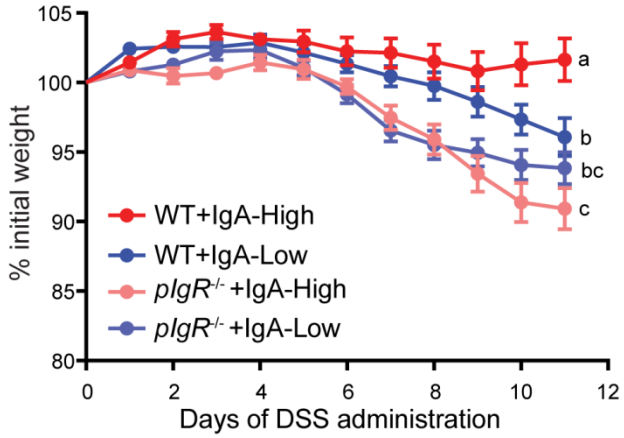

Figure 3.17. The increased DSS-induced ulceration of IgA-Low mice is due to altered IgA levels.

DSS treatment of WT and *pIgR*$^{-/-}$ mice from Facility 2 after 14 days of VNAM treatment and IgA-High/IgA-Low fecal transplantation. Mice were treated with 2.5% DSS in drinking water for 11 days, when colons were harvested for histology. **(a)** Representative hematoxylin and eosin stained histologic sections. Bars = 1 mm; boxes indicate areas of ulceration. **(b)** percentage of ulcerated distal colon. All values are indicated as mean±s.e.m. Statistical analysis by One-way analysis of variance: $F=8.272$, $P<0.0007$, $n\geq3$ mice per group. Means with different letters are significantly different by Tukey's multiple comparison test.

Figure 3.17. The increased DSS-induced ulceration of IgA-Low mice is due to altered IgA levels.

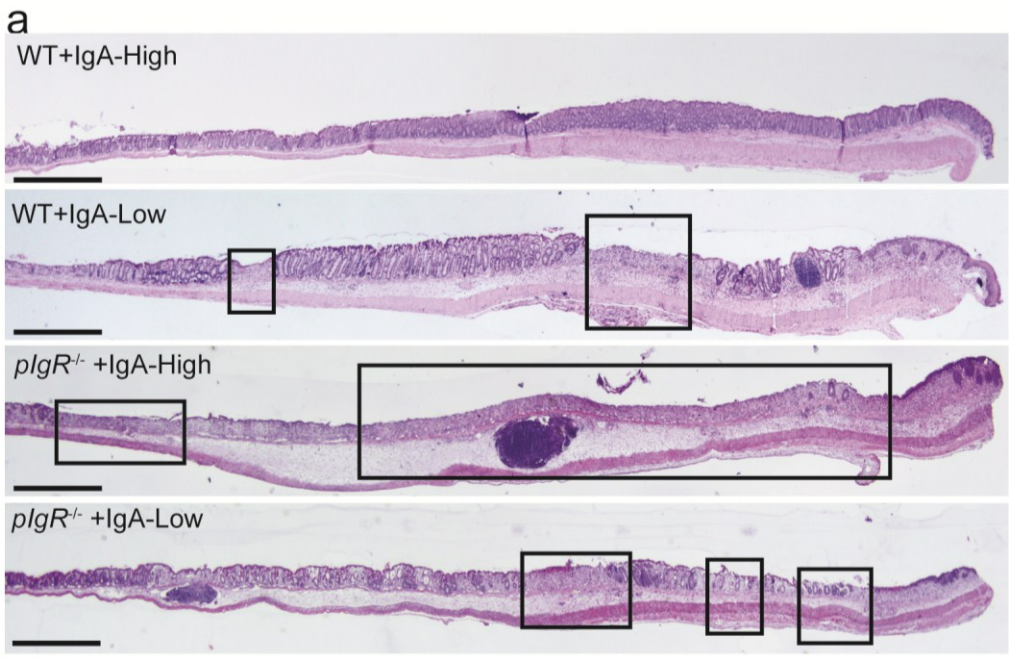

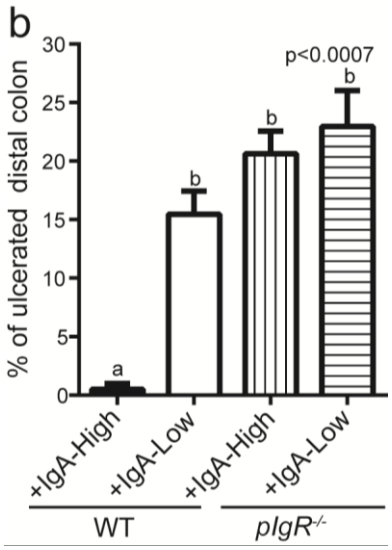

Figure 3.18. Intestinal plasma cell numbers are unchanged between IgA-High and IgA-Low mice.

Ileal **(a,b)** and colonic **(c,d)** sections from IgA-High and IgA-Low mice were stained with anti-IgA (green) and bis-benzamide dye (blue); representative images are shown. Bars = 100 μm. Quantification of ileal plasma cells per villus (**e**) and colonic plasma cells per 20X field (**f**) based on IgA staining. All values are indicated as mean±s.e.m. Statistical analysis by unpaired *t*-test: (**e**) $P<0.6638$, n=10 mice per group, and (**f**) $P<0.3158$, $n\geq 9$ mice per group.

Figure 3.18. Intestinal plasma cell numbers are unchanged between IgA-High and IgA-Low mice.

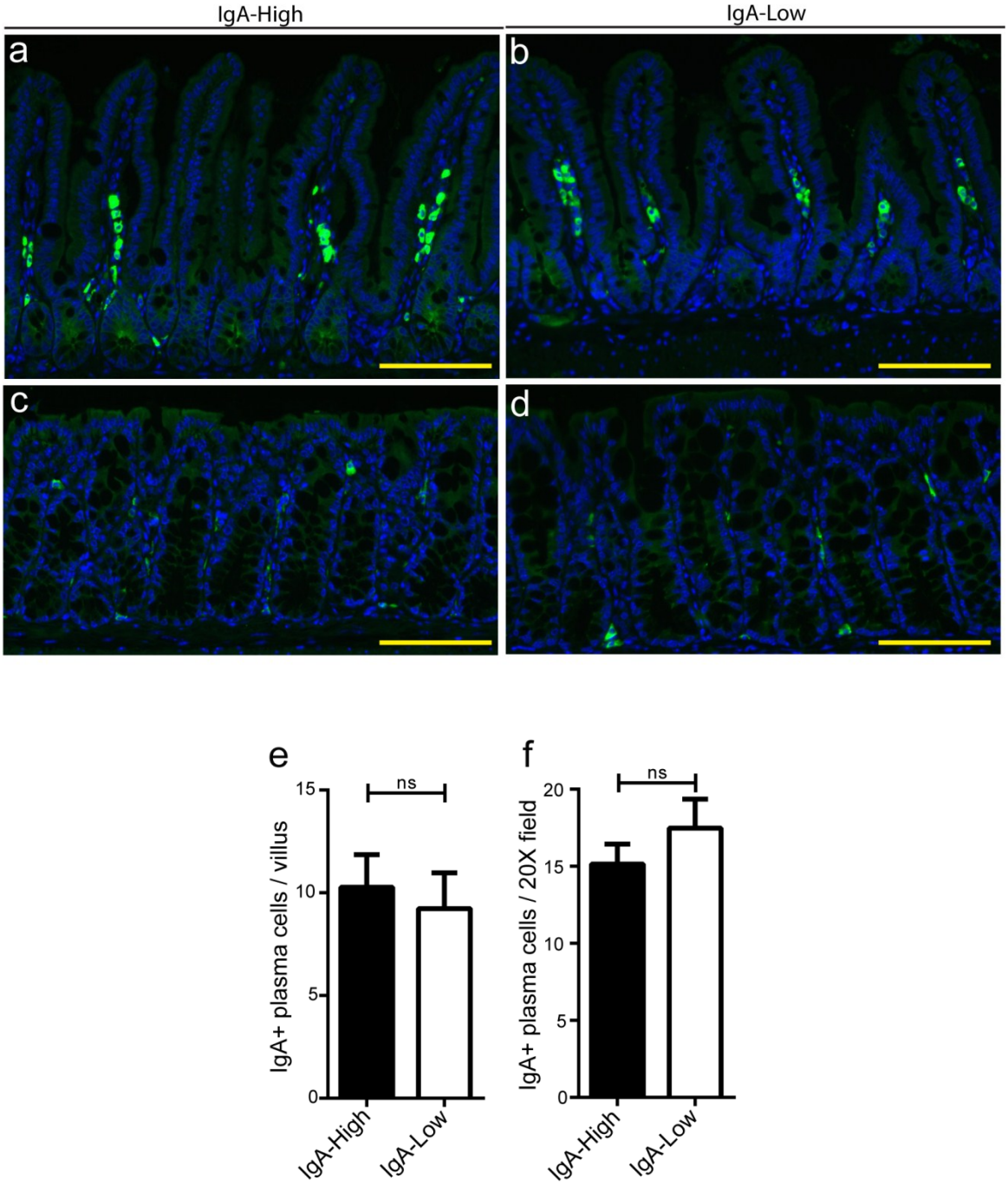

Figure 3.19. Intestinal pIgR immunostaining is not different between IgA-High and IgA-Low mice.

Ileal **(a,b)** and colonic **(c,d)** sections from IgA-High and IgA-Low mice were stained with anti-pIgR (red) and bis-benzamide dye (blue); representative images are shown (n=10 mice per group). Bars = 100 μm.

Figure 3.19. Intestinal pIgR immunostaining is not different between IgA-High and IgA-Low mice.

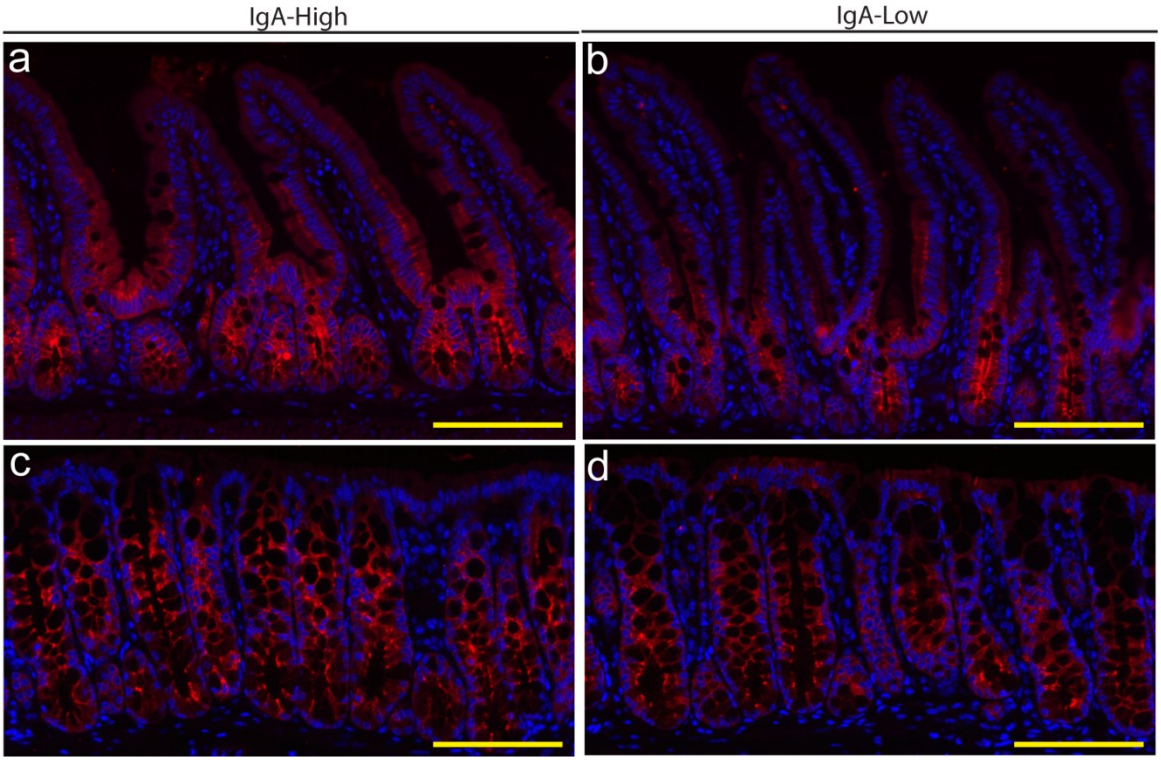

Figure 3.20. Secretory component is absent in IgA-Low fecal samples.

(a) Representative anti-pIgR/SC immunoblot of intestinal tissue and fecal samples from IgA-High (lanes 1-4) and IgA-Low (lanes 5-7) mice. Ileal and colonic pIgR was normalized to actin. Fecal samples were normalized by fecal weight. **(b-d)** Quantification of immunoblots for **(b)** ileal pIgR, **(c)** colonic pIgR, and **(d)** fecal SC using ImageJ. Colonic and ileal pIgR were normalized to actin, and fecal SC was normalized to average IgA-High values=100%. All values are indicated as mean±s.e.m. Statistical analysis by unpaired t-test: (b) $P<0.6150$, $n>5$ mice per group; (c) $P<0.0933$, $n>10$ mice per group; (d) $P<0.0001$, $n\geq5$ mice per group.

Figure 3.20. Secretory component is absent in IgA-Low fecal samples.

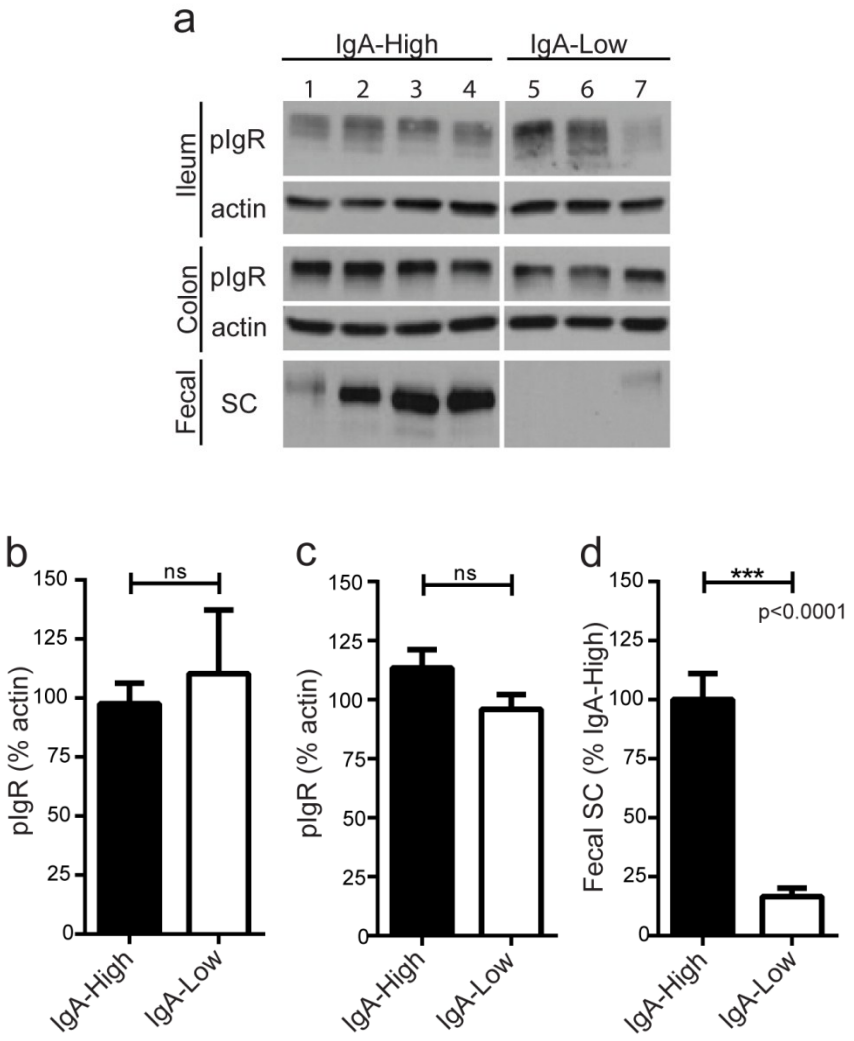

Figure 3.21. The IgA-Low-associated microbes are culturable.

(a) Schematic of bacterial culturing experiments. **(b)** Fecal IgA was measured in IgA-High mice before and after administration with cultured microbes as depicted in **(a)**. The dotted lines represent the limit of detection by ELISA. All values are indicated as mean±s.e.m. One-way analysis of variance: $F=18.60$, $P<0.0001$, $n\geq 9$ mice per group. Means with different letters are significantly different by Tukey's multiple comparison test.

Figure 3.21. The IgA-Low-associated microbes are culturable.

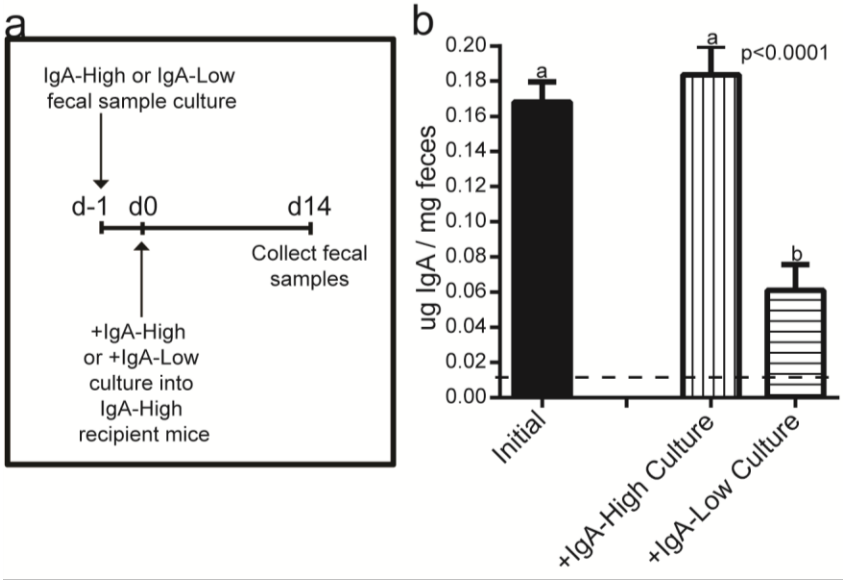

Figure 3.22: Schematic of intestinal epithelial:bacterial co-culture for IgA transcytosis

On day 3 post seeding primary intestinal epithelial cell monolayers, 3 μg of normal mouse IgA is added to the lower compartment of the Transwells. At the same time, IgA-High or IgA-Low bacterial cultures are added to the apical compartment of the Transwells. Apical Transwell supernatants are collected at 3 and 6 hours for detection of SIgA by various methods.

Figure 3.22: Schematic of intestinal epithelial:bacterial co-culture for IgA transcytosis

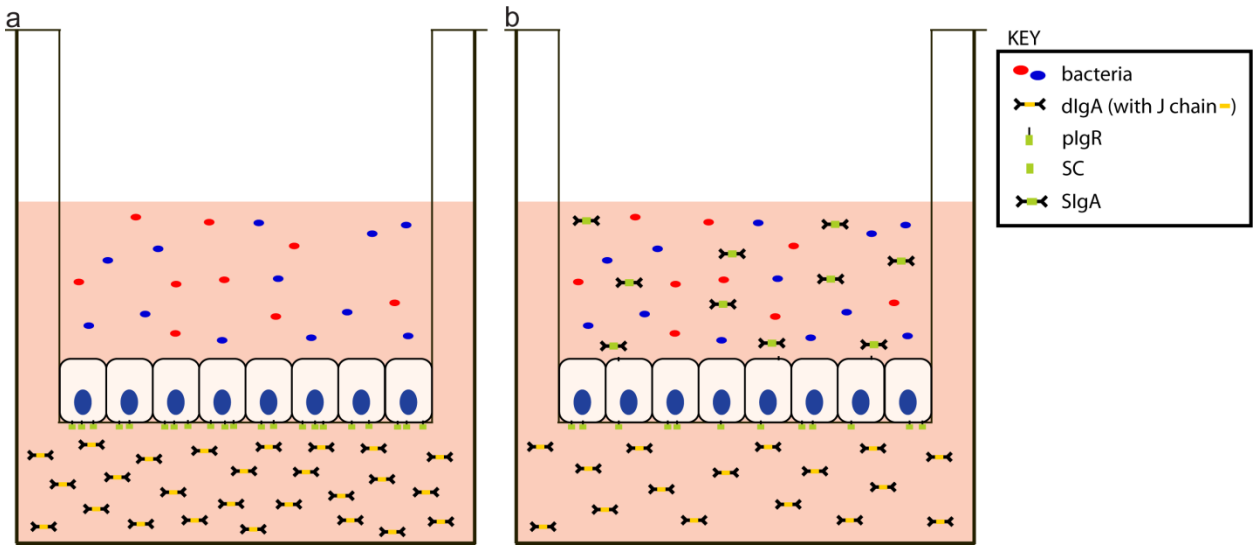

Figure 3.23. pIgR is expressed equally in intestinal epithelial monolayers in all treatment conditions.

Representative immunoblot of intestinal epithelial monolayers stained for anti-pIgR and anti-actin (one of three experiments). Cells were pre-treated with 10 μM DAPT + 1μg ml^{-1} LPS on days 1 and 2 post seeding to induce differentiation and pIgR expression. Some wells were left untreated as negative controls. On day 3 post seeding, 3 μg of normal mouse IgA was added to the lower compartment of the Transwells. At the same time, a subset of the DAPT+LPS-treated Transwells was also treated with IgA-High/IgA-Low bacterial cultures (either the pelleted bacterial or supernatant fraction) in the apical compartment.

Figure 3.23. pIgR is expressed equally in intestinal epithelial monolayers in all treatment conditions.

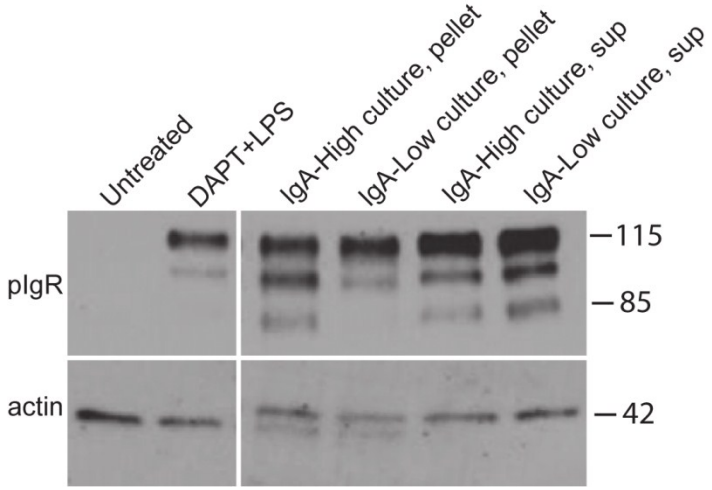

Figure 3.24. IgA-Low cultured microbes degrade SC *in vitro.*

Primary intestinal epithelial cell monolayers were pre-treated with 10 μM DAPT + 1μg ml^{-1} LPS on days 1 and 2 post seeding to induce differentiation and pIgR expression. Some wells were left untreated as negative controls. On day 3 post seeding, 3 μg of normal mouse IgA was added to the lower compartment of the Transwells. At the same time, a subset of the DAPT+LPS-treated Transwells was also treated with IgA-High/IgA-Low bacterial cultures (either the pelleted bacterial or supernatant fraction) in the apical compartment. Apical Transwell supernatants were collected at 3 and 6 hours, and the amount of SC was measured by anti-SC immunoblot. **(a)** Representative anti-SC immunoblot and quantification of the full length SC normalized to the DAPT+LPS treatment group at 3 hours **(b)** and 6 hours **(c)** over 5 independent experiments by ImageJ. All values are indicated as mean±s.e.m. One-way analysis of variance: **(b)** $F=13.50$, $P<0.0001$, $n\geq3$ per group; **(c)** $F=62.56$, $P<0.0001$, $n=5$ per group. Means with different letters are significantly different by Tukey's multiple comparison test.

Figure 3.24. IgA-Low cultured microbes degrade SC in vitro.

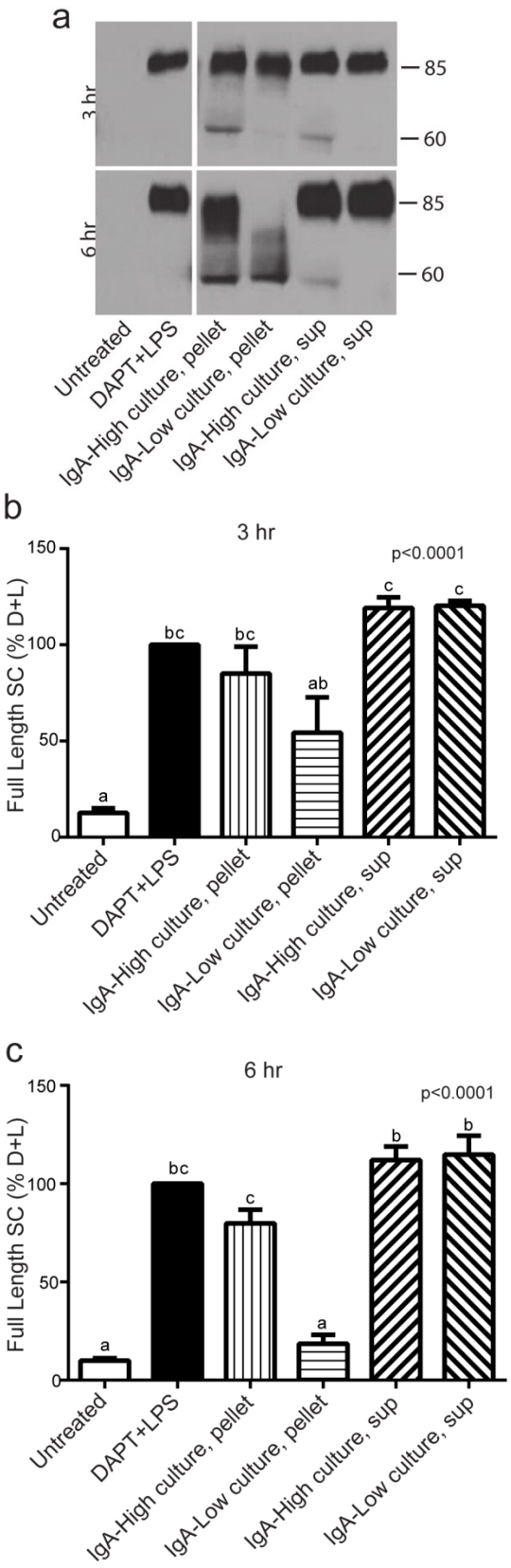

Figure 3.25. Summary and working model.

Wild-type mice bred in the same facility have a binary phenotype in fecal IgA levels (IgA-High vs IgA-Low). This phenotype was found to be heritable and transmissible. Surprisingly, the IgA-Low phenotype was dominant and microbially driven by ampicillin-susceptible bacteria. These IgA-Low mice had an increased susceptibility to DSS injury that was directly dependent on the IgA status. Mechanistically, we found the IgA-Low microbes had proteolytic activity *in vitro*, leading to the degradation of SC. This is consistent with the model in which SC degradation by IgA-Low microbes would make IgA more susceptible to degradation itself.

Figure 3.25. Summary and working model.

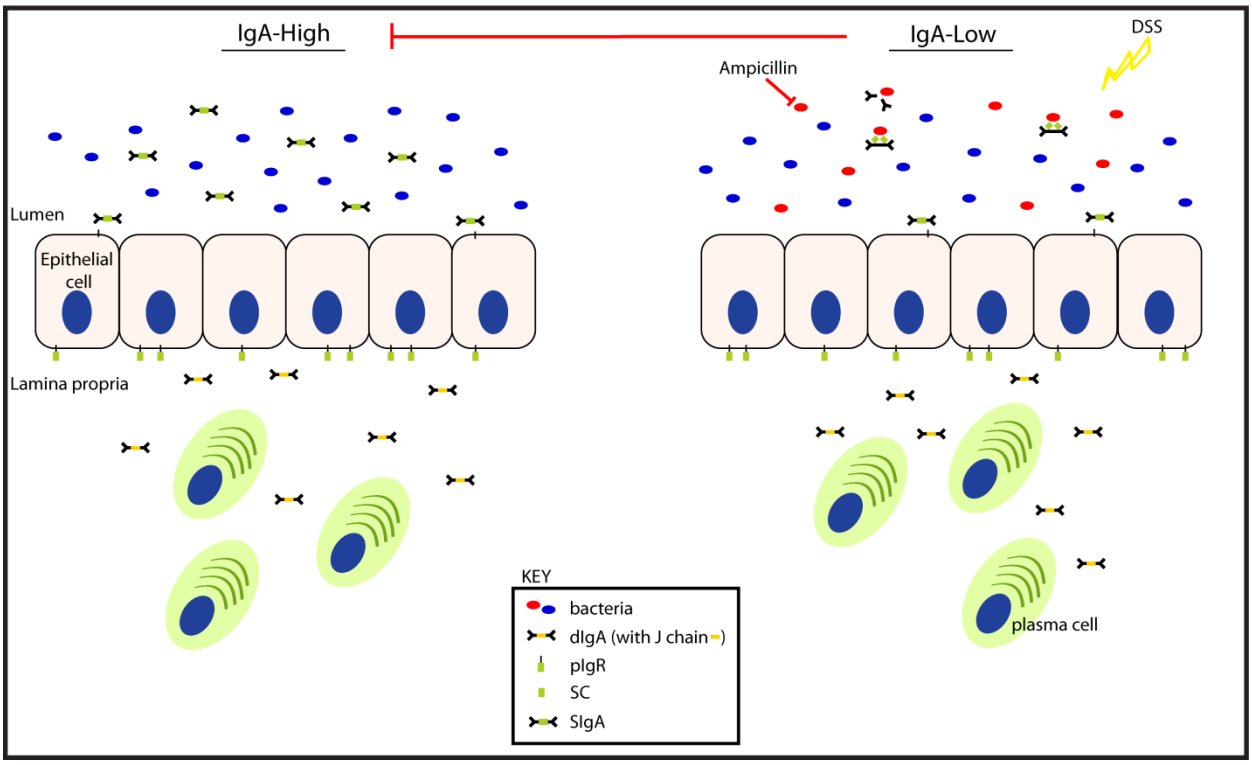

CHAPTER FOUR

Summary and future directions

SUMMARY

The overarching theme of this thesis was to investigate host-microbial interactions in the intestine. More specifically, we were interested in investigating the role of IgA, which is at a critical intersection between the host immune system and the microbiota. To do this, we developed an *in vitro* system and utilized *in vivo* mouse models to examine a mechanism by which commensal bacteria can modulate luminal IgA.

The first aim was to develop a primary intestinal epithelial monolayer system to study the cell biology of intestinal epithelial cells *in vitro*. Until recent advancements allowing for the culture and propagation of primary intestinal epithelial stem cells *in vitro*[82-84], various colon cancer cells lines and non-intestinal epithelial cell lines have been utilized to model physiologic and cell biologic processes. While studies using Caco-2, HT-29, T84, MDCK, and other cell lines have provided invaluable insights into epithelial cell biology, there are many well-recognized limitations to these systems[85,86,89-91]. However, one of the major advantages these various cell lines have over the current primary cell culture systems is their ability to form polarized monolayers. We therefore adapted the primary spheroid culture system to grow polarized primary intestinal epithelial cell monolayers, and functionally tested these monolayers by looking at the process of IgA transcytosis[116]. Our ultimate goal was to be able to use this system to not only investigate epithelial cell biology, but also epithelial cell interactions with other host cells as well as the commensal microbiota.

Our *in vivo* studies highlight the ability of the microbiota to produce significant phenotypic effects in genetically identical mice. We found that WT mice in a single mouse facility had dichotomous levels of fecal IgA, and this phenotype was found to be heritable in a non-chromosomal manner. In addition, the IgA-Low phenotype was found to be dominant,

microbially driven, and led to increased intestinal injury by DSS. *In vitro* co-culture studies utilizing the primary intestinal epithelial monolayer system and anaerobically cultured bacteria revealed proteolytic activity present in the IgA-Low cultured microbes that led to the degradation of SC. These findings are consistent with a model in which SC degradation by IgA-Low microbes makes IgA more susceptible to degradation itself, leading to the low IgA levels observed in these mice. The studies presented in this thesis have just begun to dive into the mechanism of this microbially driven phenotypic difference, and brings up multiple avenues for future studies that are the subject of this final chapter.

FUTURE DIRECTIONS

As detailed in chapter 3 and summarized in Figure 3.25, we observed that genetically identical mice in the same facility had a dichotomous fecal IgA phenotype that was heritable and transmissible. Furthermore, the IgA-Low phenotype was found to be dominant and microbially driven. *In vitro* studies utilizing the primary intestinal epithelial monolayers along with anaerobically cultured bacteria from the mice indicated that the IgA-Low-associated microbes may have proteolytic activity capable of degrading SC (**Fig. 3.24**). This is consistent with the model in which SC degradation by these IgA-Low microbes would make IgA more susceptible to degradation itself, potentially explaining the diminished luminal IgA levels in the IgA-Low mice.

Preliminary experiments using the epithelial:bacterial cell co-culture system show that in fact IgA itself may be degraded *in vitro* (**Figure 4.1**). Treatment of the epithelial monolayers with the IgA-Low culture supernatants showed comparable levels of IgA in the apical Transwell compartment to the DAPT+LPS treated positive controls. However, co-culture of the monolayers with the bacterial fraction from the IgA-Low culture showed IgA levels near the lower limit of detection. This data suggested that the IgA-Low microbes have a biologic effect on the IgA itself in addition to the SC *in vitro*. Further experiments need to be performed using cultured microbes from IgA-High mice as a control. In addition, to show that this decrease in SC and IgA is due to biologic effects of the microbes, these studies need to be repeated using heat-killed and antibiotic-treated bacterial cultures. To show that the decrease in SIgA is specifically due to proteolytic degradation, broad-spectrum bacterial protease inhibitors can be used during the co-culture experiments. Not all bacterial proteases may be inhibited by these cocktails, however if

inhibition was observed, specific bacterial protease inhibitors can be used to classify and narrow down the type of protease(s) involved in the IgA-Low phenotype.

Also at this point, we cannot determine whether the microbes affecting SC levels are the same ones affecting IgA levels. To do this, we would first need to identify specific bacterial isolates that are capable of degrading SC and IgA *in vitro*. While we have been successful in culturing a community of microbes from IgA-Low mice that is able to confer the IgA-Low phenotype *in vivo* and degrade SC and IgA *in vitro*, we have had some difficulty growing specific bacterial isolates. Through 16S sequencing (**Figure 4.2**), we have identified *Prevotella* and *Sutterella* as potential candidates associated with the IgA-Low phenotype. These microbes were present in the IgA-Low mice, but absent in the IgA-High mice. We will attempt to isolate single colonies of *Prevotella* and *Sutterella* on LKV and Brucella blood agar respectively. It is possible that while these microbes show an association by sequencing, they may not be the protease-producing microbes directly responsible for the degradation of the SIgA. These microbes may be acting in concert with other bacteria to produce this effect or may need a community of microbes to grow efficiently in culture.

Therefore a complementary approach will be used to identify the microbe(s) with IgA-degrading activity utilizing a functional screen. To do this, different combinations of antibiotics will be added to the IgA-Low chopped meat broth cultures to selectively eliminate pools of bacteria while trying to retain the IgA-Low inducing microbes. In addition, dose curves of the antibiotics could be tested. The *in vitro* co-culture system will allow us to systematically and efficiently test these pools of microbes without initially worrying about potential issues of intestinal colonization in the *in vivo* model.

Furthermore, the *in vitro* assay could be further simplified to a no-cell system: cultured microbes could be added to media containing SIgA to look for direct degradation as an initial screen prior to using the co-culture system, allowing for an even quicker screening tool. Both mouse IgA and recombinant mouse SC are sold commercially and can be incubated *in vitro* to form SIgA complexes. While some optimization will need to be performed to set up this system, it would ultimately save time in performing the screen.

In these approaches, we can functionally test pools of microbes using our *in vitro* co-culture system and potentially narrow down our IgA-Low community without the pressure of relying on one single isolate that may or may not grow well in isolation. There is also the possibility that one bacterial species alone may not be able to induce the phenotype, and a community of microbes is needed. Using these approaches to gradually narrow down pools of bacteria would address that possibility.

In addition to identifying the IgA-Low phenotype-inducing bacteria, another big question is the identity of the putative protease. Knowing the identity of the bacteria would provide a great advantage in addressing this question. If we can identify a specific bacterial species, the genome sequence could provide insight into potential candidate proteases. Candidate genes could then be cloned into *E.coli* to test for SIgA-degrading activity. In addition, we could also try to isolate and purify the protease from the bacterial cultures. If the protease of interest can be identified, it would be interesting to determine the specificity of the protease: is SIgA a specific substrate, or is there a wider range of substrates that include additional host proteins, as observed for ZapA produced by *P. mirabilis*[79]? It would be interesting to determine whether our microbe(s) of interest is(are) an opportunistic pathogen and/or a commensal microbe in the

mouse intestine, and whether these proteases function as virulence factors (which has typically been the case for the IgA proteases found thus far).

Looking at the bigger picture, it would be interesting to determine whether related microbes and/or proteases were present in the human intestine, and how this relates to luminal IgA levels in humans. While the majority of IgA is produced at mucosal sites such as the intestine, human IgA levels are mainly tested by serum analysis. Even in the case of IgA deficiency, the clinical diagnosis is performed by measuring serum IgA levels. And while alterations in IgA levels have been associated with intestinal diseases such as celiac disease and IBD, luminal IgA levels have not really been investigated in human patients. Our work has shown that serum IgA, lamina propria IgA^+ plasma cell numbers, and epithelial pIgR expression may not necessarily correlate with IgA levels in the intestinal lumen (where IgA is thought to exert most of its effects). Therefore, the investigation of mucosal, and specifically luminal IgA levels in human patients would be of great value.

Figure 4.1. IgA-Low cultured microbes degrade SIgA *in vitro*

Primary intestinal epithelial cell monolayers were pre-treated with 10 μM DAPT + 1μg ml^{-1} LPS on days 1 and 2 post seeding to induce differentiation and pIgR expression. Some wells were left untreated as negative controls. On day 3 post seeding, 3 μg of normal mouse IgA was added to the lower compartment of the Transwells. At the same time, a subset of the DAPT+LPS-treated Transwells was also treated with IgA-High/IgA-Low bacterial cultures (either the pelleted bacterial or supernatant fraction) in the apical compartment. Apical Transwell supernatants were collected at 3 and 6 hours, and the amount of IgA transcytosed to the apical compartment was measured by ELISA. The dotted lines represent the limit of detection by ELISA. All values are indicated as mean±s.e.m. One-way analysis of variance: $F=43.15$, $P<0.0001$, $n\geq3$ per group. Means with different letters are significantly different by Tukey's multiple comparison test.

Figure 4.1. IgA-Low cultured microbes degrade SIgA *in vitro*

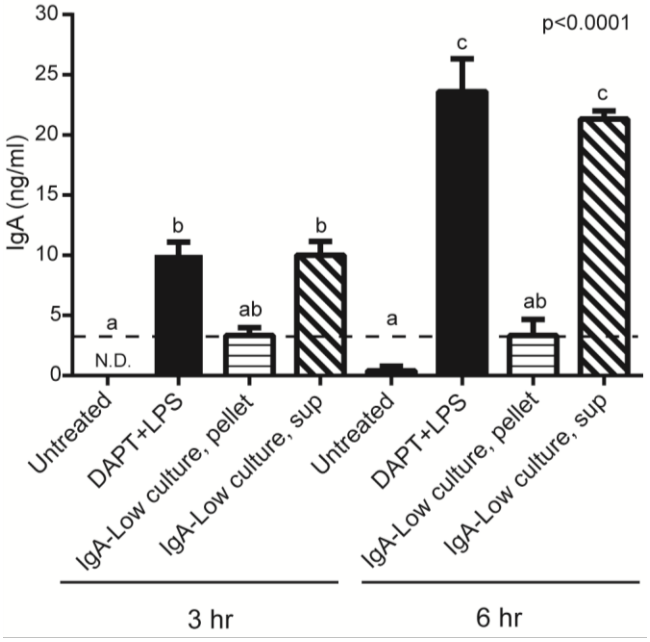

Figure 4.2. Identification of IgA-Low-associated microbes by 16S sequencing

DNA was purified from IgA-High and IgA-Low fecal samples from two different mouse facilities (Facility 1 = CSRB, Facility 2 = SRF). Each sample was amplified in triplicate, combined, and confirmed by gel electrophoresis using Golay-barcoded primers specific for the V4 region (F515/R806). The final pooled samples were sent to the Center for Genome Sciences (Washington University School of Medicine) for sequencing using the 2x250bp protocol with the Illumina MiSeq platform. 16S sequence analysis was performed using QIIME (Quantitative Insights Into Microbial Ecology, version 1.8.0) (Caporaso et al., 2010). Relative OTU abundance data was input into LEfSe to determine biomarkers with significant LDA effect size (Segata et. al 2010). Biomarkers were graphically annotated on phylogenetic trees using GraPhlAn (Segata et. al 2012). Depicted below are the biomarkers specific for the IgA-Low associated microbes. This work was performed by Dr. Megan T. Baldridge, M.D. Ph.D.

Figure 4.2. Identification of IgA-Low-associated microbes by 16S sequencing

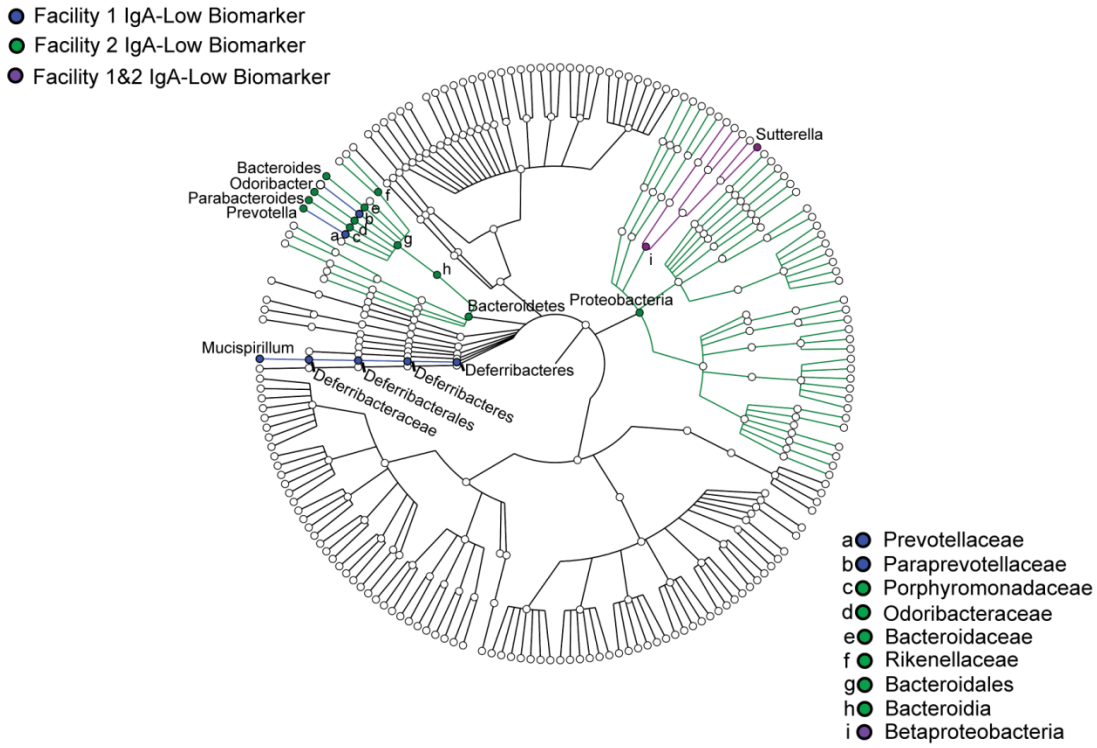

REFERENCES

1 Artis, D. Epithelial-cell recognition of commensal bacteria and maintenance of immune homeostasis in the gut. *Nature reviews immunology* **8**, 411-420 (2008).

2 Cho, J. H. The genetics and immunopathogenesis of inflammatory bowel disease. *Nat Rev Immunol* **8**, 458-466, doi:10.1038/nri2340 (2008).

3 Hooper, L. V. Do symbiotic bacteria subvert host immunity. *Nature reviews microbiology* **7**, 367-374 (2009).

4 Suzuki, K., Maruya, M., Kawamoto, S. & Fagarasan, S. Roles of B-1 and B-2 cells in innate and acquired IgA-mediated immunity. *Immunological reviews* **237**, 180-190 (2010).

5 Macpherson, A. J., Geuking, M. B., Slack, E., Hapfelmeier, S. & McCoy, K. D. The habit, double life, citizenship, and forgetfulness of IgA. *Immunological reviews* **245**, 132-146 (2012).

6 Tsuji, M. *et al.* Requirement for lymphoid tissue-inducer cells in isolated follicle formation and T cell-independent immunoglobulin A generation in the gut. *Immunity* **29**, 261-271, doi:10.1016/j.immuni.2008.05.014 (2008).

7 Macpherson, A. J., Geuking, M. B. & McCoy, K. D. Immunoglobulin A: a bridge between innate and adaptive immunity. *Curr Opin Gastroenterol* **27**, 529-533, doi:10.1097/MOG.0b013e32834bb805 (2011).

8 Wei, M. *et al.* Mice carrying a knock-in mutation of Aicda resulting in a defect in somatic hypermutation have impaired gut homeostasis and compromised mucosal defense. *Nat Immunol* **12**, 264-270, doi:10.1038/ni.1991 (2011).

9 Lycke, N. Y. & Bemark, M. The role of Peyer's patches in synchronizing gut IgA responses. *Front Immunol* **3**, 329, doi:10.3389/fimmu.2012.00329 (2012).

10 Brandtzaeg, P. History of Oral Tolerance and Mucosal Immunity. *Annals of the New York Academy of Sciences* **778**, 1-27 (1996).

11 Rojas, R. & Apodaca, G. Immunoglobulin transport across polarized epithelial cells. *Nat Rev Mol Cell Biol* **3**, 944-955, doi:10.1038/nrm972 (2002).

12 Musil, L. S. & Baenziger, J. U. Cleavage of membrane secretory component to soluble secretory component occurs on the cell surface of rat hepatocyte monolayers. *The journal of cell biology* **104**, 1725-1733 (1987).

13 Brown, W. R., Newcomb, R. W. & Ishizaka, K. Proteolytic degradation of exocrine and serum immunoglobulins. *The journal of clinical investigation* **49**, 1374-1380 (1970).

14 Lindh, E. Increased resistance of immunoglobulin A dimers to proteolytic degradation after binding of secretory component. *The journal of immunology* **114**, 284-286 (1975).

15 Resendiz-Albor, A. A. *et al.* Regionalization of pIgR expression in the mucosa of mouse small intestine. *Immunol Lett* **128**, 59-67, doi:10.1016/j.imlet.2009.11.005 (2010).

16 Renston, R. H., Jones, A. L., Christiansen, W. D., Hradek, G. T. & Underdown, B. J. Evidence for a vesicular transport mechanism in hepatocytes for biliary secretion of immunoglobulin A. *Science* **208**, 1276-1278 (1980).

17 Delacroix, D. L., Malburny, G. N. & Vaerman, J. P. Hepatobiliary transport of plasma igA in the mouse: contribution to clearance of intravascular IgA. *Eur J Immunol* **15**, 893-899 (1985).

18 Mostov, K. E. Transepithelial transport of immunoglobulins. *Annual review of Immunology* **12**, 63-84 (1994).

19 Kaetzel, C. S. The polymeric immunoglobulin receptor: bridging innate and adaptive immune responses at mucosal surfaces. *Immunological reviews* **206**, 83-99 (2005).
20 Hamburger, A. E., Bjorkman, P. J. & Herr, A. B. Structural insights into antibody-mediated mucosal immunology. *Current topics in microbiology and immunology* **308**, 173-204 (2006).
21 Mostov, K. E. & Deitcher, D. L. Polymeric immunoglobulin receptor expressed in MDCK cells transcytose IgA. *Cell* **46**, 613-621 (1986).
22 Hirt, R. P. *et al.* Transcytosis of the polymeric Ig receptor requires phosphorylation of serine 664 in the absence but not presence of dimeric IgA. *Cell* **74**, 245-255 (1993).
23 Cardone, M. H., Smith, B. L., Song, W., Mochly-Rosen, D. & Mostov, K. E. Phorbol myristate acetate-mediated stimulation of transcytosis and apical recycling in MDCK cells. *Journal of cell biology* **124**, 717-727 (1994).
24 Cardone, M. H. & Mostov, K. E. Wortmannin inhibits transcytosis of dimeric IgA by the polymeric immunoglobulin receptor. *Federation of European Biochemical Societies letters* **376**, 74-76 (1995).
25 Song, W., Bomsel, M., Casanova, J., Vaerman, J. P. & Mostov, K. E. Stimulation of transcytosis of the polymeric immunoglobulin receptor by dimeric IgA. *Proc Natl Acad Sci U S A* **91**, 163-166 (1994).
26 Giugliano, L. G., Ribeiro, S. T. G., Vainstein, M. H. & Ulhoa, C. J. Free secretory component and lactoferrin of human milk inhibit the adhesion of enterotoxigenic Escherichia coli. *Journal of medical microbiology* (1995).
27 de Araújo, A. N. & Giugliano, L. G. Lactoferrin and free secretory component of human milk inhibit the adhesion of enteropathogenic Escherichia coli to HeLa cells. *BMC Microbiology* **1** (2001).
28 Dallas, S. D. & Rolfe, R. D. Binding of Clostridium difficile toxin A to human milk secretory component. *Journal of medical microbiology* **47**, 879-888 (1998).
29 Asano, M. *et al.* Multiple cleavage sites for polymeric immunoglobulin receptor. *Immunology* **112**, 583-589, doi:10.1046/j.1365-2567.2004.01914.x (2004).
30 Asano, M. & Komiyama, K. Polymeric immunoglobulin receptor. *Journal of oral science* **53**, 147-156 (2011).
31 Hooper, L. V. Molecular Analysis of Commensal Host-Microbial Relationships in the Intestine. *Science* **291**, 881-884, doi:10.1126/science.291.5505.881 (2001).
32 Bruno, M. E. C. *et al.* Regulation of the polymeric immunoglobulin receptor in intestinal epithelial cells by Enterobacteriaceae: implications for mucosal homeostasis. *Immunol Invest* **39**, 356-382, doi:10.3109/08820131003622809 (2010).
33 Schneeman, T. A. *et al.* Regulation of the polymeric Ig receptor by signaling through TLRs 3 and 4: linking innate and adaptive immune responses. *The journal of immunology* **175**, 376-384 (2005).
34 Diebel, L. N. & Liberati, D. M. Disparate effects of bacteria and Toll-like receptor-dependant bacterial ligand stimulation on immunoglobulin A transcytosis. *J Trauma* **70**, 691-700, doi:10.1097/TA.0b013e31820c780e (2011).
35 Nakamura, Y. *et al.* Up-regulation of polymeric immunoglobulin receptor expression by the heat-inactivated potential probiotic Bifidobacterium bifidum OLB6378 in a mouse intestinal explant model. *Scand J Immunol*, doi:10.1111/j.1365-3083.2011.02645.x (2011).

36 Cao, A. T., Yao, S., Gong, B., Elson, C. O. & Cong, Y. Th17 cells upregulate polymeric Ig receptor and intestinal IgA and contribute to intestinal homeostasis. *J Immunol* **189**, 4666-4673, doi:10.4049/jimmunol.1200955 (2012).
37 Hempen, P. M. *et al.* Transcriptional regulation of the human polymeric Ig receptor gene: analysis of basal promoter elements. *The journal of immunology* **169**, 1912-1921 (2002).
38 Johansen, F. E. & Kaetzel, C. S. Regulation of the polymeric immunoglobulin receptor and IgA transport: new advances in environmental factors that stimulate pIgR expression and its role in mucosal immunity. *Mucosal Immunol* **4**, 598-602, doi:10.1038/mi.2011.37 (2011).
39 Frantz, A. L. *et al.* Targeted deletion of MyD88 in intestinal epithelial cells results in compromised antibacterial immunity associated with downregulation of polymeric immunoglobulin receptor, mucin-2, and antibacterial peptides. *Mucosal Immunol* **5**, 501-512, doi:10.1038/mi.2012.23 (2012).
40 Moreau, M. C., Ducluzeau, R., Guy-Grand, D. & Muller, M. C. Increase in the population of duodenal immunoglobulin A plasmocytes in axenic mice associated with different living of dead bacterial strains of intestinal origin. *Infect Immun* **21**, 532-539 (1978).
41 Hapfelmeier, S. *et al.* Reversible Microbial Colonization of Germ-Free Mice Reveals the Dynamics of IgA Immune Responses. *Science* **328**, 1705-1709, doi:10.1126/science.1188454 (2010).
42 Mattioli, C. A. & Tomasi, T. B. The life span of IgA plamsa cells from the mouse intestine. *J Exp Med* **138**, 452-460 (1973).
43 Johansen, F. E. *et al.* Absence of epithelial immunoglobulin A transport, with increased mucosal leakiness, in polymeric immunoglobulin receptor/secretory component-deficient mice. *J Exp Med* **190**, 915-921 (1999).
44 Shimada, S. *et al.* Generation of polymeric immunoglobulin receptor-deficient mouse with marked reduction of secretory IgA. *The journal of immunology* **163**, 5367-5373 (1999).
45 Uren, T. K. *et al.* Role of the polymeric Ig receptor in mucosal B cell homeostasis. *The journal of immunology* **170**, 2531-2539 (2003).
46 Hendrickson, B. A. *et al.* Altered hepatic transport of immunoglobulin A in mice lacking the J chain. *Journal of experimenal medicine* **182**, 1905-1911 (1995).
47 Lycke, N., Erlandsson, L., Ekman, L., Schon, K. & Leanderson, T. Lack of J chain inhibits the transport of gut IgA and abrogates the development of intestinal antitoxic protection. *The journal of immunology* **163**, 913-919 (1999).
48 Harriman, G. R. *et al.* Targeted deletion of the IgA constant region in mice leads to IgA deficiency with alterations in expression of other Ig isotypes. *The journal of immunology* **162**, 2521-2529 (1999).
49 Uren, T. K. *et al.* Vaccine-induced protection against gastrointestinal bacterial infections in the absence of secretory antibodies. *Eur J Immunol* **35**, 180-188, doi:10.1002/eji.200425492 (2005).
50 Sun, K., Johansen, F. E., Eckmann, L. & Metzger, D. W. An important role for polymeric Ig receptor-mediated transport of IgA in protection against *Streptococcus pneumoniae* nasopharyngeal carriage. *the journal of immunology* **173**, 4576-4581 (2004).

51 Sait, L. C. *et al.* Secretory antibodies reduce systemic antibody responses against the gastrointestinal commensal flora. *Int Immunol* **19**, 257-265, doi:10.1093/intimm/dxl142 (2007).
52 Suzuki, K. *et al.* Aberrant expansion of segmented filamentous bacteria in IgA-deficient gut. *Proc Natl Acad Sci U S A* **101**, 1981-1986, doi:10.1073/pnas.0307317101 (2004).
53 Robinson, J. K., Blanchard, T. G., Levine, A. D., Emancipator, S. N. & Lamm, M. E. A mucosal IgA-mediated excretory immune system *in vivo*. *The journal of immunology* **166**, 3688-3692 (2001).
54 Yel, L. Selective IgA deficiency. *J Clin Immunol* **30**, 10-16, doi:10.1007/s10875-009-9357-x (2010).
55 Strober, W., Krakauer, R., Klaeveman, H. L., Reynolds, H. Y. & Nelson, D. L. Secretory Component Deficiency - A Disorder of the IgA Immune System. *The New England Journal of Medicine* **294**, 351-356 (1976).
56 Arsenescu, R. *et al.* Signature biomarkers in Crohn's disease: toward a molecular classification. *Mucosal Immunol* **1**, 399-411, doi:10.1038/mi.2008.32 (2008).
57 Savage, D. C., Dubos, R. & Schaedler, R. W. The gastrointestinal epithelium and its autochthonous bacterial flora. *Journal of experimenal medicine* **127**, 67-76 (1968).
58 Funkhouser, L. J. & Bordenstein, S. R. Mom knows best: the universality of maternal microbial transmission. *PLoS Biol* **11**, e1001631, doi:10.1371/journal.pbio.1001631 (2013).
59 Friswell, M. K. *et al.* Site and strain-specific variation in gut microbiota profiles and metabolism in experimental mice. *PLoS One* **5**, e8584, doi:10.1371/journal.pone.0008584 (2010).
60 Peterson, D. A., Frank, D. N., Pace, N. R. & Gordon, J. I. Metagenomic Approaches for Defining the Pathogenesis of Inflammatory Bowel Diseases. *Cell Host Microbe* **3**, 417-427 (2008).
61 Nava, G. M., Friedrichsen, H. J. & Stappenbeck, T. S. Spatial organization of intestinal microbiota in the mouse ascending colon. *Isme J* **5**, 627-638, doi:10.1038/ismej.2010.161 (2011).
62 Hao, L. Y., Liu, X. & Franchi, L. Inflammasomes in inflammatory bowel disease pathogenesis. *Curr Opin Gastroenterol* **29**, 363-369, doi:10.1097/MOG.0b013e32836157a4 (2013).
63 Garrett, W. S. *et al.* Enterobacteriaceae act in concert with the gut microbiota to induce spontaneous and maternally transmitted colitis. *Cell Host Microbe* **8**, 292-300, doi:10.1016/j.chom.2010.08.004 (2010).
64 Elinav, E. *et al.* NLRP6 inflammasome regulates colonic microbial ecology and risk for colitis. *Cell* **145**, 745-757, doi:10.1016/j.cell.2011.04.022 (2011).
65 Zenewicz, L. A. *et al.* IL-22 deficiency alters colonic microbiota to be transmissible and colitogenic. *J Immunol* **190**, 5306-5312, doi:10.4049/jimmunol.1300016 (2013).
66 Ubeda, C. *et al.* Familial transmission rather than defective innate immunity shapes the distinct intestinal microbiota of TLR-deficient mice. *J Exp Med* **209**, 1445-1456, doi:10.1084/jem.20120504 (2012).
67 Brinkman, B. M. *et al.* Gut microbiota affects sensitivity to acute DSS-induced colitis independently of host genotype. *Inflamm Bowel Dis* **19**, 2560-2567, doi:10.1097/MIB.0b013e3182a8759a (2013).

68 Robertson, S. J. *et al.* Nod1 and Nod2 signaling does not alter the composition of intestinal bacterial communities at homeostasis. *Gut Microbes* **4**, 222-231, doi:10.4161/gmic.24373 (2013).
69 Letran, S. E. *et al.* TLR5-deficient mice lack basal inflammatory and metabolic defects but exhibit impaired CD4 T cell responses to a flagellated pathogen. *J Immunol* **186**, 5406-5412 (2011).
70 Plaut, A. G., Gilbert, J. V., Artenstein, M. S. & Capra, J. D. *Neisseria gonorrhoeae* and *Neisseria meningitidis*: extracellular enzyme cleaves human immunoglobulin A. *Science* **190**, 1103-1105 (1975).
71 Kilian, M., Mestecky, J. & Schrohenloher, R. E. Pathogenic species of the genus *haemophilus* and *Streptococcus pneumoniae* produce Immunoglobulin A1 protease. *Infect Immun* **26**, 143-149 (1979).
72 Male, C. J. Immunoglobulin A1 protease production by *Haemophilus influenzae* and *Streptococcus pneumoniae*. *Infect Immun* **26**, 254-261 (1979).
73 Senior, B. W., Albrechtsen, M. & Kerr, M. A. *Proteus mirabilis* strains of diverse type have IgA protease activity. *Journal of medical microbiology* **24**, 175-180 (1987).
74 Mulks, M. H. & Plaut, A. G. IgA protease production as a characteristic distinguishing pathogenic from harmless *neisseriaceae*. *The New England Journal of Medicine* **299**, 973-976 (1978).
75 Janoff, E. N. *et al.* Pneumococcal IgA1 protease subverts specific protection by human IgA1. *Mucosal Immunol* **7**, 249-256, doi:10.1038/mi.2013.41 (2014).
76 Fujiyama, Y. *et al.* A novel IgA protease from *Clostridium sp.* capable of cleaving IgA1 and IgA2 A2m(1) allotype but not IgA2 A2m(2) allotype paraproteins. *The journal of immunology* **134**, 573-576 (1985).
77 Loomes, L. M., Senior, B. W. & Kerr, M. A. A proteolytic enzyme secreted by *Proteus mirabilis* degrades immunoglobulins of the immunoglobulin A1 (IgA1), IgA2, and IgG isotypes. *Infect Immun* **58**, 1979-1985 (1990).
78 Wassif, C., Cheek, D. & Belas, R. Molecular Analysis of a Metalloprotease from *Proteus mirabilis*. *Journal of bacteriology* **177**, 5790-5798 (1995).
79 Belas, R., Manos, J. & Suvanasuthi, R. Proteus mirabilis ZapA metalloprotease degrades a broad spectrum of substrates, including antimicrobial peptides. *Infect Immun* **72**, 5159-5167, doi:10.1128/IAI.72.9.5159-5167.2004 (2004).
80 Spahich, N. A. & St. Geme, J. W. Structure and function of the Haemophilus influenzae autotransporters. *Frontiers in cellular and infection microbiology* **1**, 1-9 (2011).
81 Kapatais-Zoumbos, K., Chandler, D. K. F. & Barile, M. F. Survey of Immunoglobulin A Protease Activity Among Selected Species of Ureaplasma and Mycoplasma: Specificity for Host Immunoglobulin A. *Infect Immun* **47**, 704-709 (1985).
82 Sato, T. *et al.* Single Lgr5 stem cells build crypt-villus structures in vitro without a mesenchymal niche. *Nature* **459**, 262-265, doi:10.1038/nature07935 (2009).
83 Miyoshi, H., Ajima, R., Luo, C. T., Yamaguchi, T. P. & Stappenbeck, T. S. Wnt5a potentiates TGF-beta signaling to promote colonic crypt regeneration after tissue injury. *Science* **338**, 108-113, doi:10.1126/science.1223821 (2012).
84 Miyoshi, H. & Stappenbeck, T. S. In vitro expansion and genetic modification of gastrointestinal stem cells in spheroid culture. *Nat Protoc* **8**, 2471-2482, doi:10.1038/nprot.2013.153 (2013).

85 Duizer, E., Penninks, A. H., Stenhuis, W. H. & Groten, J. P. Comparison of permeability characteristics of the human colonic Caco-2 and rat small intestinal IEC-18 cell lines. *Journal of controlled release* **49**, 39-49 (1997).
86 Irvine, J. D. *et al.* MDCK (Madin-Darby canine kidney) cells: A tool for membrane permeability screening. *Journal of pharmaceutical sciences* **88**, 28-33 (1999).
87 Kuratnik, A. & Giardina, C. Intestinal organoids as tissue surrogates for toxicological and pharmacological studies. *Biochem Pharmacol* **85**, 1721-1726, doi:10.1016/j.bcp.2013.04.016 (2013).
88 Sun, H., Chow, E. C. Y., Liu, S., Du, Y. & Pang, K. S. The Caco-2 cell monolayer: usefulness and limitations. *Expert opinion on drug metabolism and toxicology* **4**, 395-411 (2008).
89 Sambuy, Y. *et al.* The Caco-2 cell line as a model of the intestinal barrier: influence of cell and culture-related factors on Caco-2 cell functional characteristics. *Cell biology and toxicology* **21**, 1-26 (2005).
90 Meunier, V., Bourrié, M., Berger, Y. & Fabre, G. The human intestinal epithelial cell line Caco-2; pharmacological and pharmacokinetic applications. *Cell biology and toxicology* **11**, 187-194 (1995).
91 Rousset, M. The human colon carcinoma cell lines HT-29 and Caco-2: two *in vitro* models for the study of intestinal differentiation. *Biochimie* **68**, 1035-1040 (1986).
92 Brandtzaeg, P. & Prydz, H. Direct evidence for an integrated function of J chain and secretory component in epithelial transport of immunoglobulins. *Nature* **311**, 71-73 (1984).
93 Mostov, K. E., Kraehenbuhl, J. P. & Blobel, G. Receptor-mediated transcellular transport of immunoglobulin: synthesis of secretory component as multiple and large transmembrane forms. *Proc Natl Acad Sci U S A* **77**, 7257-7261 (1980).
94 Mostov, K. E., Verges, M. & Altschuler, Y. Membrane traffick in polarized epithelial cells. *Current opinion in cell biology* **12**, 483-490 (2000).
95 Blanch, V. J., Piskurich, J. F. & Kaetzel, C. S. Cutting Edge: Coordinate regulation of IFN regulatory factor-1 and the polymeric Ig receptor by proinflammatory cytokines. *The journal of immunology* **162**, 1232-1235 (1999).
96 Piskurich, J. F. *et al.* Transcriptional regulation of the human polymeric immunoglobulin receptor gene by interferon-y. *Molecular immunology* **34**, 75-91 (1997).
97 Schjerven, H., Brandtzaeg, P. & Johansen, F. E. A Novel NFkB/Rel Site in Intron 1 Cooperates with Proximal Promoter Elements to Mediate TNFa-Induced Transcription of the Human Polymeric Ig Receptor. *The journal of immunology* **167**, 6412-6420 (2001).
98 Hayashi, M. *et al.* The polymeric immunoglobulin receptor (secretory component) in a human intestinal epithelial cell line is up-regulated by interleukin-1. *Immunology* **92**, 220-225 (1997).
99 Poltorak, A. *et al.* Defective LPS signaling in C3H/HeJ and C57BL/10ScCr mice: mutations in Tlr4 gene. *Science* **282**, 2085-2088 (1998).
100 Bloom, S. M. *et al.* Commensal Bacteroides species induce colitis in host-genotype-specific fashion in a mouse model of inflammatory bowel disease. *Cell Host Microbe* **9**, 390-403 (2011).
101 Schneider, C. A., Rasband, W. S. & Eliceiri, K. W. NIH Image to ImageJ: 25 years of image analysis. *Nature methods* **9**, 671-675 (2012).

102 Kang, S. S. *et al.* An antibiotic-responsive mouse model of fulminant ulcerative colitis. *Plos medicine* **5**, e41 (2008).
103 VanDussen, K. L. *et al.* Notch signaling modulates proliferation and differentiation of intestinal crypt base columnar stem cells. *Development* **139**, 488-497 (2012).
104 van Es, J. H. *et al.* Notch/gamma-secretase inhibition turns proliferative cells in intestinal crypts and adenomas into goblet cells. *Nature* **435**, 959-963 (2005).
105 Stevenson, B. R., Siliciano, J. D., Mooseker, M. S. & Goodenough, D. A. Identification of ZO-1: a high molecular weight polypeptide associated with the tight junction (zonula occludens) in a variety of epithelia. *Journal of cell biology* **103**, 755-766 (1986).
106 Bretscher, A. & Weber, K. Villin: the major microfilament-associated protein of the intestinal microvillus. *Proc Natl Acad Sci U S A* **76**, 2321-2325 (1979).
107 O'Connor, D. T., Burton, D. & Deftos, L. J. Chromogranin A: immunohistology reveals its universal occurrence in normal polypeptide hormone producing endocrine glands. *Life Sciences* **33**, 1657-1663 (1983).
108 Falk, P., Roth, K. A. & Gordon, J. I. Lectins are sensitive tools for defining differentiation programs of mouse gut epithelial cell lineages. *Am J Physiol Gastrointest Liver Physiol* **G987-1003.**, G987-1003. (1994).
109 Cash, H. L., Whitham, C. V., Behrendt, C. L. & Hooper, L. V. Symbiotic bacteria direct expression of an intestinal bactericidal lectin. *Science* **313**, 1126-1130, doi:10.1126/science.1127119 (2006).
110 Maunoury, R. *et al.* Villin expression in the visceral endoderm and in the gut anlage during early mouse embryogenesis. *EMBO Journal* **11**, 3321-3329 (1988).
111 Nakamura, Y. *et al.* Upregulation of Polymeric Immunoglobulin Receptor Expression by the Heat-Inactivated Potential Probiotic Bifidobacterium bifidum OLB6378 in a Mouse Intestinal Explant Model. *Scand J Immunol* **75**, 176-183, doi:10.1111/j.1365-3083.2011.02645.x (2012).
112 Ezeonu, I., Wang, M., Kumar, R. & Dutt, K. Density-dependent differentiation in nontransformed human retinal progenitor cells in response to basic fibroblast growth factor- and transforming growth factor-alpha. *DNA and cell biology* **22**, 607-620 (2003).
113 Lee, Y. S., Yuspa, S. H. & Dlugosz, A. A. Differentiation of cultured human epidermal keratinocytes at high cell densities is mediated by endogenous activation of the protein kinase C signaling pathway. *Journal of investigative dermatology* **111**, 762-766 (1998).
114 McBeath, R., Pirone, D. M., Nelson, C. M., Bhadriraju, K. & Chen, C. S. Cell shape, cytoskeletal tension, and RhoA regulate stem cell lineage commitment. *Developmental Cell* **6**, 483-495 (2004).
115 Mestecky, J. e. a. *Mucosal Immunology*. (Academic Press, 2005).
116 Moon, C., VanDussen, K. L., Miyoshi, H. & Stappenbeck, T. S. Development of a primary mouse intestinal epithelial cell monolayer culture system to evaluate factors that modulate IgA transcytosis. *Mucosal Immunol* **7**, 818-828, doi:10.1038/mi.2013.98 (2014).
117 Tsuji, M., Suzuki, K., Kinoshita, K. & Fagarasan, S. Dynamic interactions between bacteria and immune cells leading to intestinal IgA synthesis. *Semin Immunol* **20**, 59-66, doi:10.1016/j.smim.2007.12.003 (2008).
118 Blutt, S. E. & Conner, M. E. The Gastrointestinal Frontier: IgA and Viruses. *Front Immunol* **4**, 402, doi:10.3389/fimmu.2013.00402 (2013).

119 Rakoff-Nahoum, S., Paglino, J., Eslami-Varzaneh, F., Edberg, S. & Medzhitov, R. Recognition of commensal microflora by toll-like receptors is required for intestinal homeostasis. *Cell* **118**, 229-241, doi:10.1016/j.cell.2004.07.002 (2004).
120 Fagarasan, S. *et al.* Critical roles of activation-induced cytidine deaminase in the homeostasis of gut flora. *Science* **298**, 1424-1427 (2002).
121 Murthy, A. K., Dubose, C. N., Banas, J. A., Coalson, J. J. & Arulanandam, B. P. Contribution of polymeric immunoglobulin receptor to regulation of intestinal inflammation in dextran sulfate sodium-induced colitis. *J Gastroenterol Hepatol* **21**, 1372-1380, doi:10.1111/j.1440-1746.2006.04312.x (2006).
122 Virgin, H. W. & Todd, J. A. Metagenomics and Personalized Medicine. *Cell* **147**, 44-56 (2011).
123 Ichinohe, T. *et al.* Microbiota regulates immune defense against respiratory tract influenza A virus infection. *Proc Natl Acad Sci U S A* **108**, 5354-5359 (2011).